PLATINUM ON CARBON NANOFIBERS AS CATALYST FOR CINNAMALDEHYDE HYDROGENATION

Arjan Plomp

ISBN: 978-90-393-5015-7

Cover photograph and lay-out by Arjan & Annemieke Plomp
GVO drukkers & vormgevers B.V. | Ponsen & Looijen

PLATINUM ON CARBON NANOFIBERS AS CATALYST FOR CINNAMALDEHYDE HYDROGENATION

Platina op Koolstofnanovezels als Katalysator
voor de Hydrogenering van Kaneelaldehyde

(met een samenvatting in het Nederlands)

Proefschrift

ter verkrijging van de graad van doctor aan de Universiteit Utrecht op gezag van de rector magnificus, prof. dr. J.C. Stoof, ingevolge het besluit van het college voor promoties in het openbaar te verdedigen op woensdag 15 april 2009 des middags te 12.45 uur

door

Arie Jan Plomp

geboren op 18 juli 1980 te Zeist

Promotor: Prof. dr. ir. K.P. de Jong

Co-promotor: Dr. J.H. Bitter

Het in dit proefschrift beschreven onderzoek werd mede mogelijk gemaakt met financiële steun van EU Nanocat project 506621

Contents

1

General Introduction

Introduction

Catalysis is defined as reaction rate acceleration by presence of a substance, which is not consumed during reaction and does not alter the thermodynamic equilibrium. This substance is called a catalyst and allows a reaction process to take place more efficient and under milder conditions. The concept of catalysis has been described by Berzelius in 1836 for the first time [1-3]. Since that time, scientific knowledge as well as industrial applications of catalysis developed tremendously and because of its crucial role during manufacture of valuable consumer products, catalysis has become essential for the society [2, 4].

In heterogeneous catalysis, catalysts are in a different phase compared to the reactants and products. This type of catalysts is widely used in industrial applications. In general, reactants and products are either in liquid phase or gas phase and catalysts in solid phase. Catalysts often consist of a catalytically active phase (e.g. metals, metal oxides, acids etc.) on a (porous) support. For metal-based, heterogeneous catalysts, reactions are catalyzed on the metal surface. To that purpose, high metal dispersions are often preferred since in that way the largest available metal surface is created. Thus the supports should have a large surface area to facilitate high metal dispersions. Moreover, supports should not affect the catalytic performance negatively and should be mechanically strong. Support materials which are often used include silica, alumina and carbon [4].

Heterogeneous catalysts are used for a wide variety of reactions, such as hydrogenations, dehydrogenations and oxidations [4]. Selective hydrogenation of multiple unsaturated molecules towards one particular product is a major challenge [5]. For example, the selective hydrogenation of α,β-unsaturated aldehydes towards unsaturated alcohols is important from an industrial point of view [5-8]. Moreover, it is an attractive test reaction from a fundamental point of view, since C=C hydrogenation is thermodynamically more favored than C=O hydrogenation. Thus the selectivity to the unsaturated alcohol must be controlled kinetically. There are various ways to control the selectivity, e.g. by tuning the support, metal particle size and via addition of a second (promoter) metal(oxide) [5, 6, 9]. Cinnamaldehyde is an α,β-unsaturated aldehyde for which support effects, particle size effects and influence of promoters has been reported [6, 10, 11]. For example, cinnamaldehyde hydrogenation activity turned out to depend on the amount of oxygen surface groups on the catalyst support when platinum on carbon nanofibers (CNF) catalysts were used: removal of oxygen groups from the catalyst support surface resulted in an enhanced hydrogenation rate [12, 13]. In this thesis, cinnamaldehyde hydrogenation was used as a showcase to investigate the influence of the nature of CNF supports and promoters on the catalytic action of platinum based catalysts.

Selective hydrogenation of cinnamaldehyde

Hydrogenation of cinnamaldehyde results in cinnamyl alcohol and hydrocinnamaldehyde as intermediary products and hydrocinnamyl alcohol as final product (see Fig. 1 grey box). As mentioned before, the reaction path via hydrocinnamaldehyde is thermodynamically favored, but cinnamyl alcohol is the desired product for industrial applications [5, 6]. Both cinnamyl alcohol and cinnamaldehyde are used for their flavoring and fragrance properties. For commercial applications, only the trans-configuration of these materials is employed [7, 8, 14]. Furthermore, cinnamyl alcohol is used to synthesize pharmaceuticals, such as chloramphenicol which is used as an antibiotic agent in chloromycetin [8, 15]. Other synthesis routes towards cinnamyl alcohol like the Meerwein-Ponndorf-Verley reduction, are either expensive or result in large amounts of waste. Therefore, heterogeneous catalysts are used to perform the selective hydrogenation of cinnamaldehyde on industrial scale and it is the goal to obtain and maintain high activities and selectivities for the cinnamaldehyde hydrogenation [5-7, 16]. In general, noble metal based catalysts are used and the selectivity decreases in the following order Ir > Pt > Ru > Rh > Pd, while the activity increases in the same order. Because of its acceptable activity, stability and selectivity, platinum and ruthenium catalysts are in general used for this type of selective hydrogenations. Moreover, the selectivity can be significantly enhanced by the use of promoters [6, 10, 17].

By-products can be formed due to decarbonylation and hydrogenolysis reactions and subsequent hydrogenation of these by-products (see Fig. 1). The formation of CO due to decarbonylation is often associated with catalyst poisoning [6, 10, 11, 18]. Because of its stability, it is difficult to hydrogenate the phenyl ring. Only starting from hydrocinnamyl alcohol the phenyl ring can become hydrogenated and result in cyclohexylpropanol [10]. When using hydrogenation catalysts with acidic properties and alcohols as reaction solvent, the formation of acetals as by-product has been observed as well and this often results in a decreasing catalytic activity and/or selectivity [6, 10, 11].

Platinum catalysts are already employed for almost a century for the hydrogenation of cinnamaldehyde [19, 20]. Tuley and Adams described in 1925 that the selectivity to cinnamyl alcohol was enhanced when platinum catalysts were combined with promoters. To that purpose, iron salts were added to the reaction mixture which resulted in a higher selectivity [21]. Addition of alkali metal salts to the reaction system has been described as well [22, 23]. Also bimetallic catalysts resulted in enhanced selectivities towards cinnamyl alcohol. Examples of such promoters are tin [24], germanium [25] and iron [26]. Two mechanisms of promotion have been proposed in literature. (1) The promoter can act as an electron donor

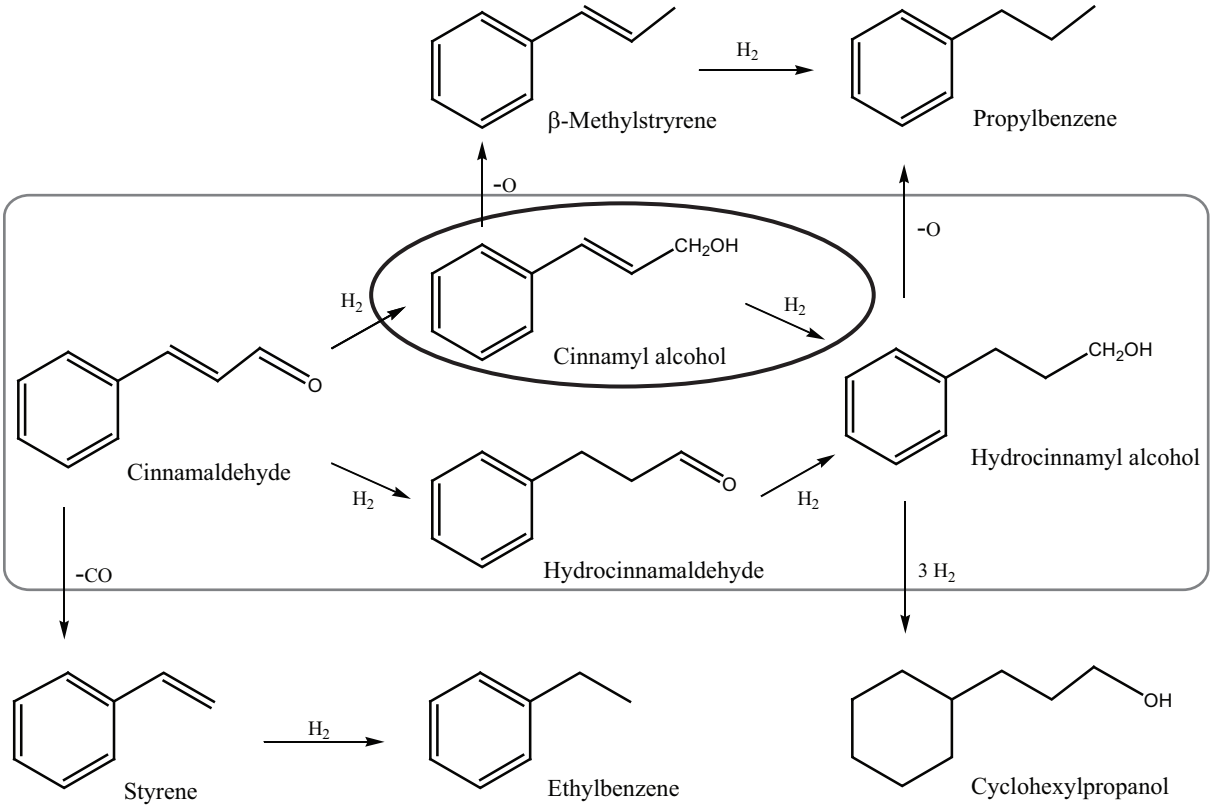

Fig. 1 Reaction scheme of the cinnamaldehyde hydrogenation towards the major hydrogenation products (grey box) together with side-products which can be observed. The desired product, i.e. cinnamyl alcohol, is encircled. Adapted from [10].

thereby increasing the electron density on the catalytic metal. This decreases the adsorption energies, particularly that of the C=C bond thereby favoring C=O bond hydrogenation over C=C bond hydrogenation. (2) The promoter metal oxide interacts with and activates the C=O bond because of its valence state, bringing it into close contact with the catalytic metal and thereby resulting in a higher selectivity [6]. The latter explanation seems to be more adhered in literature [27, 28].

Next to influence of promoters, also metal particle sizes have been reported to affect the selectivity for cinnamaldehyde hydrogenations. Several reports show that larger platinum and ruthenium particles result in a higher selectivity towards cinnamyl alcohol [6, 29-32]. This has been ascribed to phenyl ring repulsion by the catalytic metal. For large metal particles, the C=C bond cannot approach metal surfaces due to this repulsion, while for small metal particles the morphology enables the C=C bond to approach metal surfaces and thus become hydrogenated. Therefore, selectivity towards cinnamyl alcohol is higher for larger metal particles [30].

The applied reaction conditions for the selective hydrogenation of cinnamaldehyde significantly affect the activity and selectivity [6]. In general higher reaction temperatures

result in higher hydrogenation activities. The influence of temperature on selectivity is more complex since both decreasing selectivities as well as constant selectivities have been reported with increasing temperatures [33-35]. It has also been described that increasing hydrogenation pressures resulted in increasing activities combined with decreasing selectivities to cinnamyl alcohol [36] though, depending on the catalyst, the selectivity might also remain constant [27, 33].

Other reaction parameters which affect the selectivity are the reactant concentration and the reaction solvent. High cinnamaldehyde concentrations resulted in enhanced selectivities towards cinnamyl alcohol [36, 37]. When alcohols are used as reaction solvent, higher hydrogenation activities are obtained in general when compared to non-polar solvents [36, 38]. Next to alcohols, also toluene, frequently combined with an aqueous alkaline solution as biphasic system, is used for the cinnamaldehyde hydrogenation to obtain high activities and selectivities [23, 27, 39].

Carbon nanofibers

In general, the advantage of carbon supports is their high surface area and good chemical stability in liquid media. By combustion of carbon supports, reclaim of catalytic metals can be performed easily. Activated carbon is widely used and is often prepared by pyrolysis of natural materials, like wood. Unfortunately, the natural origin results in a wide variety of hetero atoms in the carbon, which may affect the catalytic performance. Moreover these carbons are microporous which increases the risk of diffusion limitations during catalysis [40].

Since the 1980s, nanostructured carbons such as carbon nanofibers (CNF) attracted interest as catalyst support [4, 41, 42]. These carbons consist of graphene layers with different orientations towards the fiber axis. Three orientations are distinguished: carbon nanotubes (CNT) in which the graphene layers are aligned parallel with the central axis, carbon nanoplatelets (CNP) in which the graphene layers are perpendicular with the central axis and carbon nanofibers (CNF) in which the graphene layers are at an angle between 0 and 90 degrees with the central axis (see Fig. 2). Nanostructured carbons are most conveniently prepared by catalytic decomposition of carbon containing gases, e.g. carbon monoxide, methane or ethylene, on metal catalysts, e.g. iron, cobalt or nickel. Variations of these parameters and growth conditions will result in different orientations of the graphene layers, mean fiber diameter, density and surface area [41, 42]. CNF are a very pure, chemically inert material and can be used in acidic or basic reaction media. Moreover, properly prepared CNF skeins are mechanically strong and are therefore suitable as catalyst support [43, 44].

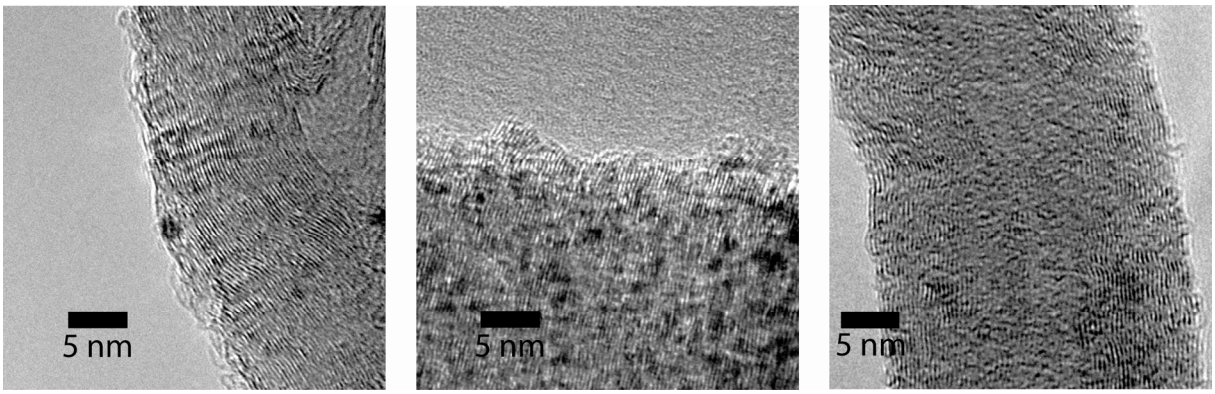

Fig. 2 TEM images of nanostructured carbons: CNF (left image), CNP (middle image) and CNT (right image).

Cost estimations showed that commercial production of CNF at large-scale may result in a cost price of less than 10 US$ per kg [41]. Establishment of companies which produce nanostructured carbons such as FutureCarbon GmbH, Pyrograf Products Inc, Nanocyl, Bayer MaterialScience and Hyperion Catalysis International Inc, shows that commercial production of this type of materials is within reach. Further development of large-scale production combined with good performance as catalyst support may result in industrial application of nanostructured carbons for catalysis in the future [41, 42].

It has been shown that catalytically active metals, such as platinum, palladium, rhodium, iridium, cobalt and nickel, can be deposited on all types of nanostructured carbons. Metals can be deposited directly on the nanostructured carbons using non-aqueous deposition techniques [42]. Via these synthesis techniques, it is believed that metals are anchored on defect sites on the surface of nanostructured carbons [42]. Oxidation of nanostructured carbons in e.g. nitric acid before metal deposition results in the creation of oxygen surface groups, such as carboxylic acid groups, hydroxyl groups, carbonyl groups or ether groups. Wetting of nanostructured carbons by polar solvents is possible due to the presence of these oxygen surface groups and therefore, aqueous synthesis techniques can be applied for oxidized nanostructured carbons. Also (part of) these oxygen surface groups anchor metals during deposition. Moreover, a higher metal dispersion is obtained in general upon oxidation of nanostructured carbons [41, 42, 45, 46]. In our laboratory it has been shown earlier by Toebes et al. [47] that surface oxidation of CNF is required to enable platinum deposition, when aqueous synthesis techniques are employed. Homogeneous deposition precipitation (HDP) turned out to be a suitable synthesis method resulting in metal loadings of at least 3 wt-% and metal particles sizes ranging from 1-3 nm. Platinum on CNF demonstrated a high activity for the cinnamaldehyde hydrogenation [12]. Next to platinum, also ruthenium was deposited on CNF resulting in high metal dispersion and catalytic activity for cinnamaldehyde hydrogenation [47-49].

The catalytic performance of platinum on CNF is affected to a large extent by the presence or absence of oxygen surface groups. It has been demonstrated that after platinum deposition on CNF, the oxygen surface groups could be removed via heat-treatments in inert atmosphere even up to 973 K. Sintering of platinum and a loss of metal dispersion has not been observed [12]. Thus prepared platinum on CNF, i.e. without oxygen surface groups via heat-treatment at 973 K, resulted in a higher activity for the cinnamaldehyde hydrogenation compared to the non heat-treated catalysts, i.e. with oxygen surface groups. The observed cinnamaldehyde hydrogenation activity increased with a factor of 8, while it was calculated that intrinsic reaction rate increased up to a factor of 120 upon heat-treatment at 973 K. Unfortunately, the increase in hydrogenation activity was accompanied by a loss in selectivity towards cinnamyl alcohol. The selectivity towards cinnamyl alcohol decreased from 37% to 8% upon heat-treatment (determined at 60% cinnamaldehyde conversion). The authors concluded that enhanced adsorption of the reactant accounts for the observed increase in hydrogenation activity. They proposed that before heat-treatment, the reactant is repelled from the CNF surface and is therefore hindered to approach the catalytic metal. After heat-treatment, the phenyl ring of the reactant is strongly adsorbed, thereby directing the α,β-unsaturated group towards the catalytic metal and forcing its hydrogenation (see also Fig. 3) [12, 13].

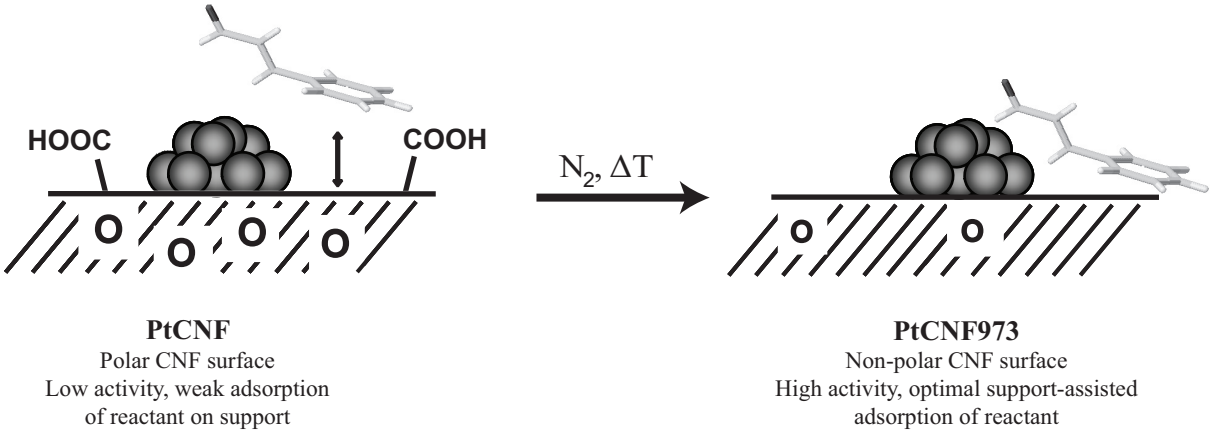

Fig. 3 Repulsion and adsorption of cinnamaldehyde on polar and non-polar catalyst surfaces. Reproduced from [13], with permission from Elsevier.

Scope and outline of this thesis

Aim of the work described in this thesis is to investigate the role of the nature of the CNF support and promoters on platinum based catalysts for the selective hydrogenation of cinnamaldehyde. Precise catalyst synthesis, characterization and testing are essential to arrive at structure-performance relations for this reaction.

In **Chapter 2** an exploratory study on the influence of reaction conditions, in particular solvent effects and concentration effects was performed using heat-treated platinum on CNF catalysts. Next, different elements, i.e. iridium, ruthenium, platinum, palladium and rhodium were deposited on CNF and tested before as well as after heat-treatment to investigate the role of the active phase.

It is known that oxygen surface groups are required to enable platinum deposition on CNF when aqueous synthesis techniques are applied. The influence and type of oxygen surface groups which determine platinum deposition on CNF via HDP, was investigated using XPS and titrations in **Chapter 3**.

Nanostructured carbons display graphene sheets with different orientations towards the fiber axis. In literature it is described that especially on CNT a large variation of deposited metal particles sizes was obtained. This might be associated with the reduction behavior related to the graphene sheet orientation for nanostructured carbons. This was investigated in **Chapter 4.** Platinum was deposited on oxidized nanostructured carbons, i.e. CNF, CNP and CNT and their reducibility was investigated by TPR.

Particle size effects have been described in literature and larger metal particles result in a higher selectivity towards cinnamyl alcohol. Variation of metal particle sizes was sometimes obtained via heat-treatments, but for carbon supports this affects the amount of oxygen surface groups as well. Therefore, particle size effects for platinum and ruthenium on CNF with similar amounts of acidic oxygen surface groups were explored and described in **Chapter 5**. Smaller and larger platinum and ruthenium particles were deposited on CNF via HDP and atomic layer deposition (ALD). The amount of oxygen surface groups on these catalysts was varied via heat-treatments and resulting catalysts were tested for the selective hydrogenation of cinnamaldehyde.

The selectivity towards cinnamyl alcohol for platinum on CNF catalysts was enhanced by combining these catalysts with promoters. The challenge was to create and characterize the platinum-promoter phase in close contact and relate this interaction to the catalytic performance. In **Chapter 6**, CNF-supported platinum was combined with promoters, namely tin and gallium via synthesis under hydrogen atmosphere, referred to as reductive deposition precipitation. A detailed characterization study was executed to relate the extent of platinum-promoter interaction to the catalytic behavior of the catalysts.

In **Chapter 7** a summary of all results described in the preceding chapters is given, together with concluding remarks and suggestions for further research.

Literature

1. J.J. Berzelius, Jahresbuch (translation by F. Wöhler), 15, 1836, 237-245.
2. B. Lindstrom, L.J. Pettersson, CATTECH, 7(4), 2003, 130-138.
3. A.J.B. Robertson, Platinum Metals Rev., 19, 1975, 64-69.
4. R.A. van Santen, P.W.N.M. van Leeuwen, J.A. Moulijn, B.A. Averill, Catalysis: An Integrated Approach, Second, Revised and Enlarged Edition, Elsevier, Amsterdam, 1999.
5. S. Schimpf, J. Gaube, P. Claus, Springer Series in Chemical Physics, 75(Basic Principles in Applied Catalysis), 2004, 87-123.
6. P. Gallezot, D. Richard, Cat. Rev. - Sci. Eng., 40(1-2), 1998, 81-126.
7. R.G. Eilerman, in: R.E. Kirk, D.F. Othmer (Eds.), Concise encyclopedia of chemical technology, 4th ed., Wiley, New York, 1999.
8. K.-G. Fahlbusch, F.-J. Hammerschmidt, J. Panten, W. Pickenhagen, D. Schatkowski, K. Bauer, D. Garbe, H. Surburg, Ullmann's Encyclopedia of Industrial Chemistry, 7th ed., Wiley-VCH, electronic release 2007.
9. P. Claus, Top. Catal., 5(1-4), 1998, 51-62.
10. T. Vergunst, PhD-thesis, Delft University of Technology, Delft, 1999.
11. P. Maki-Arvela, J. Hajek, T. Salmi, D.Y. Murzin, Appl. Catal. A, 292, 2005, 1-49.
12. M.L. Toebes, Y. Zhang, J. Hájek, T.A. Nijhuis, J.H. Bitter, A.J. van Dillen, D.Y. Murzin, D.C. Koningsberger, K.P. de Jong, J. Catal., 226(1), 2004, 215-225.
13. M.L. Toebes, T.A. Nijhuis, J. Hájek, J.H. Bitter, A.J. van Dillen, D.Y. Murzin, K.P. de Jong, Chem. Eng. Sci., 60(21), 2005, 5682-5695.
14. R.A. Sheldon, H. van Bekkum, Fine chemicals through heterogeneous catalysis, Wiley VCH, New York, 2001.
15. H.F. Rase, Handbook of commercial catalysts: heterogeneous catalysts, CRC Press, Boca Raton, 2000.
16. R.G. Eilerman, in: R.E. Kirk, D.F. Othmer (Eds.), Encyclopedia of chemical technology, 4th ed., Wiley, New York, 1993.
17. V. Ponec, Appl. Catal. A, 149(1), 1997, 27-48.
18. P. Maki-Arvela, N. Kumar, K. Eranen, T. Salmi, D.Y. Murzin, Chem. Eng. J., 122(3), 2006, 127-134.
19. G. Vavon, Compt. Rend., 154, 1912, 359-361.
20. A. Skita, Ber. Dtsch. Chem. Ges., 48, 1915, 1685-1698.
21. W.F. Tuley, R. Adams, J. Am. Chem. Soc., 47, 1925, 3061-3068.

22. J.M.A. Dautzenberg, J.M.C.A. Mulders, P.A.M.J. Stijfs, Pat. Appl. US 4247718, Stamicarbon B.V., The Netherlands, 1979.
23. C.G.M. van de Moesdijk, M.A.R. Bosma, Pat. Appl. EP 219905, Stamicarbon B.V., The Netherlands, 1987.
24. Z. Poltarzewski, S. Galvagno, R. Pietropaolo, P. Staiti, J. Catal., 102(1), 1986, 190-198.
25. S. Galvagno, Z. Poltarzewski, A. Donato, G. Neri, R. Pietropaolo, J. Chem. Soc., Chem. Commun., 23, 1986, 1729-1731.
26. D. Goupil, P. Fouilloux, R. Maurel, React. Kinet. Catal. Lett., 35(1-2), 1987, 185-193.
27. W. Koo-amornpattana, J.M. Winterbottom, Catal. Today, 66(2-4), 2001, 277-287.
28. G. Neri, S. Galvagno, Recent Research Developments in Catalysis, 2, 2003, 121-141.
29. D. Richard, P. Fouilloux, P. Gallezot, Proc. Int. Congr. Catal., 9th, 3, 1988, 1074-1081.
30. A. Giroir-Fendler, D. Richard, P. Gallezot, Catal. Lett., 5(2), 1990, 175-182.
31. S. Galvagno, C. Milone, G. Neri, A. Donato, R. Pietropaolo, Stud. Surf. Sci. Catal., 78(Heterogeneous Catalysis and Fine Chemicals III), 1993, 163-170.
32. M. Lashdaf, J. Lahtinen, M. Lindblad, T. Venalainen, A.O.I. Krause, Appl. Catal. A, 276(1-2), 2004, 129-137.
33. J. Hajek, PhD-thesis, Åbo Akademi University, Åbo/Turku, 2004.
34. E. Tronconi, C. Crisafulli, S. Galvagno, A. Donato, G. Neri, R. Pietropaolo, Ind. Eng. Chem. Res., 29(9), 1990, 1766-1770.
35. G. Neri, L. Bonaccorsi, L. Mercadante, S. Galvagno, Ind. Eng. Chem. Res., 36(9), 1997, 3554-3562.
36. M. Shirai, T. Tanaka, M. Arai, J. Mol. Catal. A: Chem., 168(1-2), 2001, 99-103.
37. T. Vergunst, F. Kapteijn, J.A. Moulijn, Catal. Today, 66(2-4), 2001, 381-387.
38. J. Hajek, N. Kumar, P. Maki-Arvela, T. Salmi, D.Y. Murzin, I. Paseka, T. Heikkila, E. Laine, P. Laukkanen, J. Vayrynen, Appl. Catal. A, 251(2), 2003, 385-396.
39. V. Satagopan, S.B. Chandalia, J. Chem. Technol. Biotechnol., 60(1), 1994, 17-21.
40. F. Rodriguez-Reinoso, Carbon, 36(3), 1998, 159-175.
41. K.P. de Jong, J.W. Geus, Cat. Rev. - Sci. Eng., 42(4), 2000, 481-510.
42. P. Serp, M. Corrias, P. Kalck, Appl. Catal. A, 253(2), 2003, 337-358.
43. T.G. Ros, A.J. van Dillen, J.W. Geus, D.C. Koningsberger, ChemPhysChem, 3(2), 2002, 209-214.
44. M.K. van der Lee, A.J. van Dillen, J.W. Geus, K.P. de Jong, J.H. Bitter, Carbon, 44(4), 2006, 629-637.

45. M.K. van der Lee, A.J. van Dillen, J.H. Bitter, K.P. de Jong, J. Am. Chem. Soc., 127(39), 2005, 13573-13582.
46. T.G. Ros, A.J. van Dillen, J.W. Geus, D.C. Koningsberger, Chem. Eur. J., 8(5), 2002, 1151-1162.
47. M.L. Toebes, M.K. van der Lee, L.M. Tang, M.H. Huis in 't Veld, J.H. Bitter, A.J. van Dillen, K.P. de Jong, J. Phys. Chem. B, 108(31), 2004, 11611-11619.
48. M.L. Toebes, F.F. Prinsloo, J.H. Bitter, A.J. van Dillen, K.P. de Jong, Stud. Surf. Sci. Catal., 143, 2002, 201-208.
49. M.L. Toebes, F.F. Prinsloo, J.H. Bitter, A.J. van Dillen, K.P. de Jong, J. Catal., 214(1), 2003, 78-87.

2

Exploratory Study on the Selective Hydrogenation of Cinnamaldehyde

Abstract

In this chapter an exploratory study on the selective hydrogenation of cinnamaldehyde is described. The study focused on solvent effects, cinnamaldehyde concentration effects and the nature of the catalytic metal. It has been found that 2-propanol/water mixture as reaction solvent resulted in optimum activity and selectivity and combined with 0.1 M cinnamaldehyde concentration, catalyst deactivation was not observed. Therefore these are preferred reaction conditions. Moreover, platinum on carbon nanofibers resulted in optimum selectivity combined with reasonable activity and catalyst deactivation is not observed. Therefore, platinum on carbon nanofibers was chosen for further studies.

Introduction

The selective hydrogenation of cinnamaldehyde is relevant for both fundamental and industrial research. In this reaction two different products can be formed in the first step, i.e. cinnamyl alcohol or hydrocinnamaldehyde. Selective formation of cinnamyl alcohol is relevant for chemical industry because of its flavoring properties and its use as intermediate to synthesize drugs [1, 2]. Unfortunately, thermodynamics predict that the route towards hydrocinnamaldehyde is more favored [3, 4]. Therefore the catalyst has to restrict that route kinetically. To achieve that goal, variables at hand are the used catalytic metals and/or catalyst supports as well as the reaction conditions, such as reaction solvent or reactant concentrations [3-7].

The influence of the chemical nature of the catalyst support on cinnamaldehyde hydrogenation was shown by Toebes et al. [8-10] for carbon nanofibers (CNF) supported platinum and ruthenium catalysts. A 120 fold increase in intrinsic activity has been demonstrated by those authors upon removal of the oxygen surface groups from platinum on CNF.

In general, the selectivity for carbon supported catalysts decreased in the following order: Ir > Pt > Ru > Rh > Pd, while the activity increased in the same order [4]. This has been demonstrated for activated carbon and graphite supports, but not for CNF based catalysts containing different amounts of oxygen surface groups. Therefore, the influence of variable amounts of oxygen surface groups, which were tuned via heat-treatments, was studied here for various noble metal catalysts on CNF. Platinum, ruthenium, iridium, rhodium and palladium were deposited on CNF and tested before as well as after heat-treatment.

Selective hydrogenation of cinnamaldehyde is used in this thesis as a showcase. We investigated, and describe here, in advance the role of some of the reaction parameters on the catalytic behavior of heat-treated (i.e. after removal of oxygen surface groups) Pt/CNF. The latter is the catalyst of choice (*supra vide*). These experiments were carried out at fixed temperature (i.e. 313 K) and fixed hydrogenation pressure (1200 mbar). The role of solvent effects and cinnamaldehyde concentration effects on the catalytic behavior of heat-treated Pt/CNF was investigated to determine the optimum hydrogenation activity and selectivity for this catalyst.

Experimental

CNF were prepared using $CO/H_2/N_2$ and a Ni/SiO_2 growth catalyst at 823 K followed by subsequent oxidation as described earlier [11]. Platinum [9] and ruthenium [8] were

deposited on oxidized CNF using homogeneous deposition precipitation (HDP) as described earlier. The obtained catalysts were reduced at 473 K (heating rate 5 K/min) in a H_2/N_2 flow (100 mL/min; 10% v/v) for 1 h and denoted as Pt/CNF and Ru/CNF respectively. Parts of these catalysts were heat-treated at 973 K for 2 h in N_2 flow (heating rate 5 K/min) and the resulting catalysts were denoted as Pt/CNF-973 and Ru/CNF-973.

Atomic layer deposition (ALD) was used to deposit iridium on CNF. Oxidized CNF (2.5 g) were placed in a F-120 reactor system (ASM Microchemistry) and heated to 473 K at a pressure 5-10 mbar. Subsequently, $Ir(acac)_3$ (1.2 g; Volatec; >99%) was evaporated at 453 K in flowing nitrogen and led over the CNF support for at least 3 h to ensure complete reaction. After the reaction, the excess reactants and gaseous by-products were removed by purging the system with nitrogen. The prepared catalysts were reduced at 573 K for 1 h (heating rate 5 K/min) in H_2/N_2 flow (100 mL/min; 10% v/v) and denoted as Ir/CNF. Part of the material was treated at 973 K in N_2 flow for 2 hours (heating rate 5 K/min) and the resulting catalyst was denoted as Ir/CNF-973.

Rhodium was deposited on CNF via incipient wetness impregnation (IWI). Oxidized CNF (6.0 g) were evacuated for 30 min. $Rh(NO_3)_3$ (0.7 g; 10 wt-% Rh in solution; Aldrich) was dissolved in demineralized water to a total mass of 2.5 g. Subsequently, part of this solution (2.1 g) was impregnated on CNF and the resulting material was kept under static vacuum overnight and dried overnight at 393 K. The catalyst was reduced at 423 K for 1 h (heating rate 5 K/min) in H_2/N_2 flow (100 mL/min; 10% v/v) and denoted as Rh/CNF. Part of this material was treated at 973 K for 2 h in N_2 flow (heating rate 5 K/min) and the resulting catalyst was denoted as Rh/CNF-973.

Ion adsorption was used to prepare Pd/CNF as described earlier [12]. The resulting material was reduced at 523 K for 2 h (heating rate 5 K/min) in H_2/N_2 flow and the resulting catalyst was denoted as Pd/CNF. Part of this material was treated at 773 K for 2 h in N_2 flow (heating rate 5 K/min) and the resulting catalyst was denoted as Pd/CNF-773.

Cinnamaldehyde hydrogenation was performed at 313 K and a pressure of 1200 mbar H_2. The hydrogenation set-up consisted of a thermostatic double-walled glass reactor, equipped with baffles and a gas-tight mechanical stirrer with a hollow shaft and blades for gas recirculation. The reactor was loaded with tetradecane as internal standard (4.57 g; Acros; 99%), the catalyst and the solvent (117.5 mL). The amount of catalyst was 1 g (sieve fraction 25-90 μm) for each test reaction. The stirrer was switched on (1700 rpm) and the slurry was saturated with H_2 by repeated pressurizing the system with 1200 mbar H_2 followed by short evacuation of the gasphase. Typically 9-10 of these cycles were performed during 30 min. Next, t-cinnamaldehyde (1.65 g; Acros; p.a.) was added, thereby resulting in a total reaction volume of 125 mL with a cinnamaldehyde concentration of 0.10 M. The

reactions were run in general for 5 hours. Samples were taken at different time intervals and analyzed on a Shimadzu GC 2010 equipped with auto injector, FID detector and CP WAX 52 CB column. The conversion of cinnamaldehyde (CALD) and selectivity to cinnamyl alcohol (CALC) were calculated as described earlier [6]:

$$Conversion(t) = \frac{([CALD(0)] - [CALD(t)])}{[CALD(0)]} \times 100\%$$

$$Selectivity(t) = \frac{[CALC(t)]}{([CALD(0)] - [CALD(t)])} \times 100\%$$

In Table 1 the varied reaction parameters for Pt/CNF-973 are summarized.

The platinum loading was determined by using calibrated X-ray fluorescence spectroscopy (Spectro X-lab 2000). For analysis 2-4 g of the dry catalyst powder was used. The palladium loading was determined using ICP-MS (Agilent 7500a) and the ruthenium loading was determined using ICP-AES (Varian Liberty series II ICP-AES). Each sample was destructed with aqua regia (1:3 mixture of HNO_3: HCl) before ICP analysis. The iridium content of the sample was determined by instrumental neutron activation analysis using a Triga Mk II research reactor [13]. $(NH_4)_2IrCl_6$ was used as a standard and $Ir(acac)_3$ as a control sample. Since impregnation was used, the rhodium content was calculated.

Table 1. Variations of reaction solvents and reactant concentrations.

Solvents		**Concentrations of cinnamaldehyde**
Pt/CNF-973 **0.10 M CALD** **25-90 µm** **1700 rpm**		**Pt/CNF-973** **25-90 µm** **1700 rpm** **2-propanol/water**
2-propanol (100 mL)/water (demineralized; 17.5 mL)		0.01 M CALD
		0.10 M CALD
2-propanol		1.01 M CALD
ethanol		
toluene (78.5 mL)/KOH-water (demineralized 39 mL with 3.9 g KOH) [18]		
toluene		
n-hexane		
tetrahydrofuran (THF)		
dimethylformamide (DMF)		
dimethyl sulfoxide (DMSO)		

Nitrogen physisorption, to determine the BET surface area, was performed at 77 K using a Micromeritics Tristar 3000 V6.04 A. Prior to the physisorption measurements, the samples were dried at 473 K for about 14 hours under nitrogen flow.

TEM was performed on a Tecnai 20 FEG TEM operating at 200 kV and a point resolution of 2.7 Å. The samples were suspended in ethanol using an ultrasonic treatment and brought onto a holey carbon film on a copper grid.

Results and Discussion

Physical properties of the synthesized catalysts

Nitrogen physisorption results showed that the BET surface area of the oxidized CNF batches varied from 153 to 184 m^2/g, which is within the reproducibility range of CNF synthesis.

Metal weight-loadings for the different catalysts are summarized in Table 2 and ranged from 1 to 3 wt-%. Representative TEM images of all catalysts before and after heat-treatment are depicted in Fig. 1. The average particle sizes and particle size ranges based on these TEM measurements are compiled in Table 2 as well. Clearly the particle sizes before heat-treatment were small and varied from 0.8 nm for Rh/CNF to 2.0 nm for Pd/CNF. Significant differences in particle sizes were found after heat treatment. For platinum, ruthenium and iridium only a minor increase in size was observed, while this was more significant for palladium and rhodium.

Investigation of solvent effects using Pt/CNF-973

As depicted in Fig. 2, hydrogenation of cinnamaldehyde (CALD) can result in cinnamyl alcohol (CALC) and hydrocinnamaldehyde (HALD) intermediates and hydrocinnamyl alcohol (HALC) as final product. Selective hydrogenation towards CALC is desired. It has been reported that the solvent can have a significant influence on the activity and selectivity of the reaction, not only for the above mentioned products but also towards for example acetals due to a side reaction with the solvent. For Pt/SiO_2 catalysts, it was found that methanol resulted in the highest reported activity, but also in substantial amounts of acetals and other by-products [14]. For this catalyst, the activity as function of the solvent decreased in the following order: methanol > ethanol > 2-propanol > cyclohexane [14]. For ruthenium-based catalysts it has been reported that 2-propanol resulted in substantially higher activities than hexane or cyclohexane [15].

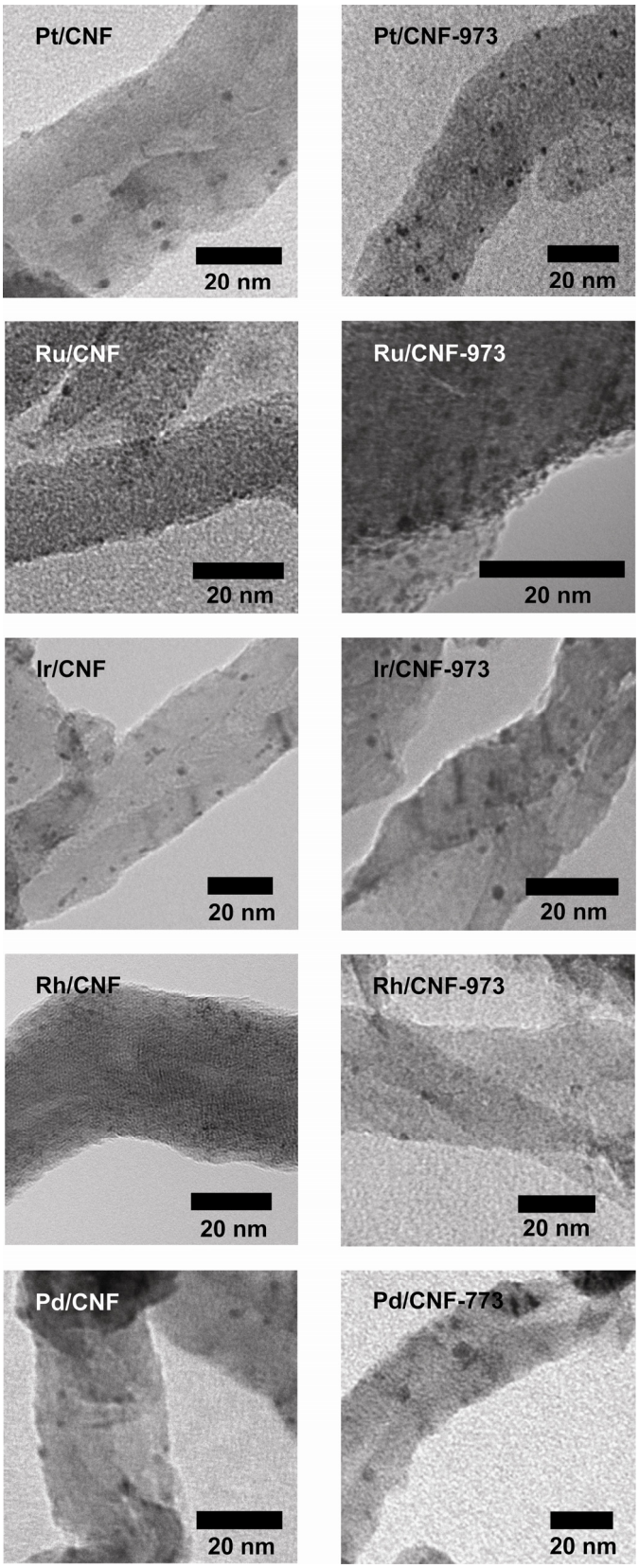

Fig. 1 TEM images of as-reduced and heat-treated CNF supported metal catalysts. The rhodium and palladium catalysts displayed substantial sintering upon heat-treatment, which has not been observed for the other catalysts.

Table 2. Physical properties of the catalysts and their corresponding initial cinnamaldehyde hydrogenation activities.

Non heat-treated catalysts				
Catalyst	**Metal loading (wt-%)**	**Average TEM particle size (nm)**	**TEM particle size range (nm)**	**Initial activity ($mmol.s^{-1}.g_{metal}^{-1}$)**
Pt/CNF	3.0	1.8	1-3	0.17
Ru/CNF	2.1	1.8	1-3	0.25
Ir/CNF	2.5	1.9	1-4	0.06
Rh/CNF	1.0	0.8	0.3-1	1.36
Pd/CNF	1.0	2.0	1-3	2.85
Heat-treated catalysts				
Catalyst	**Metal loading (wt-%)**	**Average TEM particle size (nm)**	**TEM particle size range (nm)**	**Initial activity ($mmol.s^{-1}.g_{metal}^{-1}$)**
Pt/CNF-973	3.0	2.0	1-3	0.21
Ru/CNF-973	2.1	2.2	1-3	0.41
Ir/CNF-973	2.5	2.1	1-4	0.33
Rh/CNF-973	1.0	2.6	1-5	0.41
Pd/CNF-773	1.0	4.1	2-8	1.06

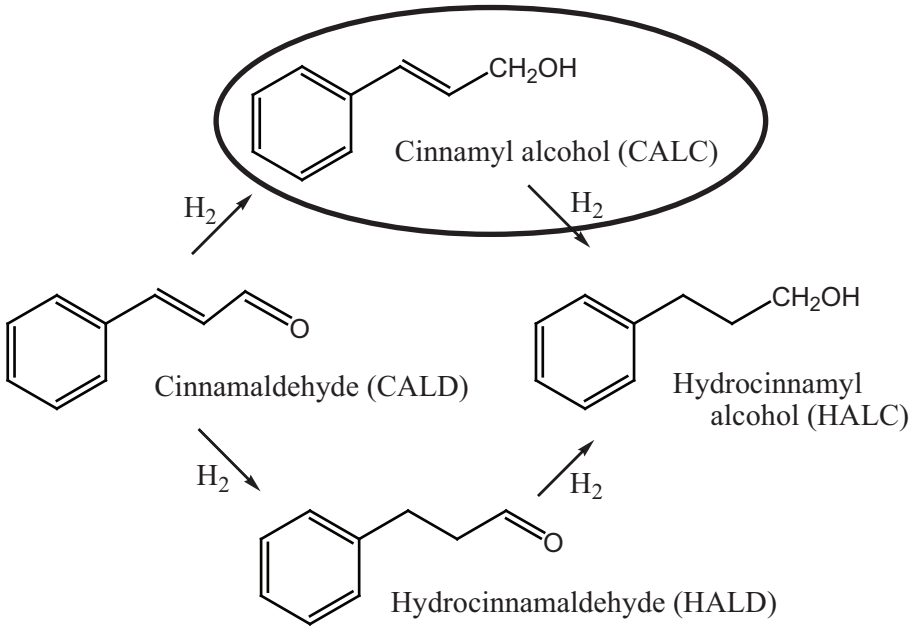

Fig. 2 Hydrogenation pathway of cinnamaldehyde; the desired product is encircled.

Since high hydrogenation activities have been obtained when using alcohols, these are frequently used as solvents. However the main drawback of the use of alcohols, especially in combination with acidic catalysts, is the formation of acetals as by-products, which deactivate the catalyst [7]. Acetal formation can be prevented by using non-alcoholic solvents [4, 15]. In addition, the equilibrium of the acetal formation, which is accompanied by water formation, can be driven to the aldehyde side by using alcohol-water mixtures as solvent [16].

Next to alcohols, also toluene and toluene/base-solutions (KOH) have been studied frequently. The latter biphasic system boosted the CALD hydrogenation activity and selectivity when compared to pure toluene [17-19].

To investigate the optimum activity and selectivity under the conditions applied in our studies, the influence of different solvents was investigated using Pt/CNF-973 as catalyst and 2-propanol/water, 2-propanol, ethanol, toluene, toluene/KOH in water, hexane, THF, DMF or DMSO as solvent (see also Table 1 for additional details).

After 90 min of reaction time, the sequence in hydrogenation activity is: toluene/KOH in water ≥ 2-propanol/water > ethanol ≥ 2-propanol > hexane ≥ THF > toluene > DMF >> DMSO (Fig. 3). The activity in DMSO was insignificant and therefore omitted in the further discussion. In Table 3 the resulting selectivities at 50% CALD conversion are summarized and 2-propanol/water resulted in the highest selectivity towards CALC.

When using hexane, THF, toluene or DMF, formation of by-products is negligible. Toluene/KOH in water, 2-propanol/water, ethanol and 2-propanol resulted in 0.7%, 1.3%, 2.1% and 2.6% by-products respectively. These by-products were mainly β-methylstyrene and propylbenzene. In addition, for 2-propanol and ethanol respectively 0.6% and 0.3% of acetals were found. The formation of larger amounts of by-products, in particular acetals, might affect the performance of the catalyst and therefore explains the lower observed activity for ethanol and 2-propanol when compared to 2-propanol/water [7].

Based on this study it was decided to use 2-propanol/water as solvent due to the high activity and selectivity observed, absence of acetal formation and its easy handling.

Concentration effects

It has been described that increasing CALD concentrations resulted in enhanced selectivities towards CALC [14, 20]. This concentration effect has been attributed to a self-assembling effect of the phenyl groups at higher concentrations thereby forcing adsorption and reaction of the aldehyde group [20, 21].

Table 3. Observed selectivities to cinnamyl alcohol for variable reaction solvents using Pt/CNF-973 catalyst.

Solvent	Selectivity at 50% CALD conversion
2-Propanol/water	59
2-Propanol	54
Ethanol	45
Toluene/KOH-water	48
Toluene	40% → at 30% CALD conversion
n-Hexane	40
Tetrahydrofuran (THF)	41
Dimethylformamide (DMF)	18-27% → not stable during reaction
Dimethyl sulfoxide (DMSO)	0

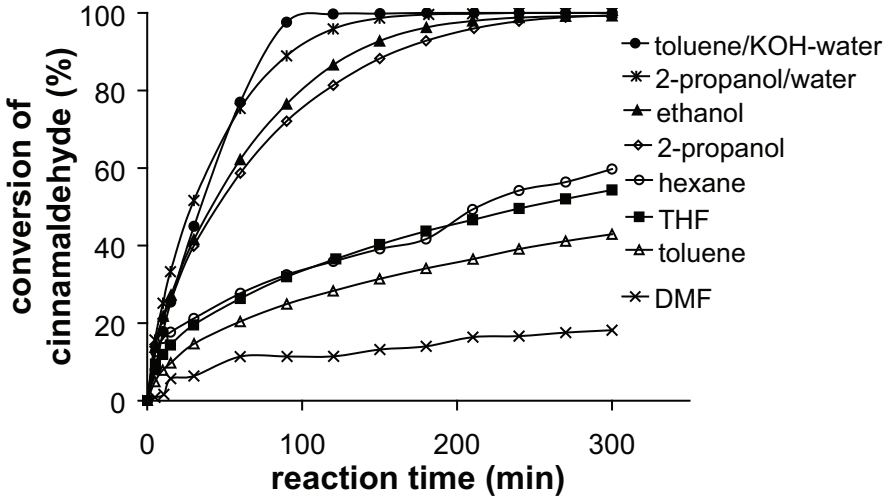

Fig. 3 Activity of Pt/CNF-973 for cinnamaldehyde hydrogenation using various solvents (0.1 M CALD, 1 g catalyst, 1200 mbar H_2, 313 K).

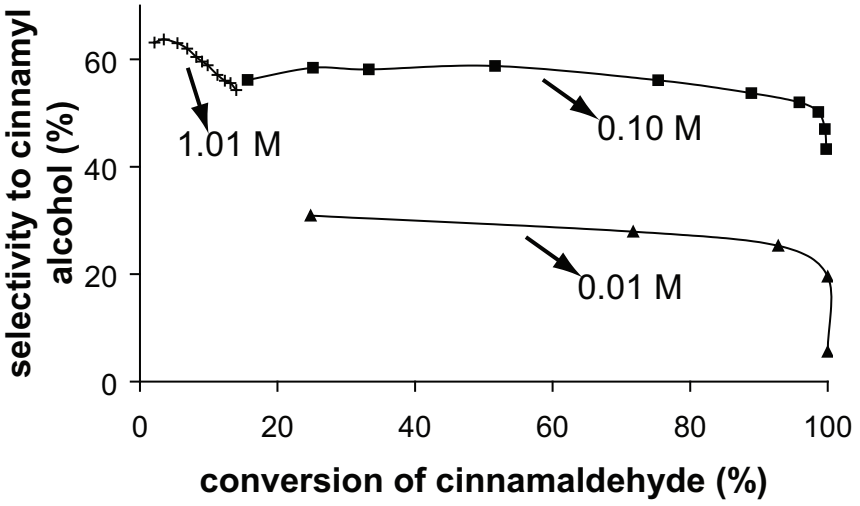

Fig. 4 Conversion vs. selectivity plots at variable cinnamaldehyde concentrations for Pt/CNF-973 (2-propanol/water solvent, 1 g catalyst, 1200 mbar H_2, 313 K).

To investigate concentration effects under the conditions applied here, CALD concentrations of 0.01 M (low), 0.10 M (medium) and 1.01 M (high) were employed. Pt/CNF-973 was used as catalyst and reactions were performed in 2-propanol/water. Conversion versus selectivity plots are presented in Fig. 4. Clearly, the initial selectivities towards CALC increased with increasing concentration. For the low and medium concentrations the selectivity remained invariant with conversion (up to 95% conversion), while for the highest concentration the selectivity decreased already at lower conversions (10% conversion). This selectivity decrease might be associated with observed deactivation at this reactant concentration. Only for the test reaction at high reactant concentration, acetal formation (0.04%) is observed and this is often associated with catalyst deactivation and decreasing selectivities [7]. This might explain the observed activity and selectivity behavior.

We decided to use a reactant concentration of 0.10 M in the further experiments, since catalyst deactivation was not observed.

Different elements

To investigate the influence of the nature of the metal, all catalysts before and after heat-treatment were tested for the CALD hydrogenation in 2-propanol/water. Initial hydrogenation activities are compiled in Table 2. For the non-heat treated samples, the initial metal weight based activities decreased in the following sequence: Pd > Rh > Ru > Pt > Ir (Table 2; Fig. 5). The selectivity as function of conversion for these catalysts is displayed in Fig. 6. The selectivity decreased as follows: Ir > Ru > Rh > Pt >> Pd. Pd/CNF did not result in any CALC formation and is therefore not included in Fig. 6.

After heat-treatment the order in initial metal weight based activity changed to Pd > Rh ≈ Ru > Ir > Pt (Table 2, Fig. 7). Please, note that in Fig. 7 Rh/CNF-973 resulted in the lowest activity, which is not reflected in Table 2. This is due to the fact that in Table 2 the activity per gram of metal is reported while Fig. 7 reflects the activity per gram of catalyst.

A decrease in activity is observed for the palladium and rhodium catalysts after heat-treatment, but platinum, ruthenium and iridium resulted in an increasing activity after heat-treatment. For platinum and ruthenium this increase in activity upon heat-treatment has been reported earlier and has been ascribed to an increased coverage of the heat-treated, i.e. non-polar, catalyst surface by the reactant [8-11]. We believe that this is also the case for the iridium catalyst here. The decreasing hydrogenation activity observed for palladium and rhodium is ascribed to substantial sintering, thus loss of active metal surface, of these metals after heat-treatment as observed using TEM (Table 2).

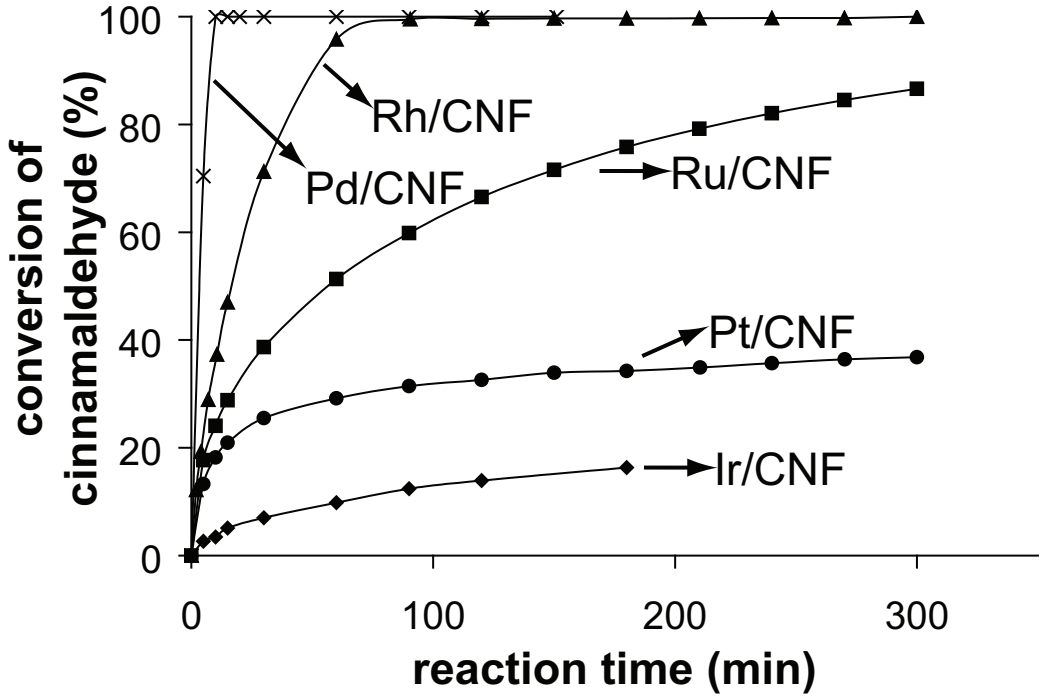

Fig. 5 Activity for cinnamaldehyde hydrogenation as observed for various non heat-treated catalysts (2-propanol/water solvent, 0.1 M CALD, 1 g catalyst, 1200 mbar H_2, 313 K).

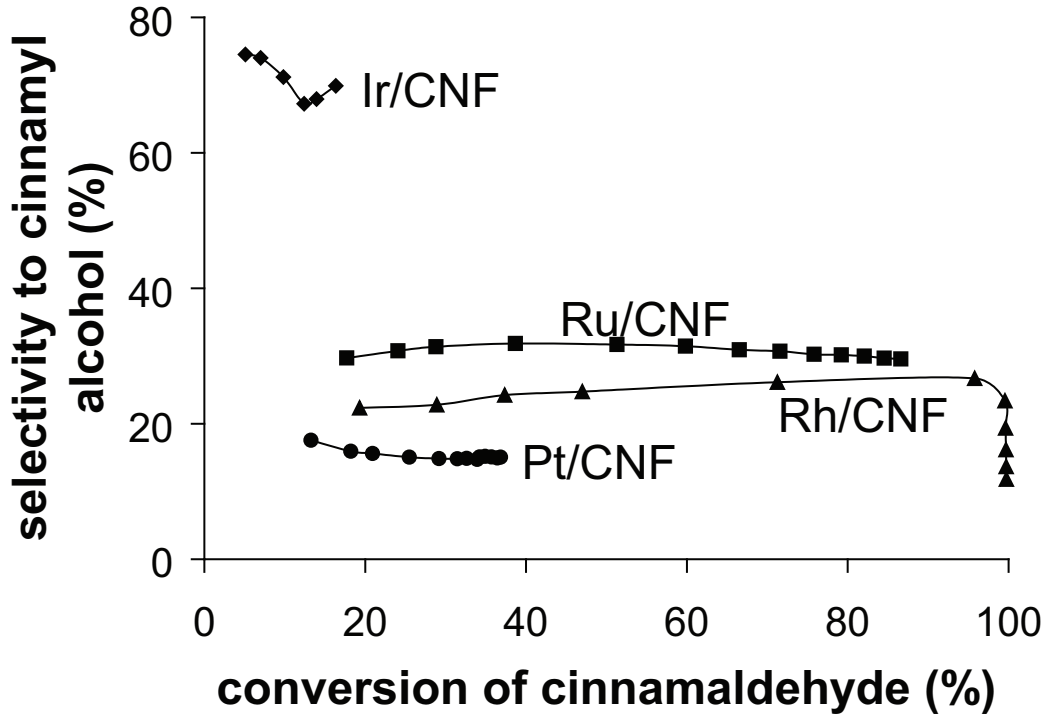

Fig. 6 Conversion vs. selectivity plots as observed for non heat-treated catalysts (2-propanol/water solvent, 0.1 M CALD, 1 g catalyst, 1200 mbar H_2, 313 K).

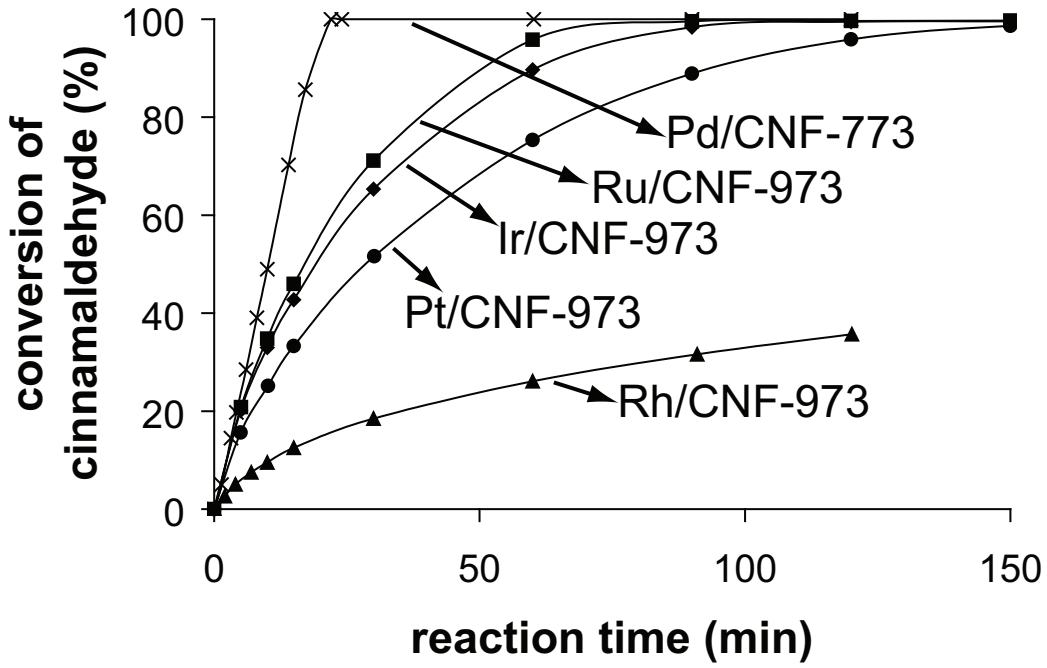

Fig. 7 Activity for cinnamaldehyde hydrogenation as observed for various heat-treated catalysts (2-propanol/water solvent, 0.1 M CALD, 1 g catalyst, 1200 mbar H_2, 313 K).

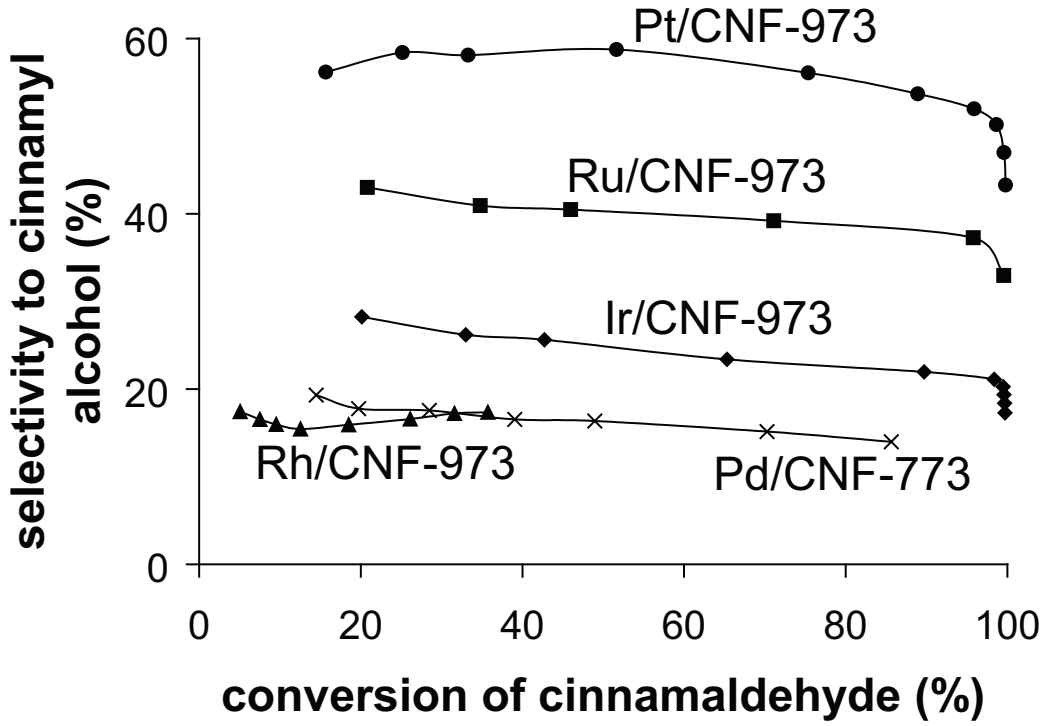

Fig. 8 Conversion vs. selectivity plots as observed for heat-treated catalysts (2-propanol/water solvent, 0.1 M CALD, 1 g catalyst, 1200 mbar H_2, 313 K).

When the conversion of CALD is plotted versus selectivity towards CALC (Fig. 8), it is observed that the selectivity of the heat-treated samples decreased in the sequence Pt > Ru > Ir > Pd ≈ Rh. When comparing these selectivities with those of the untreated samples (Fig. 6) it is clear that the selectivity for platinum, ruthenium and palladium was enhanced, while for rhodium and iridium the selectivity decreased upon heat-treatment. Selectivity enhancement for platinum on CNF catalysts under these reaction conditions has been observed earlier and the selectivity behavior of the ruthenium and palladium catalysts is in line with those results [11]. The opposite trend for the rhodium and iridium catalysts is not explained yet.

Heat-treated platinum on CNF combined the highest selectivity with reasonable activity, while deactivation was not observed. Therefore, we decided to use platinum on CNF for further studies.

Conclusions

Based on an exploratory study we decided to investigate in this thesis platinum on CNF in more detail for the hydrogenation of cinnamaldehyde. Cinnamaldehyde concentration of 0.1 M combined with 2-propanol/water solvent are preferred for testing, since full cinnamaldehyde conversion and optimum selectivity to cinnamyl alcohol are obtained.

Literature

1. K.-G. Fahlbusch, F.-J. Hammerschmidt, J. Panten, W. Pickenhagen, D. Schatkowski, K. Bauer, D. Garbe, H. Surburg, Ullmann's Encyclopedia of Industrial Chemistry, 7th ed., Wiley-VCH, electronic release 2007.
2. H.F. Rase, Handbook of commercial catalysts: heterogeneous catalysts, CRC Press, Boca Raton, 2000.
3. S. Schimpf, J. Gaube, P. Claus, Springer Series in Chemical Physics, 75(Basic Principles in Applied Catalysis), 2004, 87-123.
4. P. Gallezot, D. Richard, Cat. Rev. - Sci. Eng., 40(1-2), 1998, 81-126.
5. V. Ponec, Appl. Catal. A, 149(1), 1997, 27-48.
6. T. Vergunst, PhD-thesis, Delft University of Technology, Delft, 1999.
7. P. Maki-Arvela, J. Hajek, T. Salmi, D.Y. Murzin, Appl. Catal. A, 292, 2005, 1-49.
8. M.L. Toebes, F.F. Prinsloo, J.H. Bitter, A.J. van Dillen, K.P. de Jong, J. Catal., 214(1), 2003, 78-87.

9. M.L. Toebes, Y. Zhang, J. Hájek, T.A. Nijhuis, J.H. Bitter, A.J. van Dillen, D.Y. Murzin, D.C. Koningsberger, K.P. de Jong, J. Catal., 226(1), 2004, 215-225.
10. M.L. Toebes, T.A. Nijhuis, J. Hájek, J.H. Bitter, A.J. van Dillen, D.Y. Murzin, K.P. de Jong, Chem. Eng. Sci., 60(21), 2005, 5682-5695.
11. A.J. Plomp, H. Vuori, A.O.I. Krause, K.P. de Jong, J.H. Bitter, Appl. Catal. A, 351(1), 2008, 9-15.
12. H. Markus, A.J. Plomp, P. Maki-Arvela, J.H. Bitter, D.Y. Murzin, Catal. Lett., 113(3-4), 2007, 141-146.
13. G.N. Eby, Annual Meeting Program with Abstracts, p. 21, Invited paper for National Organization of Test, Research, and Training Reactors, 2008.
14. M. Shirai, T. Tanaka, M. Arai, J. Mol. Catal. A: Chem., 168(1-2), 2001, 99-103.
15. J. Hajek, N. Kumar, P. Maki-Arvela, T. Salmi, D.Y. Murzin, I. Paseka, T. Heikkila, E. Laine, P. Laukkanen, J. Vayrynen, Appl. Catal. A, 251(2), 2003, 385-396.
16. A.B. da Silva, E. Jordao, M.J. Mendes, P. Fouilloux, Appl. Catal. A, 148(2), 1997, 253-264.
17. C.G.M. van de Moesdijk, M.A.R. Bosma, Pat. Appl. EP 219905, Stamicarbon B.V., The Netherlands, 1987.
18. V. Satagopan, S.B. Chandalia, J. Chem. Technol. Biotechnol., 60(1), 1994, 17-21.
19. W. Koo-amornpattana, J.M. Winterbottom, Catal. Today, 66(2-4), 2001, 277-287.
20. T. Vergunst, F. Kapteijn, J.A. Moulijn, Catal. Today, 66(2-4), 2001, 381-387.
21. R.J. Berger, E.H. Stitt, G.B. Marin, F. Kapteijn, J.A. Moulijn, CATTECH, 5(1), 2001, 30-60.

3

On the Nature of Oxygen-Containing Surface Groups on Carbon Nanofibers and their Role for Platinum Deposition

Abstract

XPS and titrations were used to investigate the nature and stability of oxygen-containing surface groups on carbon nanofibers (CNF) and platinum-containing CNF. During heat-treatments in inert atmosphere at 973 K all acidic (carboxylic) oxygen surface groups were removed. Introduction of platinum decreased the temperature at which the acidic oxygen surface groups could be removed to 773 K. The role of oxygen surface groups in the synthesis of platinum on CNF when prepared via homogeneous deposition precipitation has been evaluated. It has been demonstrated that both carboxyl and phenol surface groups are able to bring about platinum ion adsorption during synthesis.

Introduction

Carbon nanofibers (CNF) display considerable potential as catalyst support materials [1, 2]. To obtain highly dispersed platinum on CNF catalysts when prepared using wet chemical (aqueous) techniques, it is essential to perform an oxidative treatment of the CNF surface in advance, for example in concentrated nitric acid [2, 3]. That treatment introduces oxygen-containing groups on the surface of CNF which may function as anchoring sites for metal deposition [2, 3].

Van der Lee et al. [4] showed that carboxylic acid surface groups are required to obtain highly dispersed nickel on CNF when prepared via homogeneous deposition precipitation (HDP). On these surface groups nickel ions adsorb which is followed by nucleation and growth of remaining nickel ions as a hydroxide phase during the pH increase.

It is known that deposition of platinum via HDP does not result in the formation of a hydroxide phase [3]. Thus the mechanism of platinum deposition must be different compared to nickel deposition. It has been described by Toebes et al. [3] that a pH-induced ion adsorption takes place during HDP synthesis for platinum on CNF. Based on titrations it was concluded that acidic oxygen-containing surface groups were essential for metal-ion adsorption. However the nature of these oxygen surface groups remains unresolved.

Therefore, in this study we investigated which types of oxygen surface groups are present on oxidized CNF before as well as after heat-treatment and their platinum loaded equivalents. This approach will lead, next to a general characterization of the oxygen surface groups present on CNF, to insights in the role of the different oxygen surface groups for platinum deposition. To investigate the nature of oxygen surface groups, XPS and acid-base titration studies for CNF and Pt/CNF catalysts were performed.

Experimental

The Ni/SiO_2 (20 wt-% nickel) growth catalyst was prepared via HDP using 17.0 g silica (Degussa, Aerosil 200), 21.1 g nickel nitrate hexahydrate (Acros; 99%) and 13.9 g urea (Acros; p.a.) in 1 L demineralized water according to an earlier described procedure [5]. CNF were grown from $CO/H_2/N_2$ at 823 K using Ni/SiO_2 as reported earlier [6]. The resulting CNF material (30 g) was collected and refluxed three times for 1 h per reflux in aqueous KOH solution (1 M; 0.6 L; Merck; p.a.) to remove the SiO_2. Subsequently, the material was refluxed two times for 1 h per reflux in concentrated nitric acid (0.6 L; Merck; 65%) to remove exposed nickel and introduce oxygen surface groups on the CNF surface. Finally, the

material was washed three times with demineralized water and dried overnight at 393 K. This sample is denoted as CNF-ox.

On part of CNF-ox the carboxylic acid surface groups were converted to phenol groups as described by Van der Lee et al. [4]. $LiAlH_4$ (1.36 g; Acros; 95%) was dissolved in dry THF (135 mL) and after filtration added to dry CNF-ox (8.0 g). After stirring for 20 hours, filtration and washing with dry THF, the sample was washed with demineralized water to protonate the alkoxide ions. All aforementioned steps were performed under argon conditions. The resulting material was washed for 1 h in an aqueous HCl solution (Merck; 250 mL; 1 M) to remove possible remaining metal oxides/alkoxides, washed again with demineralized water afterwards, dried overnight at 393 K and denoted as CNF-OH.

Platinum was deposited on CNF-ox using HDP (intended metal loading 5 wt-%) as described earlier [3, 7]. To that purpose, an acidified suspension (pH 3; 250 mL demineralized water) of CNF-ox (5 g) was stirred and heated to 363 K under inert atmosphere and subsequently urea (0.41 g; Acros) and $Pt(NH_3)_4(NO_3)_2$ (0.52 g; Aldrich) were added. After 18 h, the final pH of the slurry was 6.5 – 7 and the material was filtered, washed with demineralized water, dried overnight at 393 K and reduced at 473 K for 1 h (ramp 5 K/min) in H_2/N_2 (100 mL/min; 10% v/v). The resulting catalyst was denoted as Pt/CNF. Part of this catalyst was treated in N_2-flow at 773 K or 973 K for 2 hours (5 K/min) to remove the oxygen surface groups [7]. The resulting catalysts are denoted as Pt/CNF-773 or Pt/CNF-973.

Platinum catalysts (intended metal loading 5 wt-%) were also prepared on CNF-OH using HDP as described earlier [3, 7]. To that purpose, an acidified suspension (pH 3; 250 mL demineralized water) of CNF-OH (1 g) was stirred and heated to 363 K under inert atmosphere and subsequently urea (0.41 g; Acros) and $Pt(NH_3)_4(NO_3)_2$ (0.10 g; Aldrich) were added. After 18 h, the final pH of the slurry was 6.5 – 7 and the material was filtered, washed with demineralized water, dried overnight at 393 K and reduced at 473 K for 1 h (ramp 5 K/min) in H_2/N_2 (100 mL/min; 10% v/v). The resulting material was denoted as Pt/CNF-OH.

Non-metal containing CNF-ox was also reduced at 473 K for 1 h (ramp 5 K/min) in H_2/N_2 (100 mL/min; 10% v/v) and denoted as CNF-red. Non-metal containing CNF-ox was heat-treated in N_2-flow at 773 K or 973 K for 2 hours (5 K/min) as well to remove the oxygen surface groups and denoted as CNF-773 or CNF-973.

The metal weight-loading of the samples was determined using ICP-OES. The measurements were performed using a SPECTRO CIROS^{CCD} ICP-Spectrometer. Each sample was destructed by heating in aqua regia (1:3 mixture of HNO_3: HCl) before analysis.

XPS was performed using a modified LHS/SPECS EA200 MCD system equipped with XPS (radiation source: Mg Kα 1253.6 eV and 168 W power). Fixed analyser pass

energy of 48 eV was used resulting in a resolution of 0.9 eV FWHM of the Ag $3d_{5/2}$ intensity. The binding energy scale was calibrated using Au $4f_{7/2}$ = 84.0 eV and Cu $2p_{3/2}$ = 932.67 eV. The base pressure of the UHV analysis chamber was 1.5 x 10^{-10} mbar. The sample was mounted on a stainless steel sample holder. To obtain O/C atomic ratios, Shirley backgrounds were subtracted from the experimental data and empirical cross sections were used [8, 9].

The O1s peaks were, before peak deconvolution, normalized at the C1s peak position. It is assumed that the C1s peak will remain unaltered upon the different synthesis methods and treatments applied, since all CNF were graphite-like material. Moreover, all samples originate from the same CNF batch. Peak deconvolution (Gaussian distribution) was performed using Peakfit V4.12 of Systat Software.

Acid-base titrations were performed using a Titralab TIM 880 apparatus. To 60 mL of 0.1 M KCl 0.05 g of the material of interest was added. A solution of 0.01 M NaOH and 0.1 M KCl was used as titrant. The total titrant consumption at pH 5 and at pH 7.5 was used to calculate respectively the amount of strong acidic groups and the total amount of acidic groups on the catalysts [4, 10].

Nitrogen physisorption measurements were performed at 77 K using a Micromeritics Tristar 3000 V6.04 A. The obtained data were used to calculate the BET surface area. Prior to the physisorption measurements, the samples were dried at 473 K for about 14 hours under nitrogen flow.

TEM was performed using a Tecnai 20 FEG operating at 200 kV and a point resolution of 2.7 Å. The samples were suspended in ethanol using an ultrasonic treatment and brought onto a holey carbon film on a copper grid.

Table 1. Physical properties of the catalyst.

Catalyst	**Metal loading (wt-%)**	**Average metal particle size (nm based on TEM)**	**Titrated mmol acidic groups/g (pH 5)**	**Titrated mmol acidic groups/g (pH 7.5)**	**O/C atomic ratio**
CNF-ox	-	-	0.16	0.22	0.082
CNF-red	-	-	0.13	0.18	0.071
CNF-OH	-	-	0.04	0.10	0.071
CNF-773	-	-	0.02	0.04	0.049
CNF-973	-	-	0.00	0.00	0.017
Pt/CNF	2.9	1.8	0.02	0.05	0.045
Pt/CNF-773	2.9	1.9	0.00	0.00	0.036
Pt/CNF-973	2.9	2.0	0.00	0.00	0.012
Pt/CNF-OH	1.4	1.9	n.d.	n.d.	n.d.

n.d. = not determined

Results and Discussion

BET surface areas were 179 m^2/g for CNF-ox and 177 m^2/g for CNF-OH with a mesopore volume of 0.26 ml/g. No micropores were found.

The platinum loading after metal deposition was 2.9 wt-% except for Pt/CNF-OH which contained only 1.4 wt-% platinum (Table 1). The platinum particle size was determined for all samples using TEM and representative images of Pt/CNF-773 and Pt/CNF-OH are depicted in Fig. 1. Histograms of the particle size distributions were compiled for all samples (Fig. 2). The particle size range for Pt/CNF, Pt/CNF-773 and Pt/CNF-973 was 1-3 nm with an average of 1.8 nm for Pt/CNF, 1.9 nm for Pt/CNF-773 and 2.0 nm for Pt/CNF-973 (Table 1). For Pt/CNF-OH the particle size range was broadened to 1-4 nm though still with an average of 1.9 nm (Table 1). Therefore we concluded that, given the experimental uncertainties, the platinum particle size was similar on all samples.

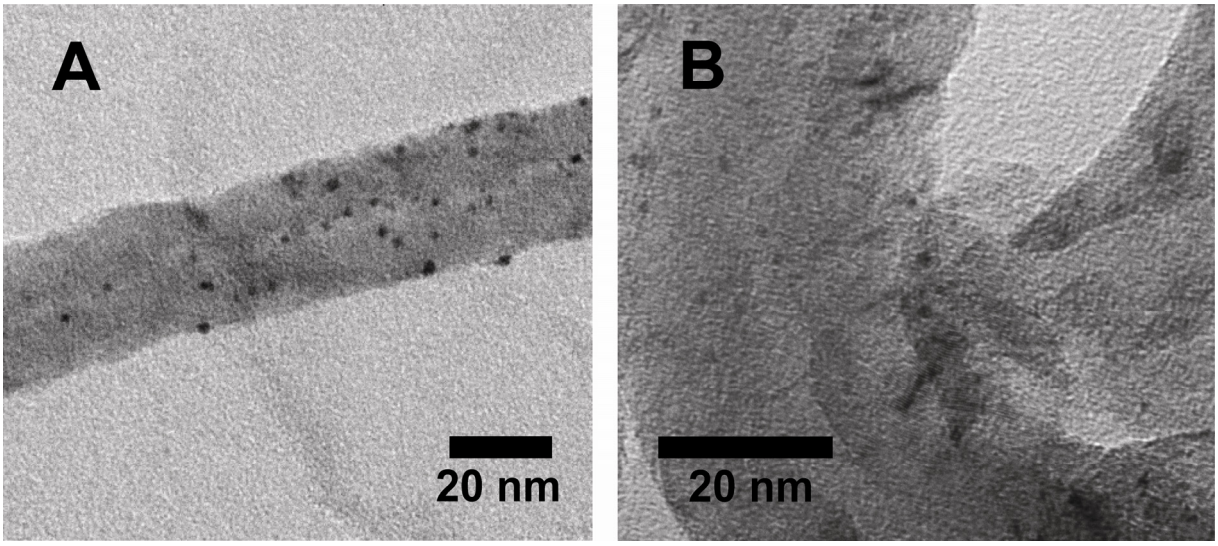

Fig. 1 Representative TEM images of A) Pt/CNF-773 and B) Pt/CNF-OH.

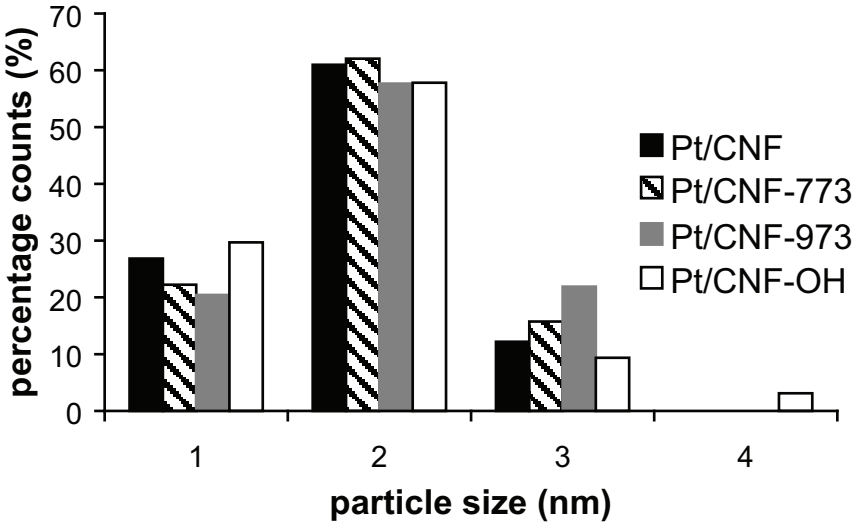

Fig. 2 TEM particle size histograms of Pt/CNF, Pt/CNF-773, Pt/CNF-973 and Pt/CNF-OH.

The acidic properties of oxygen surface groups on oxidized CNF-materials were determined using acid-base titrations [11]. Since it was claimed for nickel deposition that carboxyl groups were required, we summarized in Table 1 the amount of acidic groups at a titrant consumption at pH=5 to establish the number of carboxylic acid surface groups [4]. In addition, the titrant consumption to reach pH 7.5 was used to determine the total amount of acidic oxygen surface groups [4, 10]. For CNF-ox and CNF-red the majority of the groups present consists of carboxylic acid surface groups (pH<5). For the non-metal containing materials, i.e. CNF-ox, CNF-red, CNF-773 and CNF-973 a strong decrease of the amount of acidic oxygen surface groups was found with increasing severity of the heat-treatment. Treatment at 973 K resulted in complete decomposition of acidic groups to CO, CO_2 and H_2O [10].

Platinum deposition and subsequent reduction resulted in larger removal of acidic groups going from CNF-ox to Pt/CNF, when compared to going from CNF-ox to CNF-red. Thus the decrease in oxygen surface groups going from CNF-ox to Pt/CNF must be induced by deposition and subsequent reduction of platinum. It has been described in literature that during reduction of platinum on carbon supports, hydrogen might be dissociated on the metal and migrated onto the support. This reactive hydrogen might assist in decomposition of oxygen surface groups to CO, CO_2 and H_2O [12]. Going from CNF-ox to Pt/CNF, 0.17 mmol acidic groups/g were removed using the titration results up to pH 7.5, while titration results up to pH 5 showed that 0.14 mmol acidic groups/g were removed. It is therefore concluded that the majority of the removed groups were carboxylic acid groups.

Heat-treatment in N_2-flow of Pt/CNF at 773 K resulted in complete removal of the acidic groups. For non-metal containing materials the temperature had to be increased to 973 K (i.e. CNF-973) to remove all acidic groups (Table 1). This clearly shows the assisting role of platinum in the decomposition of acidic oxygen surface groups.

Treatment of CNF-ox with $LiAlH_4$, thus producing CNF-OH, resulted in a decrease of the total amount of acidic groups (up to pH=5) on the CNF surface (Table 1). This is expected since this treatment converts carboxylic acid surface groups towards phenol groups. The total amount of titrated groups is decreasing as well indicating that oxygen surface groups are removed upon the $LiAlH_4$-treatment which is in agreement with results of Van der Lee et al. [4].

In addition to titrations, also XPS was used to study the nature of the oxygen surface groups on the different samples. The advantage of XPS is that also non-acidic surface groups and subsurface oxygen-containing groups (i.e. 1-2 nm below the surface) can be analyzed. Via peak deconvolution of the O1s peak the amount and nature of the different oxygen surface groups can be established [11, 13-15]. Peak deconvolution of the XPS binding

energies are influenced by the somewhat arbitrary inputs for the number, shape and width of the peaks [11]. As will be discussed later for the individual samples, XPS peaks obtained in this research showed clearly three different contributions in the O1s region and therefore peak deconvolution into these three contributions is applied. Several authors in literature describe the O1s deconvolution in two or three peaks and a summary is made in Table 2 [13, 14, 16-18]. Distinction is made between carbonyl groups (peak 1: 530 - 531.5 eV), phenol and/or ether groups (peak 2: 532.5 - 533.1 eV) and chemisorbed water and/or O_2 (peak 3: 534.8 - 535.8 eV). Some authors, who resolved the O1s peak in four components, agreed with the positions of carbonyl and phenol groups bonded to aromatic systems, but resolved at 533.1-533.8 eV ether oxygen atoms in esters and anhydrides and attributed the fourth position, i.e. peak 3 here, to oxygen atoms in carboxyl groups [15, 19]. The published binding energies for carbonyl and phenol/ether groups are in line with the reference spectra of polymers measured by Louette et al. [20-22] for poly(vinyl alcohol), poly(ether ether ketone) and poly(vinyl butyral). The limitations of comparing polymers with oxygen surface groups on carbon is stressed here as well: the absolute binding energy for oxygen in poly(acroleine) (532.65eV) is not in agreement with the expected binding energy (530 - 531.5 eV) [23]. Such discrepancies upon comparison of absolute binding energies for oxygen functionalities on carbon and oxygen functionalities on polymers were already observed by Proctor et al. [16]. Still, the trend observed for e.g. poly(ether ether ketone) show that binding energies for ether-type bonded oxygen (533.40 eV) and carbonyl bonded oxygen (531.31 eV) are well separated, which is therefore used in this study.

The resulting O/C atomic ratios are compiled in Table 1. Heat-treatment of the CNF-materials resulted in a decreasing amount of oxygen surface groups which is in agreement with the titration results.

Deposition of platinum and subsequent reduction in hydrogen (i.e. Pt/CNF) resulted also in a lower amount of oxygen surface groups present when compared to CNF-red. Heat-treatment of the platinum-containing CNF samples revealed the same trends as observed by titrations, i.e. a lower amount of oxygen surface groups is present on the platinum-containing materials when compared to the non-metal containing CNF samples which were heat-treated under similar conditions.

Table 2. Comparison of peak positions for XPS O1s deconvolutions.

	Peak 1 C=O	**Peak 2 C-OH/ C-O-C**	**Peak 3 chem. H_2O/O_2**
Proctor (1983) [16]	531.5	533	--
Schlögl (1983) [17]	530	533	535
Stöhr (1991) [18]	531	533	--
Gardner (1995) [14]	531.2-531.6	532.8-533.1	535.4-535.8
Biniak (1997) [13]	530.4-530.8	532.4-533.1	534.8-535.6

$LiAlH_4$ reduction (i.e. CNF-OH) resulted in removal of oxygen surface groups as well when compared to CNF-ox. The XPS results observed here, i.e. removal of oxygen surface groups upon heat-treatment, platinum deposition/reduction and $LiAlH_4$ reduction, are in line with the titration results, though the latter technique is only limited to accessible acidic oxygen surface groups.

As described earlier, peak deconvolution of the O1s scan may reveal more information about the amount and nature of the different oxygen surface groups. To that purpose, the measured O1s scans using XPS were normalized at the C1s peak position and compared to each other in Fig. 3. Peak deconvolution for the O1s signals was performed into three contributions. For three representative examples i.e., CNF-ox, CNF-OH and Pt/CNF, the raw data and peak deconvolutions are depicted in Fig. 4. Peak 1 is ascribed to carbonyl groups (binding energy position of 531 eV). Peak 2 is ascribed to phenol and/or ether type groups (binding energy position of 533 eV). Peak 3, which forms mainly a tail, has been tentatively ascribed to chemisorbed water and/or O_2 (binding energy position varies between 535 and 536 eV) [13, 14, 17]. Since the samples were exposed to air before introduction into the XPS-machine and in situ heat-treatments were not possible, chemisorption of oxygen-containing gases from the atmosphere cannot be excluded. When compared to CNF-ox, CNF-OH shows a decrease of peak 1 (carbonyl groups) and a relative increase of peak 2 (533 eV; phenol and/or ether groups). Since it is expected that CNF-OH has a high concentration of phenol type groups due to the $LiAlH_4$ reduction treatment, it is concluded that the peak at 533 eV must be attributed to the binding energy of oxygen in phenol type groups and confirms thereby earlier reported phenol peak positions [13-19].

In Fig. 5, the absolute integrated areas for all three contributions for the (heat-treated) CNF-materials with and without platinum, are depicted. As described earlier, application of heat-treatments resulted in a decreasing integrated area, while the presence of platinum and subsequent reduction in hydrogen resulted in even a further decreasing integrated area. For the non-metal containing materials, peak 2 (phenol and/or ether-type bonded oxygen) resulted in the highest surface area irrespective the applied heat-treatments. This has been observed earlier for non-metal containing carbon fibers [13, 14]. After metal deposition and reduction, peak 1 (carbonyl groups) resulted in the highest surface area throughout all heat-treatments applied. This means that upon metal deposition and reduction, XPS results show that mainly phenol groups are removed from the CNF surface. It is important to note here that using XPS, oxygen originating from the carboxylic acid surface groups cannot be resolved (see peak assignments above). Therefore XPS and titrations are complementary techniques, since titrations showed that platinum deposition and reduction resulted in a substantial removal of carboxylic acid surface groups (Table 1).

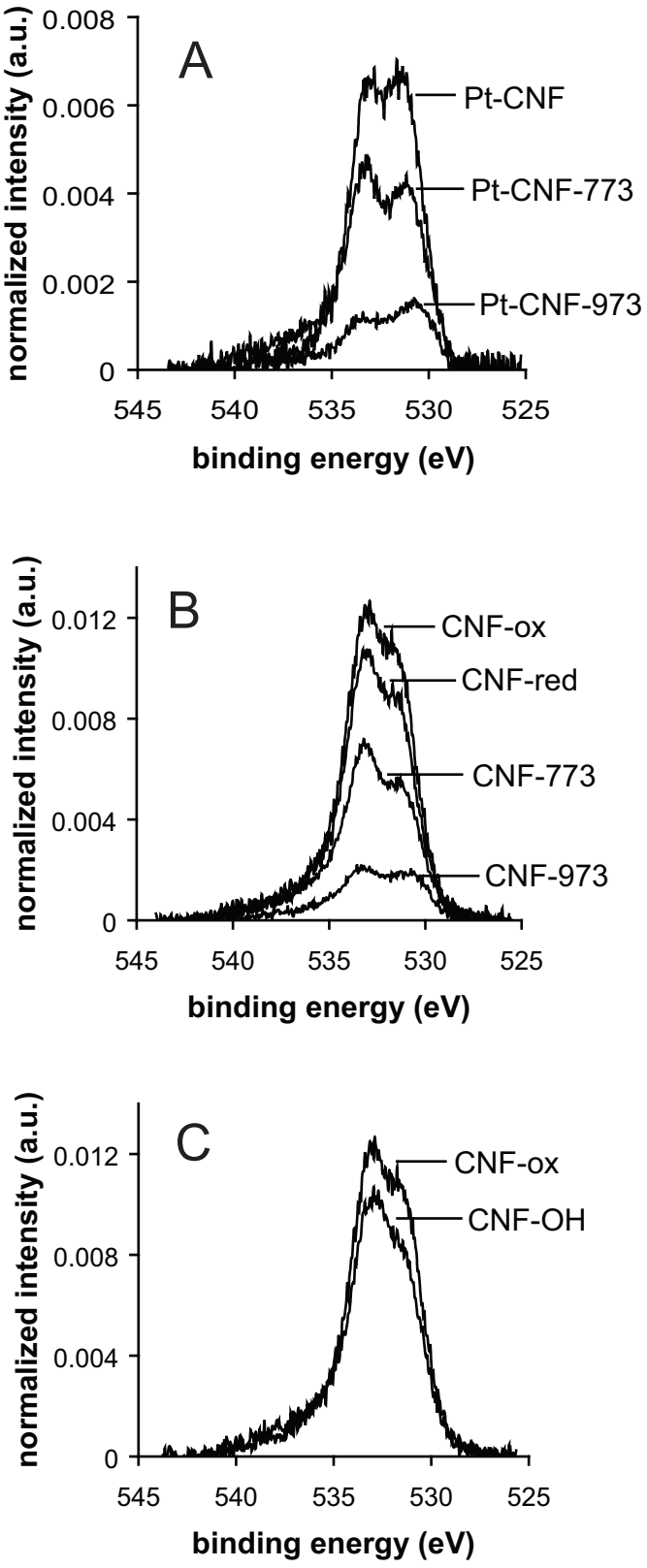

Fig. 3 XPS O1s scans normalized at C1s position. In A, the Pt-containing samples are depicted, in B the non-metal containing samples and in C the samples CNF-ox and CNF-OH are compared.

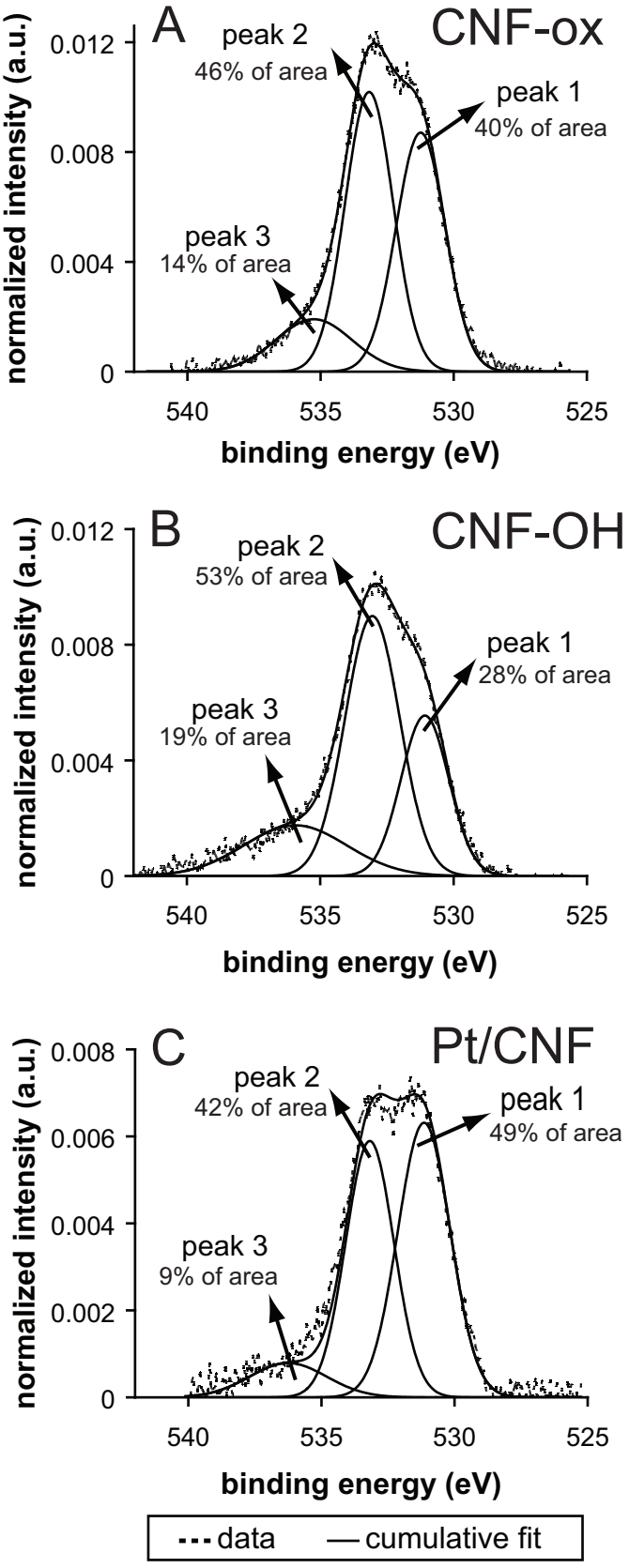

Fig. 4 Raw data and peak deconvolutions of the XPS O1s scans exemplified for A: CNF-ox, B: CNF-OH and C: Pt-CNF. Energies for peak 1: 531 eV peak 2: 533 eV peak 3: 535-536 eV.

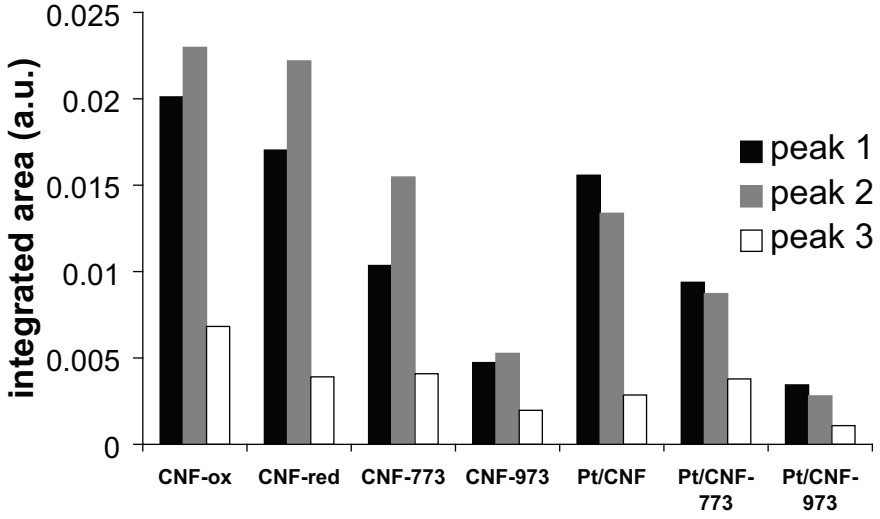

Fig. 5 Integrated areas (a.u.) of the different materials for peaks 1 till 3.

The amount of carboxylic acid surface groups for CNF-ox (0.16 mmol acidic groups/g material; pH<5) is close to the amount of platinum incorporated (i.e. 0.15 mmol Pt/g material), which is theoretically possible assuming a 1/1 ratio. Based on the metal loading and assuming a surface area of 1.98 nm^2 for a hydrated $Pt(NH_3)_4^{2+}$-complex [24], it was calculated that the surface coverage is close to a monolayer. Thus we cannot distinguish whether the amount of carboxylic groups or the surface area of the support determines the platinum loading. Therefore, we continued our investigations by deposition of platinum via HDP on CNF-OH which contained less carboxylic acid surface groups then CNF-ox. This synthesis resulted in deposition of platinum on CNF-OH, but a lower metal loading was obtained as compared to deposition on CNF-ox (1.4 wt-% for Pt/CNF-OH vs. 2.9 wt-% for Pt/CNF) and therefore shows that carboxylic acid surface groups are important for metal deposition. Since in the latter experiment the amount of platinum (i.e. 0.07 mmol Pt/g material) exceeded the amount of carboxylic acids present on CNF-OH (i.e. 0.04 mmol groups/g material at pH<5), it is concluded that also other types of oxygen surface groups are involved in platinum deposition. Using XPS analysis, it has been found that after platinum deposition, reduction and heat-treatment (i.e. Pt/CNF, Pt/CNF-773 and Pt/CNF-973) the majority of the oxygen surface groups are of the carbonyl type, but when platinum is absent (i.e. CNF-ox, CNF-red, CNF-773 and CNF-973) the majority of the oxygen surface groups are of the phenol type. This means that upon metal deposition and reduction, mainly phenol groups are removed from the CNF surface. As described earlier, deposition of platinum is not solely related to the amount of carboxylic acid surface groups. Since mainly phenol groups are present on CNF-OH and these groups are removed upon metal deposition and reduction in large amounts

when compared to carbonyl groups, it is concluded that also phenol oxygen surface groups may enable platinum deposition next to carboxylic acid surface groups. After reduction, both groups are removed, which has been confirmed for acidic groups using titrations and for phenol groups using XPS. The removal of carboxyl and phenol groups for the as-reduced Pt/CNF has been confirmed by the analysis results for the heat-treated samples when comparing platinum-containing CNF with non-metal containing CNF after heat-treatments. After removal of these oxygen surface groups, the platinum metal particles are probably stabilized directly on carbon via e.g. defects in the structure or other types of oxygen surface groups [25, 26].

These results differ from observations made by Van der Lee et al. [4] namely that only carboxylic acid surface groups are required for nickel deposition on CNF. For nickel, a hydroxide phase is formed upon increasing pH (5.5 – 6.4) which starts to nucleate on nickel ions which were adsorbed at low pH. Since only carboxylic acid surface groups become deprotonated at the low pH range, one requires these groups to adsorb and deposit nickel ions prior to complete nucleation of the nickel hydroxide [4]. Platinum does not form a hydroxide phase in the pH range of HDP synthesis and therefore, deposition of platinum is more a result of pH induced ion adsorption than deposition precipitation [3]. During HDP, phenol groups become deprotonated as well at higher pH range [27, 28]. Therefore, phenol groups are, next to carboxyl groups, also responsible for platinum ion adsorption. The ion adsorption observed here as function of pH is in line with the revised physical adsorption model as described by the group of Regalbuto, namely that at pH well above the point of zero charge (i.e. pH 2-3 for oxidized CNF [29, 30]), adsorption of cationic platinum occurs on the negatively charged support material [31, 32].

Conclusions

In this study, analysis of the nature and stability of oxygen surface groups on carbon nanofibers and platinum-containing carbon nanofibers was performed using XPS and titrations and these results were related to platinum deposition on CNF. Removal of acidic oxygen surface groups is observed when heat-treatments in inert atmosphere at 973 K were performed. Platinum deposition and reduction on CNF resulted in decreasing decomposition temperature of the acidic oxygen surface groups to 773 K. Synthesis of platinum on CNF via homogeneous deposition precipitation results in metal anchoring on carboxyl as well as on phenol oxygen surface groups. It is proposed that during synthesis both groups become deprotonated and are able to bring about platinum ion adsorption.

Literature

1. K.P. de Jong, J.W. Geus, Cat. Rev. - Sci. Eng., 42(4), 2000, 481-510.
2. P. Serp, M. Corrias, P. Kalck, Appl. Catal. A, 253(2), 2003, 337-358.
3. M.L. Toebes, M.K. van der Lee, L.M. Tang, M.H. Huis in 't Veld, J.H. Bitter, A.J. van Dillen, K.P. de Jong, J. Phys. Chem. B, 108(31), 2004, 11611-11619.
4. M.K. van der Lee, A.J. van Dillen, J.H. Bitter, K.P. de Jong, J. Am. Chem. Soc., 127(39), 2005, 13573-13582.
5. M.L. Toebes, J.H. Bitter, A.J. van Dillen, K.P. de Jong, Catal. Today, 76(1), 2002, 33-42.
6. A.J. Plomp, H. Vuori, A.O.I. Krause, K.P. de Jong, J.H. Bitter, Appl. Catal. A, 351(1), 2008, 9-15.
7. M.L. Toebes, Y. Zhang, J. Hájek, T.A. Nijhuis, J.H. Bitter, A.J. van Dillen, D.Y. Murzin, D.C. Koningsberger, K.P. de Jong, J. Catal., 226(1), 2004, 215-225.
8. D.A. Shirley, Phys. Rev. B, 5(12), 1972, 4709-4714.
9. D. Briggs, M.P. Seah, Practical Surface Analysis, 2nd ed., Wiley, 1990, pp. 635-638 (Appendix 636).
10. M.L. Toebes, J.M.P. van Heeswijk, J.H. Bitter, A.J. van Dillen, K.P. de Jong, Carbon, 42(2), 2004, 307-315.
11. H.P. Boehm, Carbon, 40(2), 2002, 145-149.
12. M.A. Fraga, E. Jordao, M.J. Mendes, M.M.A. Freitas, J.L. Faria, J.L. Figueiredo, J. Catal., 209(2), 2002, 355-364.
13. S. Biniak, G. Szymanski, J. Siedlewski, A. Swiatkowski, Carbon, 35(12), 1997, 1799-1810.
14. S.D. Gardner, C.S.K. Singamsetty, G.L. Booth, G.R. He, C.U. Pittman, Carbon, 33(5), 1995, 587-595.
15. I. Kvande, G. Oye, N. Hammer, M. Ronning, S. Raaen, A. Holmen, J. Sjoblom, D. Chen, Carbon, 46(5), 2008, 759-765.
16. A. Proctor, P.M.A. Sherwood, Carbon, 21(1), 1983, 53-59.
17. R. Schlögl, H.P. Boehm, Carbon, 21(4), 1983, 345-358.
18. B. Stöhr, H.P. Boehm, R. Schlögl, Carbon, 29(6), 1991, 707-720.
19. P.V. Lakshminarayanan, H. Toghiani, C.U. Pittman, Carbon, 42(12-13), 2004, 2433-2442.
20. P. Louette, F. Bodino, J.-J. Pireaux, Surf. Sci. Spectra, 12, 2006, 106-110.
21. P. Louette, F. Bodino, J.-J. Pireaux, Surf. Sci. Spectra, 12, 2006, 149-153.
22. P. Louette, L. Kohler, F. Bodino, J.-J. Pireaux, Surf. Sci. Spectra, 12, 2006, 159-163.

23. P. Louette, F. Bodino, J.-J. Pireaux, Surf. Sci. Spectra, 12, 2006, 154-158.
24. N. Santhanam, T.A. Conforti, W. Spieker, J.R. Regalbuto, Catal. Today, 21(1), 1994, 141-156.
25. Y. Zhang, M.L. Toebes, A. van der Eerden, W.E. O'Grady, K.P. de Jong, D.C. Koningsberger, J. Phys. Chem. B, 108(48), 2004, 18509-18519.
26. R.V. Hull, L. Li, Y.C. Xing, C.C. Chusuei, Chem. Mater., 18(7), 2006, 1780-1788.
27. H.P. Boehm, E. Diehl, W. Heck, R. Sappok, Angew. Chem., 76(17), 1964, 742-751.
28. H.P. Boehm, Carbon, 32(5), 1994, 759-769.
29. J.W. Geus, A.J. Van Dillen, M.S. Hoogenraad, Mater. Res. Soc. Symp. Proc., 368(Synthesis and Properties of Advanced Catalytic Materials), 1995, 87-98.
30. M.S. Hoogenraad, PhD-thesis, Utrecht University, Utrecht, 1995.
31. X. Hao, W.A. Spieker, J.R. Regalbuto, J. Colloid Interface Sci., 267(2), 2003, 259-264.
32. X. Hao, L. Quach, J. Korah, W.A. Spieker, J.R. Regalbuto, J. Mol. Catal. A: Chem., 219(1), 2004, 97-107.

4

Reducibility of Platinum Supported on Nanostructured Carbons

Abstract

The nanostructure of graphite like carbon, i.e. carbon nanofibers (CNF), carbon nanotubes (CNT) and carbon nanoplatelets (CNP), displayed a significant influence on the reducibility of platinum deposited on these carbons. The onset temperature for reduction increased from 461 K for Pt/CNF to 466 K for Pt/CNP and 487 K for Pt/CNT. The retarded reduction for Pt/CNT was related to the higher amount of acidic oxygen surface groups on this support resulting in a strong stabilization of the cationic platinum species. A higher reduction temperature for that sample increased the amount of metallic platinum, however the platinum particle size was larger (2-11 nm) compared to that of Pt/CNF and Pt/CNP (both 1-3 nm). The orientation of the graphene sheets had a significant influence on the selectivity for the cinnamaldehyde hydrogenation: Pt/CNP resulted in a higher selectivity towards cinnamyl alcohol compared to Pt/CNF.

Introduction

Reduction temperature and sintering behavior of the metal(oxide) phase in supported metal(oxide) catalysts depend largely on parameters such as the nature of the support used or the synthesis method [1-3]. For example, Roman-Martinez et al. [2] showed for platinum supported on activated carbons that partial oxidation of the support resulted in higher platinum reduction temperatures and substantial hydrogen spill-over compared to the non-oxidized carbon supports. Da Silva et al. [4] deposited monometallic platinum, platinum-iron and platinum-tin combinations on TiO_2 and carbon. The TPR profiles of the monometallic platinum catalysts showed that platinum is reduced at lower temperature on TiO_2 compared to carbon (443 K and 473 K respectively). The addition of a second metal affected the platinum reduction temperature: for platinum-iron an increase of 20 to 40 K was observed.

For catalysts based on nanostructured carbon it can be expected that their reduction behavior is related to the orientation of the graphene layers with respect to the central axis. Three major classes of tubular carbons are distinguished, i.e. carbon nanotubes (CNT, graphene layers aligned with central axis), carbon nanoplatelets (CNP, graphene layers perpendicular with central axis) and carbon nanofibers (CNF, graphene layers at an angle between 0 and 90 degrees with central axis) [5]. All these nanostructured carbons attracted interest as heterogeneous catalyst support [5, 6].

Different examples can be found in which it was shown that the graphene orientation has an influence on the catalytic activity of supported metal catalysts. Motoyama et al. [7] investigated CNF, CNT and CNP-supported ruthenium for the hydrogenation of various aromatic compounds. Ruthenium was well dispersed (particle size ~2.5 nm) on CNP and resulted in high and reproducible catalytic activity, while for CNF and especially for CNT supported ruthenium the coexistence of large particles (ranging from 10 to 150 nm) and small ones (<4.5 nm) was observed resulting in low hydrogenation activities. Vu et al. [8] deposited platinum and ruthenium on CNT and CNF and tested these catalysts for the cinnamaldehyde hydrogenation. They observed that in general the average metal particle size was smaller for CNF than for CNT. Two different CNT batches with different inner tube diameters (batch 1: <10 nm and batch 2: 60-100 nm) and different BET surface areas (batch 1: 400 m^2/g and batch 2: 40 m^2/g) were studied by Ma et al. [9]. The authors deposited platinum on the supports, which resulted in two different metal particles sizes (batch 1: <2 nm and batch 2: >5 nm). These catalysts were tested for the cinnamaldehyde hydrogenation and large differences with respect to catalytic selectivity were found (selectivity to cinnamyl alcohol for batch 1: <25% and batch 2: >60%) [9].

The above described results show that especially for CNT supported catalysts a wide variety of particle sizes is observed, which is accompanied by large differences with respect to catalytic activities or selectivities. This might be associated with the reduction behavior related to the graphene sheet orientation. The goal of the current study is to deposit platinum on CNF, CNT and CNP to investigate the role of graphene layer orientation on reducibility and catalytic activity of platinum for cinnamaldehyde hydrogenation. The latter reaction is sensitive to subtle changes in the support surface composition of nanostructured carbons as shown earlier by our group [10, 11].

Experimental

The Ni/SiO_2 (20 wt-%) growth catalyst was prepared via homogeneous deposition precipitation using 17.0 g silica (Degussa; Aerosil 200), 21.1 g nickel nitrate hexahydrate (Acros; 99%) and 13.9 g urea (Acros; p.a.) in 1 L demineralized water according to an earlier described procedure [12]. The growth and oxidation of CNF was performed as described earlier [13].

CNT (multi-walled class 1) and CNP (carbon nanofiber - platelets) were obtained from FutureCarbon GmbH, Germany. Both materials (9 g) were refluxed for 1 h in aqueous KOH solution (1 M; 250 mL) and, after filtering and washing, refluxed for 2 h in concentrated nitric acid (250 mL; Merck; 65%) and filtered again. The oxidized residue was washed three times with demineralized water and dried overnight at 393 K.

Platinum was deposited on oxidized CNF, CNP and CNT using ion adsorption, as described for platinum tetraammine nitrate by Hao et al. [14]. Oxidized carbon material (5.00 g) was suspended in demineralized water (250 mL) and the pH was adjusted to 10 using ammonium hydroxide (Merck; conc.). $Pt(NH_3)_4(NO_3)_2$ (0.202 g; Aldrich) was added and the slurry was stirred for two hours. If necessary, the pH was again adjusted to 10. Next, the slurry was filtered using a Millipore filter and shortly washed using aqueous ammonium hydroxide solution of pH 10. After drying overnight at 393 K, the obtained material was reduced in H_2/N_2-flow (100 mL/min; 10% v/v) at 473 K (1 h; ramp 5 K/min) and the resulting materials were denoted as Pt/CNF, Pt/CNP and Pt/CNT. A batch of Pt/CNT was also reduced in H_2/N_2-flow (100 mL/min; 10% v/v) at 503 K (1 h; ramp 5 K/min). This catalyst is denoted as Pt/CNT-red503.

Platinum on nanostructured carbon catalysts (1 g; sieve fraction 25-90 μm) were tested for the cinnamaldehyde hydrogenation as described earlier [13]. The conversion of cinnamaldehyde and selectivity to cinnamyl alcohol were calculated as described before [13].

The metal weight-loading of the samples was determined using ICP-OES. The measurements were performed using a SPECTRO CIROS^{CCD} ICP-Spectrometer. Each sample was destructed by heating in aqua regia (1:3 mixture of HNO_3: HCl) before analysis.

TPR experiments were performed using a Micromeritics AutoChem II 2920. After drying at 393 K, the non-reduced catalysts were analyzed using a flow of H_2/Ar (5% v/v; 50 mL STP/min) and a temperature ramp of 5 K/min. Different amounts of sample were used (0.17 – 0.33 g). The reproducibility of the machine was experimentally determined to be ±2 K. Hydrogen consumptions were normalized to the sample weight. The onset reduction temperature was determined by extrapolation of the baseline and extrapolation of the tangent at the inflection point of the first peak slope. The point of intersection of these two lines is reported as the onset reduction temperature.

Acid-base titrations were performed using a Titralab TIM 880 apparatus. To 60 mL of 0.1 M KCl 0.05 g Pt/CNF was added. A solution of 0.01 M NaOH and 0.1 M KCl was used as titrant. The titrant consumption to reach a pH of respectively 5 and 7.5 were used to calculate the amount of strong (at pH 5) and total (at pH 7.5) acidic sites on the catalysts. The stronger acidic groups are expected to be the carboxylic acid surface groups [15].

TEM was performed using a Tecnai 20 FEG operating at 200 kV and a point resolution of 2.7 Å. The microscope was equipped with an EDX detector.

Nitrogen physisorption was performed at 77 K using a Micromeritics Tristar 3000 V6.01 to determine BET surface areas and pore volumes (single point adsorption at $P/P_0>0.994$). Prior to the physisorption measurements, the samples were dried in flowing nitrogen at 473 K for about 14 hours.

Hydrogen chemisorption measurements were performed using a Micromeritics ASAP 2020. Samples were dried at 373 K in vacuum followed by cooling to room temperature. Next, the samples were re-reduced in flowing hydrogen at 473 K for 60 min (ramp 5 K/min). Afterwards, the samples were degassed for at least 30 min at a pressure of <13.3 Pa at 473 K to remove chemisorbed hydrogen and water. The isotherms were measured at 313 K and the mass was determined afterwards. The presented H/Pt ratios are based on the amounts adsorbed at zero pressure, which are calculated by extrapolation of the linear part of the isotherm. Estimated average particle sizes and dispersions are based on spherical geometry and an adsorption stoichiometry of H/Pt_s = 1. Based on these data and assuming full reduction, average particle sizes were calculated as described by Scholten et al. [16]:

$$d = 10^{21} \frac{6 \times M \times \rho_{site}}{D \times \rho_{metal} \times N}$$

Where d is particle size (nm), M the atomic weight (195.1 g/mol), ρ_{site} the platinum surface site density (12.5 Pt atoms/nm^2) [16], D is dispersion (H/Pt), ρ_{metal} the metal density (21.45 g/cm^3) and N the Avogadro constant giving d = 1.13/D (nm).

Results and Discussion

Some of the structural parameters of the oxidized carbons are compiled in Table 1 and high resolution TEM images are depicted in Fig. 1. The measured BET surface areas were 78 m^2/g for CNP, 178 m^2/g for CNF and 247 m^2/g for CNT. The increase in BET surface area is ascribed to a decrease in fiber diameter (Table 1) for the different carbon materials (CNP: 40-200 nm, CNF: 25-40 nm and CNT: 10-25 nm), which will result in a larger surface-to-volume ratio.

Table 1. Physical properties of the oxidized supports.

	oxidized CNF	oxidized CNP	oxidized CNT
BET surface area (m^2/g; after oxidation)	178	78	247
Pore volume based on N_2-physisorption (mL/g)	0.28	0.24	1.01
mmol acidic sites/g material at pH 5	0.17	0.10	0.50
mmol acidic sites/g material at pH 7.5	0.23	0.23	0.84
Fiber diameter (nm; based on TEM)	25-40	40-200	10-25

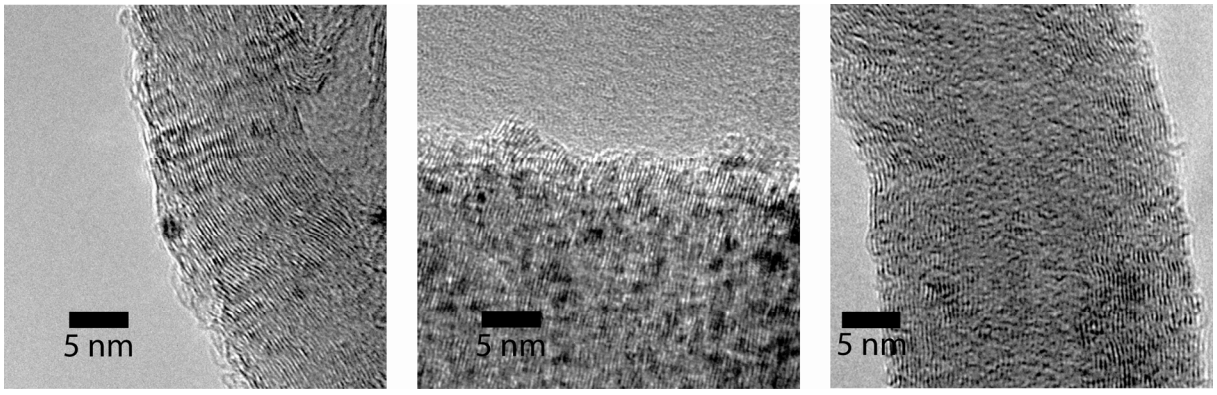

Fig. 1 High-resolution TEM image of oxidized CNF (left), CNP (middle) and CNT (right). For CNF, an image with some platinum particles is depicted.

The pore volume established from nitrogen physisorption was significantly higher for CNT (1.01 mL/g) than for CNP (0.24 mL/g) and CNF (0.28 mL/g). No micropores were found in the used materials. The substantially larger pore volume observed for CNT compared to CNF and CNP is ascribed to the fact that CNT has a lower bulk density combined with a small particle size. Therefore, a large intratubular pore volume is created. Moreover, the individual fibers in CNP and CNF seem to be more entangled as compared to the thinner CNT. This may result in a higher pore volume for CNT [17].

ICP-OES showed that platinum loadings for the catalysts were 1.7 – 1.8 wt-% (Table 2). The amount of acidic, oxygen surface groups was determined using acid-base titrations. CNT displayed 0.50 mmol strong acidic sites per gram CNT, while 0.10 mmol strong acidic sites per gram were found for CNP and 0.17 mmol strong acidic sites per gram for CNF. At pH 7.5 0.84 mmol acidic sites per gram CNT was titrated, while for CNF and CNP the results were similar: 0.23 mmol acidic sites per gram material. For CNT the oxygen containing groups must be located on defects in the graphene sheets [18], which are either present in the as prepared materials or can be formed during the nitric acid treatment used to introduce the oxygen surface groups [19]. Also after platinum deposition, titrations were performed to determine the amount of acidic, oxygen surface groups. At pH 5 this resulted in 0.02 mmol acidic sites per gram for Pt/CNF and Pt/CNP and in 0.06 mmol acidic sites per gram for Pt/CNT and Pt/CNT-red503. For Pt/CNF and Pt/CNP 0.07 mmol acidic sites per gram were found while for Pt/CNT and Pt/CNT-red503 0.14 and 0.13 mmol acidic sites per gram were present respectively at pH 7.5.

Table 2. Physical properties of the catalysts.

	Pt/CNF	Pt/CNP	Pt/CNT	Pt/CNT-red503
metal loading (wt-%)	1.8	1.8	1.7	1.7
H/Pt ratio	0.65	0.64	0.17	0.35
particle size (nm; based on H_2-chemisorption)	1.7	1.8	6.7	3.2
average particle size (nm; based on TEM)	1.6	2.1	n.d.	4.2
mmol acidic sites/g material at pH 5	0.02	0.02	0.06	0.06
mmol acidic sites/g material at pH 7.5	0.07	0.07	0.14	0.13
initial TOF (s^{-1})[a]	0.05	0.07	0.05	0.07

n.d. = not determined

[a] based on H_2-chemisorption data

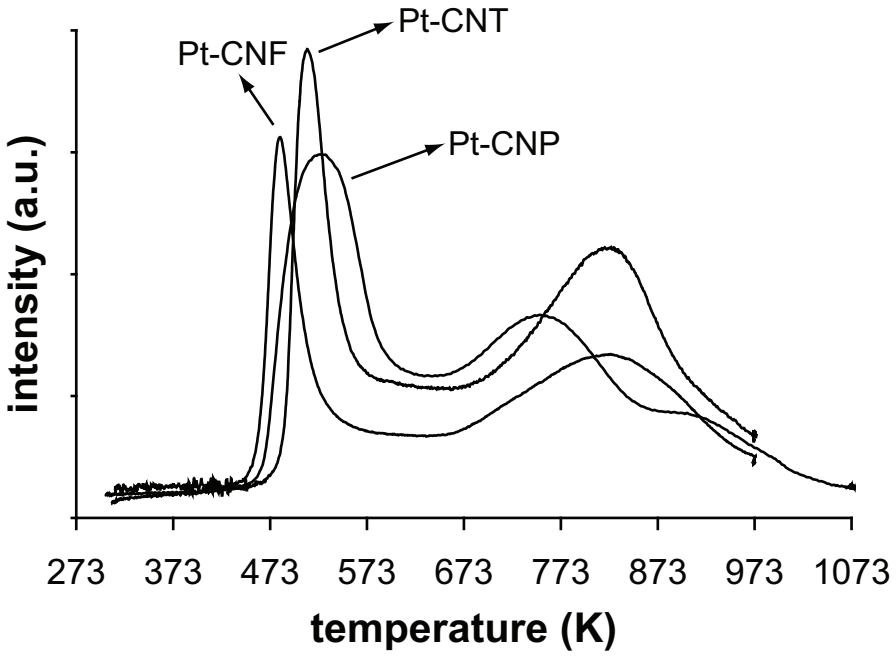

Fig. 2 TPR profiles of the non-reduced catalysts.

The TPR profiles of the materials after synthesis and drying are depicted in Fig. 2. The peak between 450 and 575 K represents the platinum reduction, while the peak at higher temperature is ascribed to gasification of the supports. The onset temperature for reduction was determined to be 461 K for Pt/CNF, 466 K for Pt/CNP and 487 K for Pt/CNT. Thus the reduction for Pt/CNT is retarded compared to Pt/CNF and Pt/CNP. The amount of platinum per gram material is approximately the same for all catalysts (i.e. 0.09 mmol Pt/g material; see also Table 2). Titrations showed that CNT have the highest amount of acidic sites i.e. 0.50 mmol acidic sites/g at pH 5 and 0.84 mmol/g at pH 7.5 which is a 5-9 time excess compared to the amount of platinum deposited on this material. It has been shown earlier by Toebes et al. [20] that acidic oxygen surface groups are required to anchor platinum on CNF. Even after metal deposition still CNT have the highest amount of acidic sites. Since it is known that acidic oxygen surface groups are required to anchor platinum, it is speculated that the high amount of acidic oxygen surface groups on CNT resulted in a strong binding and stabilization of the cationic platinum. The formation of metallic platinum particles during reduction might therefore be hindered, which in turn results in a higher reduction temperature for this sample compared to Pt/CNF and Pt/CNP (see Fig. 3). It has been described in literature that the reduction temperature of palladium on nanostructured carbon is affected by and related to the presence of stable acidic surface groups [21]. This is in good agreement with our results.

It must be noted here that during metal deposition and reduction more oxygen surface groups are removed on CNT (i.e. 0.84-0.14=0.7 mmol/g) compared to Pt/CNF and Pt/CNP (0.23-0.07=0.16 mmol/g). These groups can decompose and being removed due to e.g.

hydrogen spill-over during reduction [22]. The substantial removal of oxygen surface groups for CNT is ascribed to the fact that this material has the highest concentration of oxygen surface groups present after oxidation of this material. As a consequence, more oxygen surface groups are in the vicinity of platinum resulting in a relative high removal of these groups. The first peak in the TPR profile for Pt/CNF is clearly the smallest and is related to platinum reduction. It is calculated that for this peak the theoretical H_2/Pt ratio is around 6, which is above the expected value of 1. This is probably the result of the formation of other gases during the reduction/anion decomposition such as nitrogen oxides, ammonia, CO and CO_2 (the latter two gases originate from support gasification [22, 23]), which will affect the TCD signal making quantitative statements obsolete. H/Pt ratios of the catalysts were calculated using hydrogen chemisorption and resulted for Pt/CNF in 0.65, Pt/CNP in 0.64, Pt/CNT in 0.17 and Pt/CNT-red503 in 0.35. Based on these data, average particle sizes were calculated and the results are given in Table 2. Platinum particle sizes were also analyzed using TEM (see Fig. 4). Pt/CNF and Pt/CNP showed platinum particles of 1-3 nm, while for Pt/CNT, TEM did not show platinum particles. For the latter catalyst, the presence of platinum was confirmed using TEM-EDX and ICP-OES. For Pt/CNT-red503 large platinum particles, ranging from 2-11 nm were observed. Histograms of the observed particle size distribution of the different catalysts are compiled in Fig. 5. Based on TEM histograms the average particle sizes were calculated for all catalysts and the results are summarized in Table 2. As mentioned before, TEM did not show unambiguously the presence of platinum particles for Pt/CNT, though ICP-OES and TEM-EDX confirmed the presence of platinum. Also hydrogen chemisorption resulted in a low H/Pt ratio, which shows that at least some platinum is present in the metallic state. These results are inconsistent with the observations using TEM, unless the sample is not well-reduced. The TPR profile of Pt/CNT suggests that this might be the case and therefore a reduction of Pt/CNT at 503 K was performed. The measured H/Pt ratio of this sample was indeed larger compared to the one reduced at 473 K, which shows that a higher reduction degree is obtained. Still, the H/Pt ratio is lower compared to Pt/CNF and Pt/CNP. TEM analysis of this sample showed relatively large particles, which leads to the conclusion that sintering had occurred. The average particle

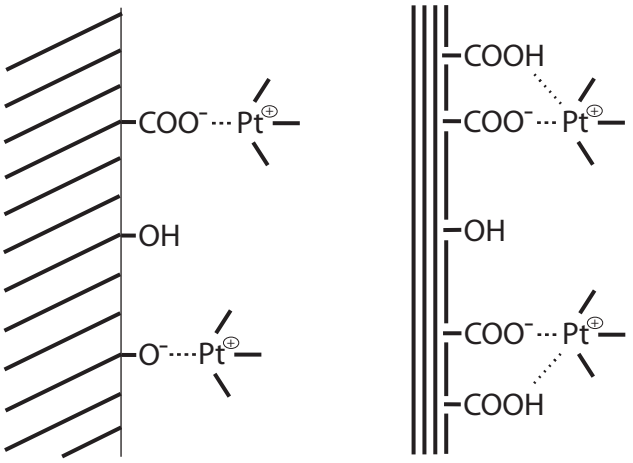

Fig. 3 Left scheme: platinum adsorption on surface oxidized CNF (and CNP). Right scheme: platinum adsorption on surface oxidized CNT.

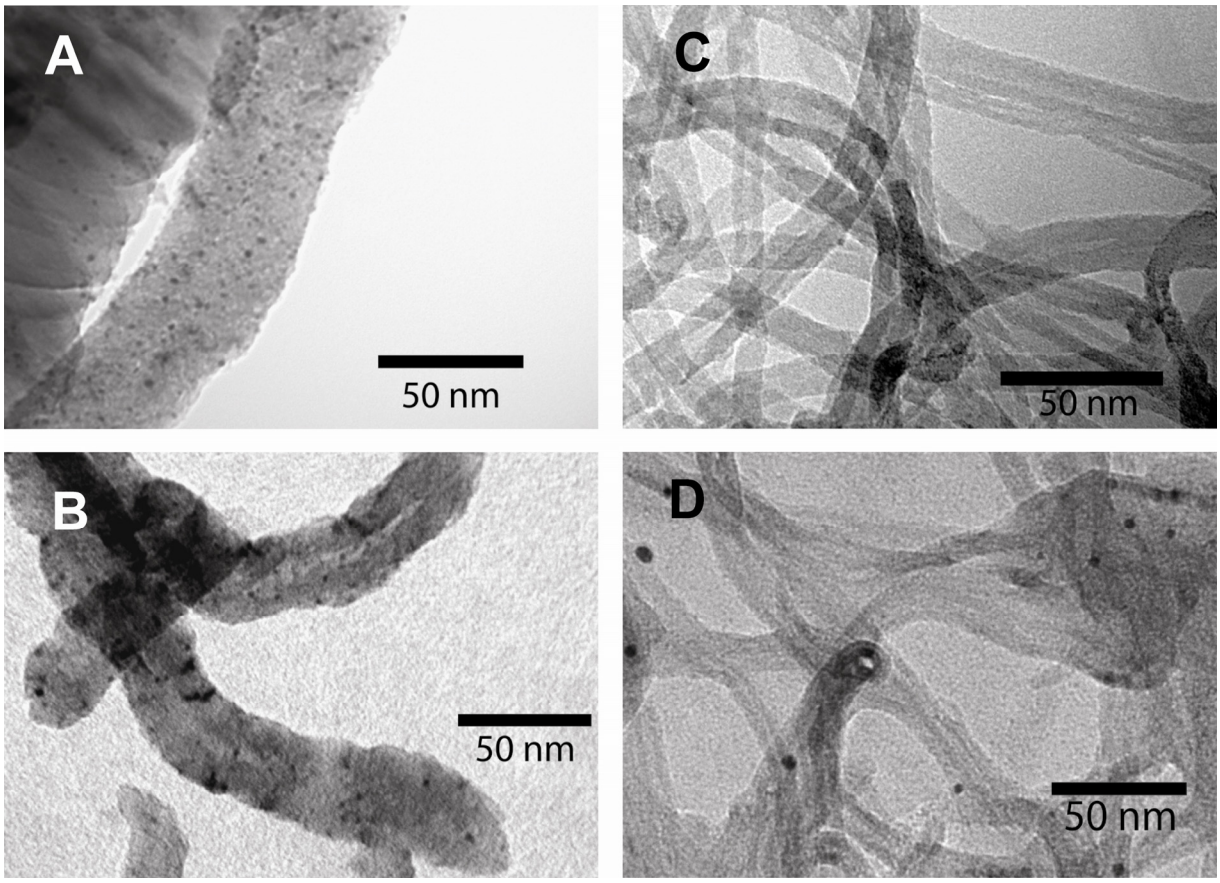

Fig. 4 TEM images of the catalysts A: Pt/CNP Pt particles of 1-3 nm B: Pt/CNF Pt particles of 1-3 nm C: Pt/CNT no Pt particles detected (the latter catalysts were reduced at 473 K) D: Pt/CNT-red503 (reduction at 503 K) Pt particles of 2-11 nm were observed.

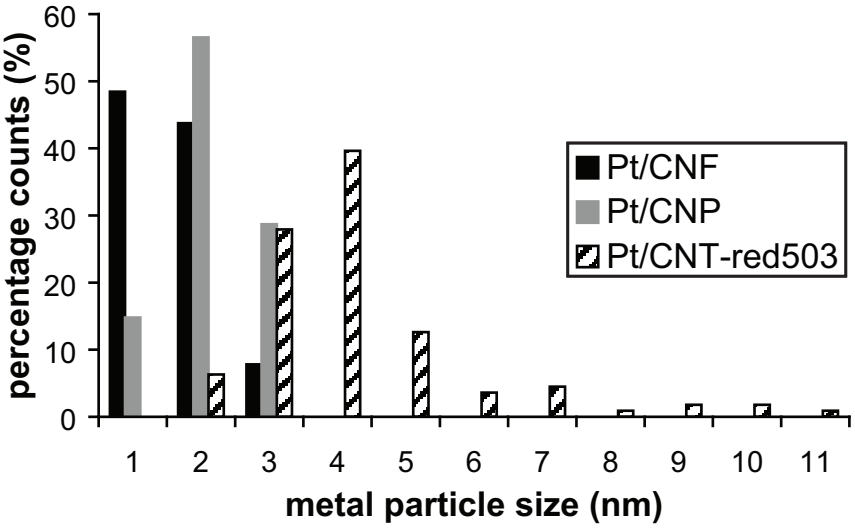

Fig. 5 Histograms of metal particle sizes observed using TEM for Pt/CNF (1-3 nm), Pt/CNP (1-3 nm) and Pt/CNT-red503 (2-11 nm).

size for Pt/CNT-red503 determined using TEM (4.2 nm) and hydrogen chemisorption (3.2 nm) are relatively close to each other and therefore, it is concluded that reduction at 503 K resulted in metallic platinum. Thus to summarize, the high amount of acidic oxygen surface groups on CNT results in a high platinum-precursor dispersion. These platinum species are more difficult to reduce and need a higher reduction temperature compared to platinum deposited on CNF and CNP. Once reduced at higher temperature, TEM and hydrogen chemisorption revealed that the platinum particles on CNT were sintered.

The catalysts were tested for the cinnamaldehyde (CALD) hydrogenation (see Fig. 6 for the used abbreviations) and the results are depicted in Fig. 7. Both Pt/CNP and Pt/CNF were active (60% and 25% CALD conversion after 300 minutes respectively), though for the latter catalyst a clear deactivation is observed. For these test reactions by-products (only propylbenzene and β-methylstyrene) were observed: for Pt/CNP this was around 2% and for Pt/CNF this was around 1%. Pt/CNT showed only in the initial state some hydrogenation activity, but deactivated rapidly resulting in no further conversion at all. This also indicates that the standard chosen reduction temperature of 473 K is not high enough to create an active metal surface. Indeed when the catalyst is reduced at a higher temperature (i.e. Pt/CNT-red503), hydrogenation activity is observed (Fig. 7) resulting in 13% conversion after 300 min of reaction time and about 0.5% of by-product was observed. This conversion is still substantially lower compared to Pt/CNF and Pt/CNP (25% and 60% respectively).

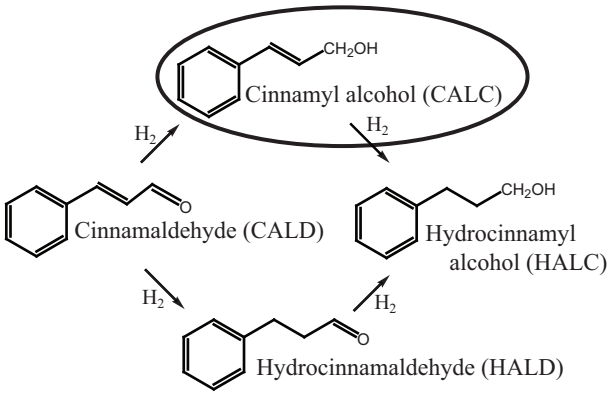

Fig. 6 Hydrogenation pathway of CALD; the desired product is encircled.

The initial turn-over frequencies (TOF) are calculated based on H/Pt ratios and are summarized in Table 2. The initial TOF is the same for all catalysts, but as mentioned before deactivation quickly starts to affect the catalytic activity for several catalysts. Since the initial TOF is similar for all catalysts, the low weight based catalytic activity of Pt/CNT-red503 must be the result of the lower metal dispersion of that catalyst.

For Pt/CNF, Pt/CNP and Pt/CNT-red503 the conversion of CALD is plotted versus the selectivity to cinnamyl alcohol (CALC) (see Fig. 8). The selectivity to CALC for Pt/CNP is significantly higher compared to that with Pt/CNF, while the platinum particle size, amount of oxygen surface groups and TOF is the same for these samples. It is therefore concluded

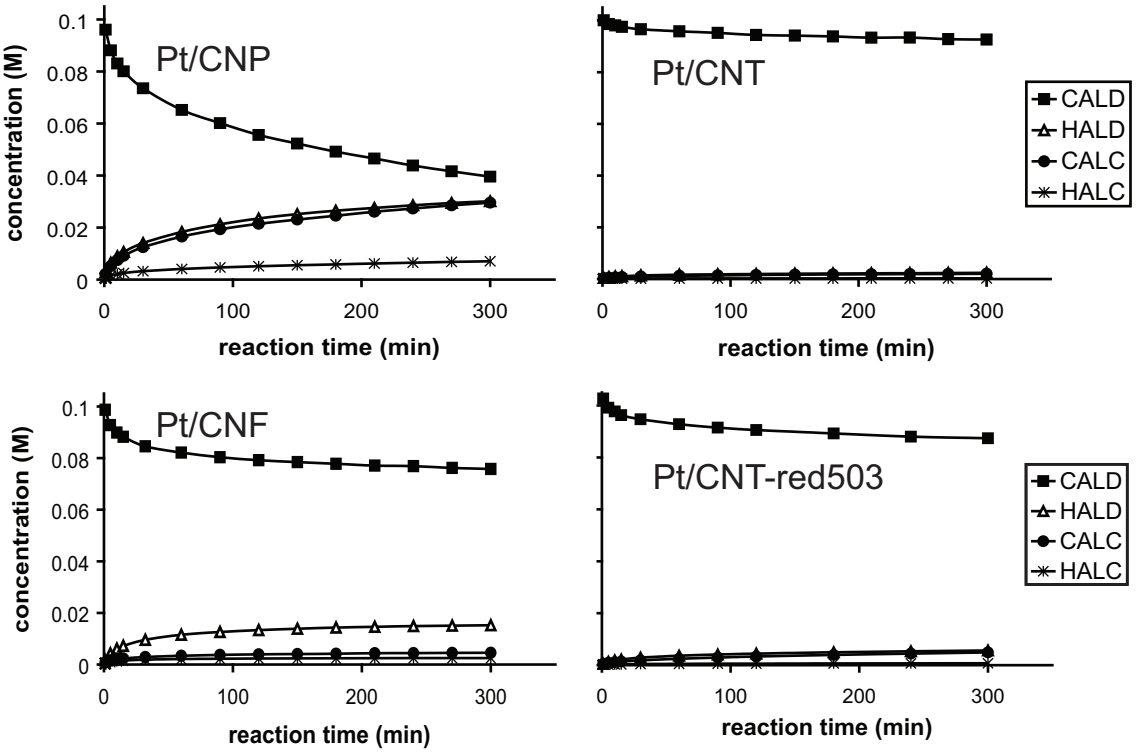

Fig. 7 Cinnamaldehyde hydrogenation results of Pt/CNP, Pt/CNF, Pt/CNT and Pt/CNT-red503. Test reactions were performed at 313 K under 1200 mbar H_2 in 2-propanol/water mixture.

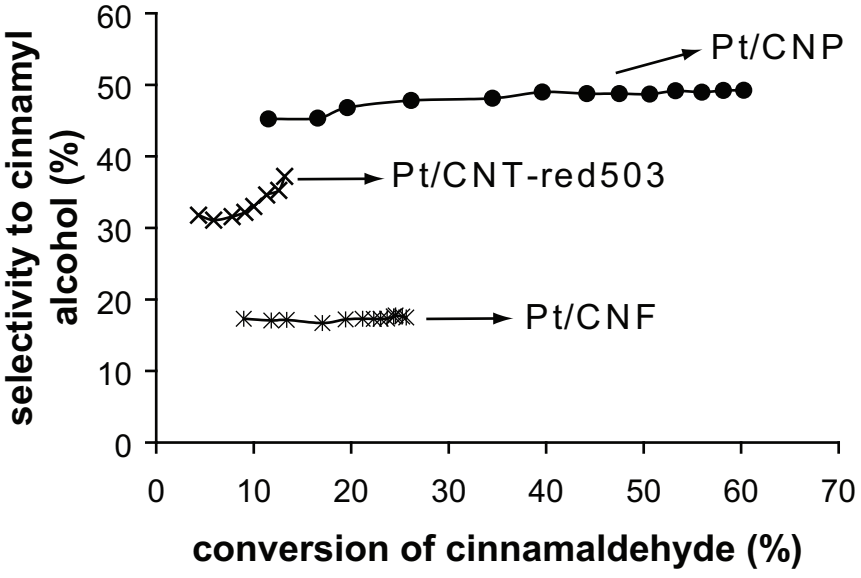

Fig. 8 Conversion vs selectivity for Pt/CNF, Pt/CNP and Pt/CNT-red503.

that the selectivity for Pt/CNP and Pt/CNF changes as a function of the graphene sheet orientation. It is tempting to ascribe this to an electronic effect which has also been used to explain catalytic differences between CNF and CNT materials [5, 24], however that requires more research. For Pt/CNT-red503, the platinum particle sizes, amount of acidic sites as well as the graphene sheet orientation are different compared to Pt/CNF and Pt/CNP. Since it is known that for example variable platinum particle sizes have a significant influence on the catalytic activity [25], it is not possible to establish an intrinsic influence of the CNT graphene sheet orientation with respect to catalytic selectivity.

Conclusions

Platinum was deposited on nitric acid oxidized CNF, CNT and CNP to investigate the influence of the orientation of the support graphene sheets on the reduction characteristics. The TPR profiles showed that the onset reduction temperature increased from 461 K for Pt/CNF to 466 K for Pt/CNP and 487 K for Pt/CNT. The reduction temperature for Pt/CNT was retarded, which we related to the high amount of acidic oxygen surface groups detected on this support. Therefore, a strong stabilization of the cationic platinum species is observed. Application of the required higher reduction temperature resulted in complete reduction for that sample, however the platinum particle size is then larger (2-11 nm) compared to that of Pt/CNF and Pt/CNP (both 1-3 nm). Therefore, the latter two catalysts turned out to be active for the cinnamaldehyde hydrogenation, while reduced platinum on CNT was not very active for this reaction. Pt/CNP is more selective towards cinnamyl alcohol in the cinnamaldehyde hydrogenation compared to Pt/CNF. Since the platinum particle size is the same for both materials, this must be the result of the different orientation of the graphene sheets for the two catalysts.

Literature

1. S.E. Wanke, P.C. Flynn, Cat. Rev. - Sci. Eng., 12(1), 1975, 93-135.
2. M.C. Roman-Martinez, D. Cazorla-Amoros, A. Linares-Solano, C. Salinas-Martinez de Lecea, Carbon, 31(6), 1993, 895-902.
3. N.W. Hurst, S.J. Gentry, A. Jones, B.D. McNicol, Cat. Rev. - Sci. Eng., 24(2), 1982, 233-309.
4. A.B. da Silva, E. Jordao, M.J. Mendes, P. Fouilloux, Appl. Catal. A, 148(2), 1997, 253-264.
5. P. Serp, M. Corrias, P. Kalck, Appl. Catal. A, 253(2), 2003, 337-358.

6. K.P. de Jong, J.W. Geus, Cat. Rev. - Sci. Eng., 42(4), 2000, 481-510.
7. Y. Motoyama, M. Takasaki, K. Higashi, S.H. Yoon, I. Mochida, H. Nagashima, Chem. Lett., 35(8), 2006, 876-877.
8. H. Vu, F. Goncalves, R. Philippe, E. Lamouroux, M. Corrias, Y. Kihn, D. Plee, P. Kalck, P. Serp, J. Catal., 240(1), 2006, 18-22.
9. H.X. Ma, L.C. Wang, L.Y. Chen, C. Dong, W.C. Yu, T. Huang, Y.T. Qian, Catal. Commun., 8(3), 2007, 452-456.
10. M.L. Toebes, Y. Zhang, J. Hájek, T.A. Nijhuis, J.H. Bitter, A.J. van Dillen, D.Y. Murzin, D.C. Koningsberger, K.P. de Jong, J. Catal., 226(1), 2004, 215-225.
11. M.L. Toebes, T.A. Nijhuis, J. Hájek, J.H. Bitter, A.J. van Dillen, D.Y. Murzin, K.P. de Jong, Chem. Eng. Sci., 60(21), 2005, 5682-5695.
12. M.L. Toebes, J.H. Bitter, A.J. van Dillen, K.P. de Jong, Catal. Today, 76(1), 2002, 33-42.
13. A.J. Plomp, H. Vuori, A.O.I. Krause, K.P. de Jong, J.H. Bitter, Appl. Catal. A, 351(1), 2008, 9-15.
14. X. Hao, L. Quach, J. Korah, W.A. Spieker, J.R. Regalbuto, J. Mol. Catal. A: Chem., 219(1), 2004, 97-107.
15. M.K. van der Lee, A.J. van Dillen, J.H. Bitter, K.P. de Jong, J. Am. Chem. Soc., 127(39), 2005, 13573-13582.
16. J.J.F. Scholten, A.P. Pijpers, M.L. Hustings, Cat. Rev. - Sci. Eng., 27(1), 1985, 151-206.
17. M.K. van der Lee, A.J. van Dillen, J.W. Geus, K.P. de Jong, J.H. Bitter, Carbon, 44(4), 2006, 629-637.
18. T.G. Ros, A.J. van Dillen, J.W. Geus, D.C. Koningsberger, Chem. Eur. J., 8(5), 2002, 1151-1162.
19. V. Datsyuk, M. Kalyva, K. Papagelis, J. Parthenios, D. Tasis, A. Siokou, I. Kallitsis, C. Galiotis, Carbon, 46, 2008, 833-840.
20. M.L. Toebes, M.K. van der Lee, L.M. Tang, M.H. Huis in 't Veld, J.H. Bitter, A.J. van Dillen, K.P. de Jong, J. Phys. Chem. B, 108(31), 2004, 11611-11619.
21. T.J. Zhao, D. Chen, Y.C. Dai, W.K. Yuan, A. Holmen, Top. Catal., 45(1-4), 2007, 87-91.
22. M.A. Fraga, E. Jordao, M.J. Mendes, M.M.A. Freitas, J.L. Faria, J.L. Figueiredo, J. Catal., 209(2), 2002, 355-364.
23. S.R. de Miguel, O.A. Scelza, M.C. Roman-Martinez, C. Salinas-Martinez de Lecea, D. Cazorla-Amoros, A. Linares-Solano, Appl. Catal. A, 170(1), 1998, 93-103.

24. J.P. Tessonnier, L. Pesant, G. Ehret, M.J. Ledoux, C. Pham-Huu, Appl. Catal. A, 288(1-2), 2005, 203-210.
25. P. Gallezot, D. Richard, Cat. Rev. - Sci. Eng., 40(1-2), 1998, 81-126.

5

Particle Size Effects for Carbon Nanofiber Supported Platinum and Ruthenium Catalysts for the Selective Hydrogenation of Cinnamaldehyde

Abstract

The selective hydrogenation of cinnamaldehyde was studied over carbon nanofibers (CNF) supported platinum and ruthenium catalysts. The catalysts differed independently in their metal particle sizes and amount of acidic oxygen groups on the CNF surface. For the catalysts with oxygen on the CNF surface, the larger metal particles (~ 3.5 nm) displayed the highest selectivity towards cinnamyl alcohol. Surprisingly, when the oxygen groups were removed from the catalyst surface, the smaller particles (~ 2.0 nm) exhibited the highest selectivity to cinnamyl alcohol. Also the hydrogenation activity increased for all catalysts after oxygen removal. A model is proposed to account for the role of the metal particle size and oxygen surface groups in the hydrogenation of cinnamaldehyde.

Introduction

The hydrogenation of cinnamaldehyde can proceed via two pathways, i.e. via the formation of cinnamyl alcohol or via the formation of hydrocinnamaldehyde. In both cases the final product is hydrocinnamyl alcohol. The reaction via hydrocinnamaldehyde is thermodynamically more favorable, however the most desired product is the partially hydrogenated product cinnamyl alcohol [1, 2]. The selectivity towards cinnamyl alcohol using platinum or ruthenium based catalysts seems to depend on the metal particle and the selectivity increased with increasing metal particle size [1, 3-9]. Giroir-Fendler et al. [5] attributed this particle size effect to a directing effect of the phenyl group. The authors proposed that the phenyl group is repelled by the metal surface in that way hampering the C=C bond to approach the metal surface. Therefore, only the C=O bond can approach the metal resulting in a higher selectivity for C=O bond hydrogenation (see Fig. 1). In contrast, on small particles the phenyl ring does not interact with the metal surface and therefore both the C=O and the C=C bond can reach the metal surface and become hydrogenated. Alternatively, Galvagno et al. [8] hypothesized that the relative amounts of corners, edges and faces exposed to the reactants vary as function of the particle size. The atoms in different crystallographic positions can have different catalytic properties, resulting in different selectivities and activities as a function of the particle size. The particle size effect is also observed when using cobalt catalysts for cinnamaldehyde and crotonaldehyde hydrogenations and when using platinum catalysts for the crotonaldehyde hydrogenation [10, 11]. On the other hand, it is not observed for citral or acrolein hydrogenations on ruthenium catalysts [6, 12, 13].

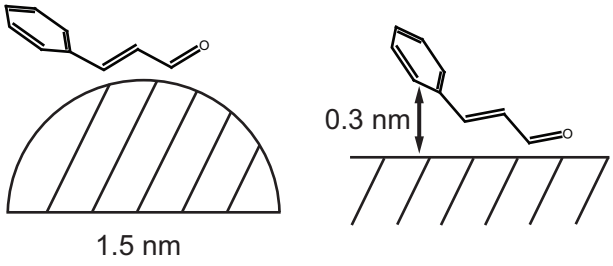

Fig. 1 Adsorption of cinnamaldehyde on a small metal particle (left) and a large non-curved particle (right). (Reproduced from Giroir-Fendler et al. [5] with kind permission of Springer Science and Business Media).

Some studies addressed the particle size effect on platinum supported on carbon-based supports [4, 5]. In those studies, the particle size was varied by using different calcination or reduction temperatures after catalyst preparation. Unfortunately, these treatments do not only influence the metal particle sizes, but the amount of oxygen groups on the surface of the carbon support is modified as well. The latter might have a significant influence on the catalytic performance of carbon based catalysts as was for example shown by Toebes et al. [14, 15]. In these studies, it was shown that the activity of Pt/CNF catalysts significantly increased after removing oxygen groups from the support surface, although the selectivity to

the desired cinnamyl alcohol decreased. Therefore we report here a systematic study on the influence of oxygen surface groups on the particle size effect of both platinum and ruthenium supported on CNF.

CNF are inert and pure graphite-like materials with a high specific surface area [16]. Therefore, CNF can be used conveniently as a model to study supported, catalytically active nanoparticles [17]. In the current study, platinum and ruthenium particle size effects were investigated for the selective hydrogenation of cinnamaldehyde using CNF as support. Samples which differed in their platinum or ruthenium particle size (1-3 and 2-6 nm for both metals) and amount of acidic oxygen groups on the CNF surface, either 0.17 groups/nm^2 or without oxygen surface groups, were studied. We opted for varying the particle size by preparing the catalysts in two different ways, i.e. atomic layer deposition (ALD) and homogeneous deposition precipitation (HDP). Via heat-treatments in inert conditions, the oxygen surface groups could be removed completely, while the metal particle sizes were not affected [14].

Experimental

The Ni/SiO_2 (20 wt-%) growth catalyst was prepared via HDP using 17.0 g silica (Degussa; Aerosil 200), 21.1 g nickel nitrate hexahydrate (Acros; 99%) and 13.9 g urea (Acros; p.a.) in 1 L demineralized water according to an earlier described procedure [18].

CNF growth was adapted from Toebes et al. [18]. For CNF growth the Ni/SiO_2 catalyst (2 g) was loaded in a quartz boat and placed horizontally in a tubular furnace. The catalyst was reduced in a H_2/N_2 mixture (276/1026 mL/min) at 973 K (ramp 5 K/min) for 2 h at 3.4-3.8 bar total pressure. Next, the temperature was decreased to 823 K and the CNF were grown for 24 h from $CO/H_2/N_2$ (441/148/704 mL/min) at 3.4-3.8 bar total pressure. The raw material (30 g) was collected and refluxed for 1 h in an aqueous KOH solution (0.6 L; 1 M) to remove the SiO_2. After washing, the material was refluxed for 2 h in concentrated nitric acid (0.6 L; Merck; 65%) to remove exposed nickel and introduce oxygen containing groups on the CNF surface. The material was filtered again, washed three times with demineralized water and dried overnight at 393 K. This material is referred to as CNF-ox.

Platinum [14] and ruthenium [19] were deposited on CNF-ox using HDP as described before. The prepared catalysts were reduced at 473 K for 1 h (ramp 5 K/min) in 10% v/v H_2/N_2 (100 mL/min) and subsequently crushed and sieved in a fraction of 25-90 μm. The resulting platinum catalyst was denoted as Pt/CNF (HDP). Part of the platinum and ruthenium catalysts was treated in N_2-flow at 973 K for 2 hours (5 K/min) to remove the oxygen surface

groups [14, 19]. The resulting catalysts are denoted as Pt/CNF-973 (HDP) and Ru/CNF-973 (HDP).

Platinum and ruthenium on CNF-ox catalysts were also prepared using ALD in a flow-type F-120 reactor (ASM Microchemistry) that operated at a reduced pressure of 5-10 mbar. CNF-ox (2.5 g) were placed in a quartz reactor and heated to 473 K. Subsequently, 1.2 g $Ru_3(CO)_{12}$ or $Pt(acac)_2$ (Volatec Oy) was evaporated at 413 K and 453 K respectively in flowing nitrogen and led over CNF-ox for at least 3 h to ensure complete reaction. After the reaction, the excess reactants and gaseous by-products were removed by purging with nitrogen. The prepared catalysts were reduced at 473 K for 1 h (ramp 5 K/min) in 10% v/v H_2/N_2 (100 mL/min) and subsequently crushed and sieved in a fraction of 25-90 μm. The resulting platinum catalyst was denoted as Pt/CNF (ALD). Part of the platinum and ruthenium catalysts was treated in N_2-flow at 973 K for 2 hours (5 K/min) to remove the oxygen surface groups [14, 19]. The resulting catalysts are denoted as Pt/CNF-973 (ALD) and Ru/CNF-973 (ALD).

Cinnamaldehyde hydrogenation was performed at 313 K and a pressure of 1200 mbar H_2. The hydrogenation set-up consisted of a thermostatic double-walled glass reactor, equipped with baffles and a gas-tight mechanical stirrer with a hollow shaft and blades for gas recirculation. The reactor was loaded with tetradecane as internal standard (4.57 g; Acros; 99%), the catalyst and the solvent (100 mL 2-propanol with 17.5 mL demineralized water). The amount of catalyst was 0.3 g for Pt/CNF (ALD) and Pt/CNF-973 (ALD) and 1 g for the other catalysts to ensure a constant amount of catalytic metal in the reactor. The stirrer was switched on (1700 rpm) and the slurry was saturated with H_2 for 30 minutes. Next, t-cinnamaldehyde (1.65 g; Acros; p.a.) was added and the reaction was run for 5 hours. Samples were taken at different time intervals. The samples were analyzed on a Shimadzu GC 2010 equipped with auto injector, FID detector and CP WAX 52 CB column. The conversion of cinnamaldehyde (CALD) and selectivity to cinnamyl alcohol (CALC) were calculated as described earlier [20]:

$$Conversion(t) = \frac{([CALD(0)] - [CALD(t)])}{[CALD(0)]} \times 100\%$$

$$Selectivity(t) = \frac{[CALC(t)]}{([CALD(0)] - [CALD(t)])} \times 100\%$$

The platinum weight-loading of the Pt/CNF (HDP) catalyst was analyzed using calibrated X-ray fluorescence spectroscopy (Spectro X-lab 2000). For analysis 2-4 g of the

dry catalyst powder was used. The metal weight loadings of the other catalysts were determined using ICP-AES. The catalysts were treated in aqua regia at 473 K to dissolve the metal. Analysis was performed using a Varian Liberty series II ICP-AES apparatus. Each sample was analyzed twice and the results were averaged.

Acid-base titrations were performed using a Titralab TIM 880 apparatus. To 0.05 g of catalyst 60 mL of 0.1 M KCl was added. This slurry was titrated with a solution containing 0.01 M NaOH and 0.1 M KCl. The required amount of titrant to reach pH 7.5 was used to calculate the amount of acidic sites on the catalysts, as described by Toebes et al. [21].

TEM was performed using a Tecnai 20 FEG operating at 200 kV and a point resolution of 2.7 Å. The samples were suspended in ethanol using an ultrasonic treatment and brought onto a holey carbon film on a copper grid. Based on TEM, particle size histograms were compiled. The average particles sizes were recalculated to dispersion values assuming spherical shapes and using the formula described by Scholten et al. [22]:

$$D = 10^{21} \frac{6 \times M \times \rho_{site}}{d \times \rho_{metal} \times N}$$

D is dispersion ($Pt_{surface}/Pt_{total}$), M the atomic weight (195.1 g/mol for Pt, 101 g/mol for Ru), ρ_{site} the platinum surface site density (12.5 Pt atoms/nm^2, 16.3 Ru atoms/nm^2) [22], d is particle size (nm), ρ_{metal} the metal density (21.45 g/cm^3 for Pt, 12.3 g/cm^3 for Ru) and N the Avogadro constant giving D = 1.13/d (nm) for Pt and D = 1.33/d (nm) for Ru.

Nitrogen physisorption was performed at 77 K using a Micromeritics Tristar 3000 V6.04 A. The obtained data were used to calculate the BET surface area. Prior to the physisorption measurements, the samples were dried at 473 K for about 14 hours under nitrogen flow.

Hydrogen chemisorption measurements were performed with pure hydrogen at 303 K using a Coulter Omnisorp 100CX apparatus in static volumetric mode. Before the measurement, the samples (0.15 g) were outgassed in situ at room temperature ($<10^{-3}$ Pa) followed by purging with helium at 373 K for 30 min. Then, samples were re-reduced in flowing hydrogen at 373 K for 60 min. After reduction, the samples were outgassed at 373 K for 30 min to remove hydrogen. Finally, the temperature was lowered to 303 K for the chemisorption measurement. The adsorption isotherm was measured twice with one hour evacuation between the measurements, thus giving both total and reversible adsorption isotherms. The total amount of adsorbed hydrogen was used for further calculations. The sample was weighed after the measurement to obtain the mass corresponding to reduced and dry sample. This value was used for the calculations.

Results and Discussion

Some of the physical-chemical properties of the platinum and ruthenium catalysts are summarized in Table 1. Two different batches of CNF were used. The BET surface area was slightly different, however this difference falls within the reproducibility range of CNF synthesis. The metal loading for the platinum catalysts prepared via ALD resulted in 11.0 wt-%, while via HDP the metal loading resulted in 3.0 wt-%. The high metal loading obtained after ALD synthesis can be explained by the gasphase-decomposition of $Pt(acac)_2$ during preparation [23]. In that way platinum does not only decompose on the oxygen surface groups of the support as desired but also directly from the gasphase without the need of adsorption sites on the support.

For the ruthenium catalysts, the metal loading was determined to be 2.1 wt-% for the HDP prepared catalyst and 2.8 wt-% for the ALD prepared catalyst (see Table 1). The metal loadings of these catalysts were much closer to each other, compared to the platinum catalysts. Apparently, $Ru_3(CO)_{12}$ does not suffer from gasphase-decomposition when deposited via ALD.

Representative TEM images of the prepared samples before and after heat-treatment are depicted in Fig. 2 and 3. The particle size distributions obtained from TEM are summarized in Fig. 4 and Table 1. Platinum particle sizes for the HDP prepared catalysts were 1-3 nm independent of the heat-treatment while ALD resulted in platinum particles which were larger, i.e. 2-6 nm, irrespective whether the samples were subjected to a temperature treatment or not. Upon heat-treatment, the average particle size increased, but as

Table 1. Physical properties of the catalysts.

	BET (m^2/g)	metal loading (wt-%)	average metal particle size (nm, based on TEM)	Dispersion based on TEM	H/M ratio (measured using H_2-chemisorption)	acidic, oxygen surface groups (nm^{-2})	initial TOF (x 10^{-2} s^{-1}, based on TEM dispersion)
Pt/CNF (HDP)	178	3.0	1.8	0.63	0.83	0.17	5.2
Pt/CNF-973 (HDP)	178	3.0	2.0	0.57	0.46	0.00	7.3
Pt/CNF (ALD)	143	11.0	3.3	0.34	0.52	0.15	9.6
Pt/CNF-973 (ALD)	143	11.0	3.4	0.33	0.39	0.00	8.1
Ru/CNF-973 (HDP)	178	2.1	2.2	0.61	0.81	0.00	6.7
Ru/CNF-973 (ALD)	178	2.8	3.5	0.38	0.29	0.00	2.7

already mentioned, the size range remained similar (see also Fig. 4). Also for the ruthenium samples the HDP synthesis resulted in smaller particles (1-3 nm) while ALD resulted in larger particles (2-6 nm). Hydrogen chemisorption showed that for all platinum samples the hydrogen chemisorption capacity decreased after the heat-treatments (Table 1). The results for the HDP-prepared platinum samples are in line with results obtained by Toebes et al. [14]. When the dispersions based on hydrogen chemisorption, i.e. H/M ratios, are compared to those based on TEM a clear discrepancy can be observed (Table 1). The dispersions based on TEM decreased less upon heat-treatment as compared to the hydrogen chemisorptions based dispersions which showed a strong decrease. Apparently, the hydrogen chemisorption capacity of all samples was significantly suppressed after heat-treatment. As described by Scholten et al. [22], different pre-treatments of catalysts may affect the chemical state of the metal or the support thereby changing the direct chemical environment, which has a significant influence on hydrogen chemisorption results. Moreover, it is described that the catalyst support is not necessarily inert towards chemisorbed hydrogen. Since in our case the heat-treatment removes most of the oxygen groups on the CNF surface, we speculate that after heat-treatment the hydrogen spill-over is less significant resulting in a lower H/M ratio. This might explain the large decrease of chemisorbed hydrogen after heat-treatment.

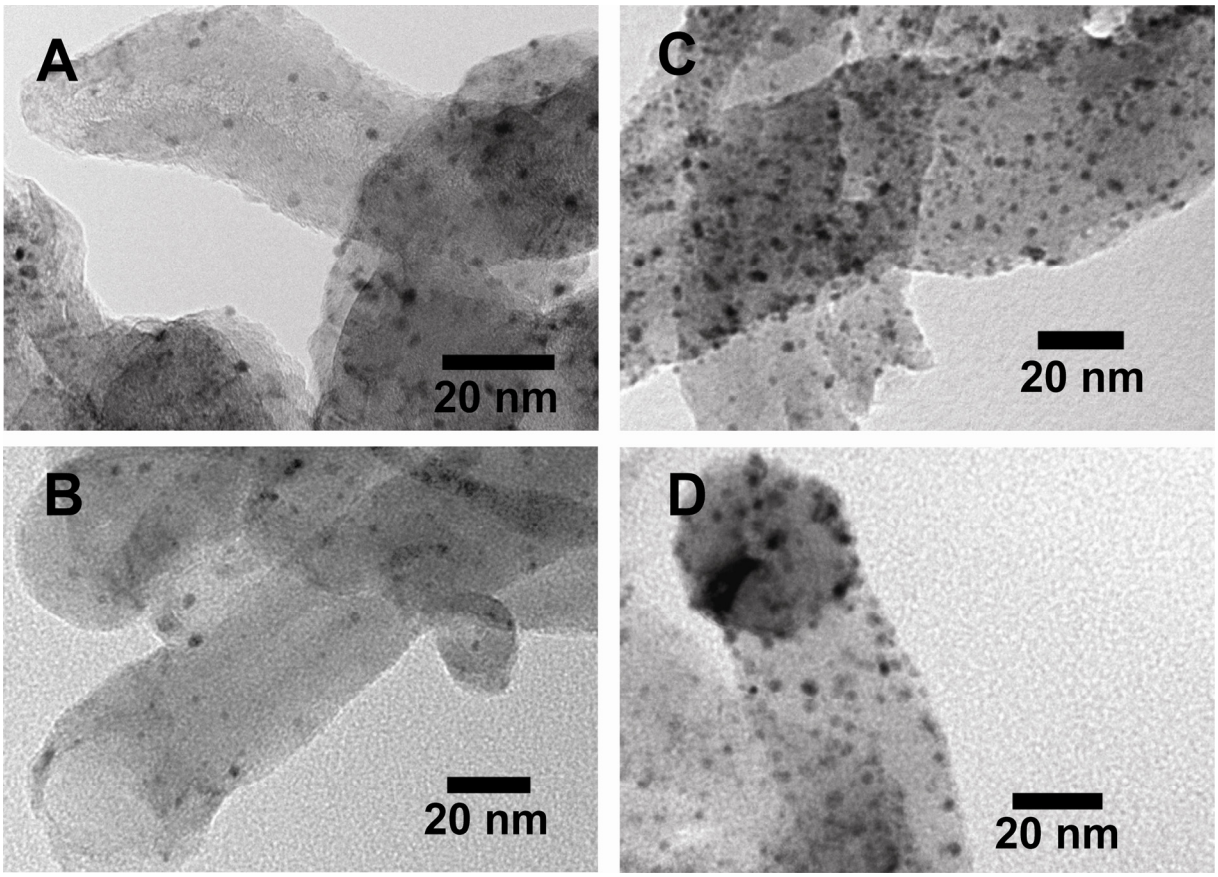

Fig. 2 TEM images of [A] Pt/CNF (HDP) [B] Pt/CNF-973 (HDP) [C] Pt/CNF (ALD) [D] Pt/CNF-973 (ALD).

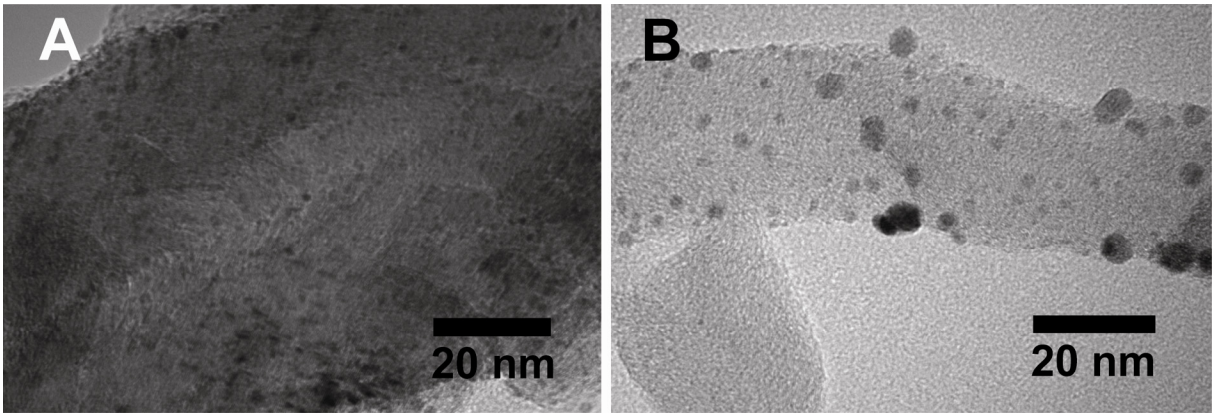

Fig. 3 TEM images of [A] Ru/CNF-973 (HDP) [B] Ru/CNF-973 (ALD).

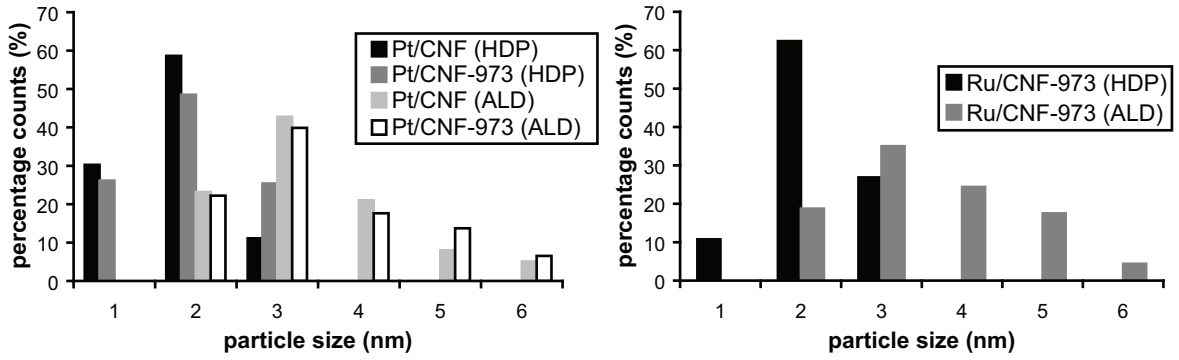

Fig. 4 TEM-based particles size histograms of the platinum catalysts (left) and ruthenium catalysts (right). Measurements are based on 90 – 160 particles per sample.

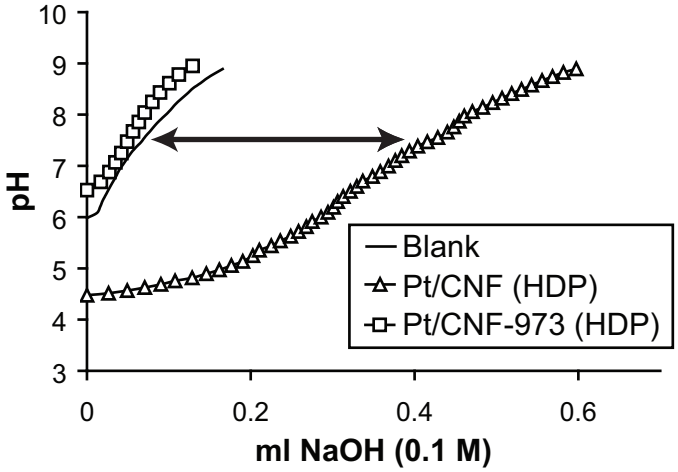

Fig. 5 Titration curves for Pt/CNF (HDP) and Pt/CNF-973 (HDP). The arrow indicates the NaOH consumption at pH 7.5, which is used for the calculation of acidic groups.

To quantify the amount of acidic oxygen surface groups (pKa<7.5), acid-base titrations were performed. Fig. 5 shows typical titrations curves for Pt/CNF (HDP) and Pt/CNF-973 (HDP). Before heat-treatment, the amount of acidic, oxygen surface groups detected by titration were similar for Pt/CNF (HDP) and Pt/CNF (ALD), i.e. 0.15-0.17 acidic, oxygen surface groups/nm^2. After heat-treatment, all these groups were removed for all catalysts, as can be observed in Fig. 5. The titration curve showed a slightly basic character for the heat-treated catalyst indicating that a small amount of basic groups remained on the CNF surface after heat-treatment [24].

The activity of the platinum based catalysts for cinnamaldehyde hydrogenation is shown in Fig. 6. Initial turn-over frequencies (TOF) based on initial conversion and dispersions based on TEM are reported in Table 1. TEM was used to determine the accessible metal surface area as we feel it is the most reliable technique. As argued above, the alternative, i.e. hydrogen chemisorption is less reliable. The hydrogen chemisorption capacity of the samples might be influenced by hydrogen spill-over which, in turn, might depend on the support composition, i.e. presence or absence of oxygen surface groups. The abbreviations used, i.e. cinnamaldehyde (CALD), hydrocinnamaldehyde (HALD), cinnamyl alcohol (CALC) and hydrocinnamyl alcohol (HALC) are explained in Fig. 7. Please, note that CALC is the desired product.

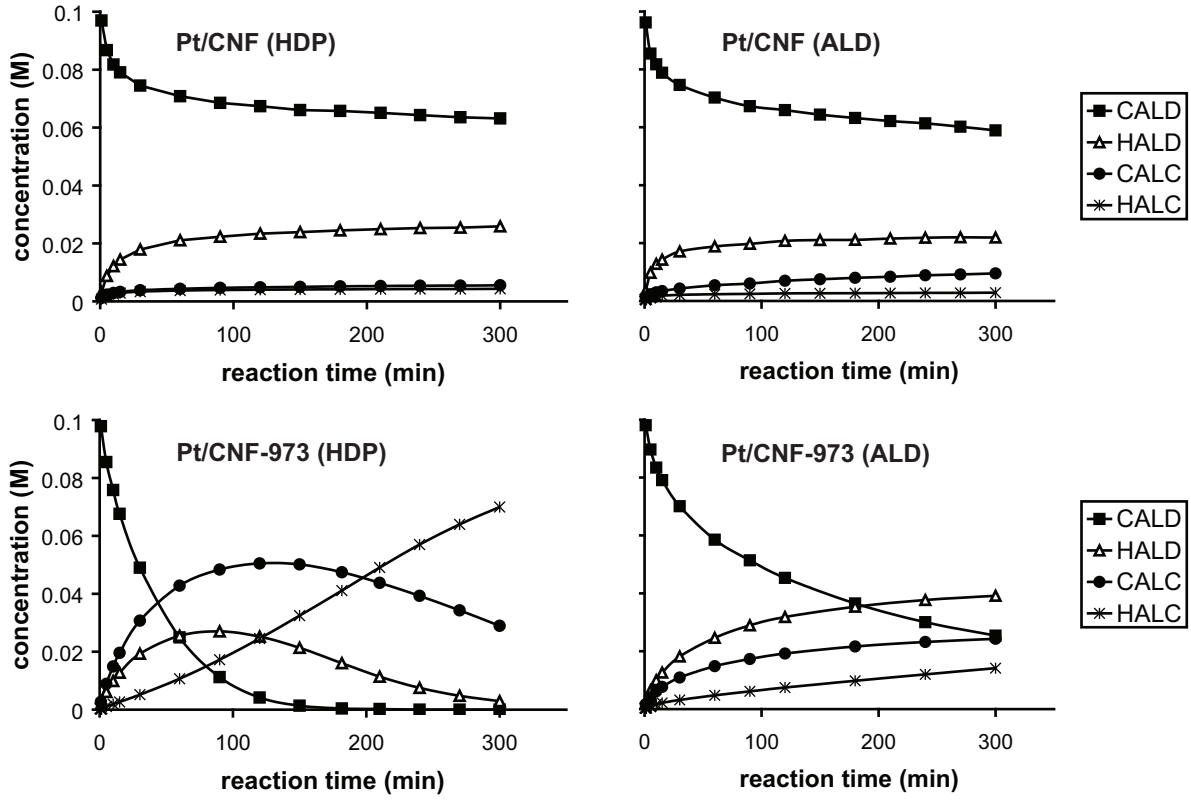

Fig. 6 Cinnamaldehyde hydrogenation results of the different platinum catalysts.

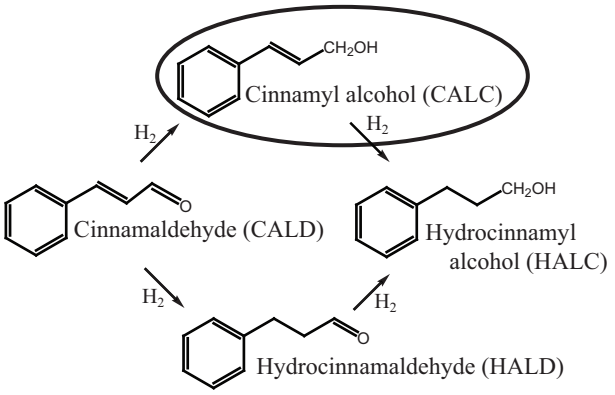

Fig. 7 Hydrogenation pathway of cinnamaldehyde, the desired product is encircled.

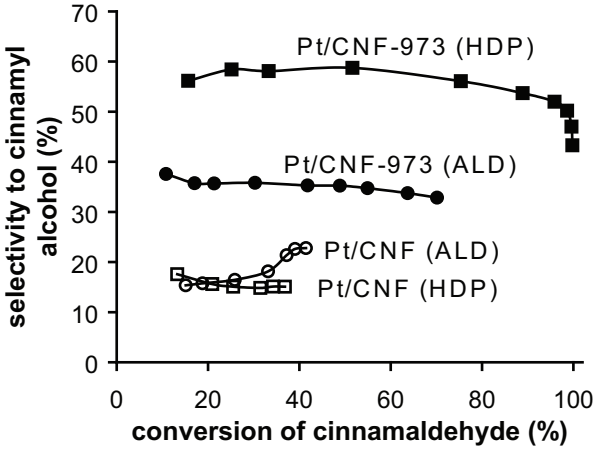

Fig. 8 Conversion vs. selectivity plot of the platinum catalysts.

Pt/CNF (HDP) and Pt/CNF (ALD) reached only about 25% conversion after 300 min forming HALD as the major product. Since the calculated TOF shows that initial activity is within the same range for all catalysts, while the activity of Pt/CNF (HDP) and Pt/CNF (ALD) levelled off, we concluded that deactivation of the latter catalysts occurred (Fig. 6). After heat-treatment, the activity of all samples increased as was also shown previously by Toebes et al. [14]. Pt/CNF-973 (HDP) converted all CALD within 150 min and Pt/CNF-973 (ALD) converted 70% of CALD in 300 min. Pt/CNF-973 (ALD) converted the majority of CALD into HALD, while for Pt/CNF-973 (HDP) the selectivity changed from initially CALC (max 59%) as primary product to the final product HALC after longer reaction time (120 min on stream). In Fig. 8 the conversion of CALD is plotted versus the selectivity to CALC. The selectivities of the non heat-treated catalysts were in the same range and independent of the CALD conversion for Pt/CNF (HDP), thereby suggesting that deactivation did not influence the selectivity to a large extent. For Pt/CNF (ALD) an increasing selectivity with conversion is observed, thereby exceeding the selectivity of Pt/CNF (HDP) at higher conversions. We cannot explain the observed selectivity increase at higher CALD conversions. Nevertheless, upon heat-treatment, the selectivity was significantly enhanced and Pt/CNF-973 (HDP) showed the highest selectivity and activity.

For all tested catalysts it is observed during CALD conversion that small amounts of by-products (less than 2%) were formed. The by-products were mainly ethylbenzene and propylbenzene. Only for Pt/CNF (ALD) 6% of by-products was observed. The non heat-treated catalysts resulted in the highest amounts of ethylbenzene, i.e. 0.3% for both platinum catalysts. After heat-treatment, Pt/CNF-973 (ALD) resulted in 0.2% ethylbenzene whereas for Pt/CNF-973 (HDP) ethylbenzene was not observed at all. The process of decarbonylation is

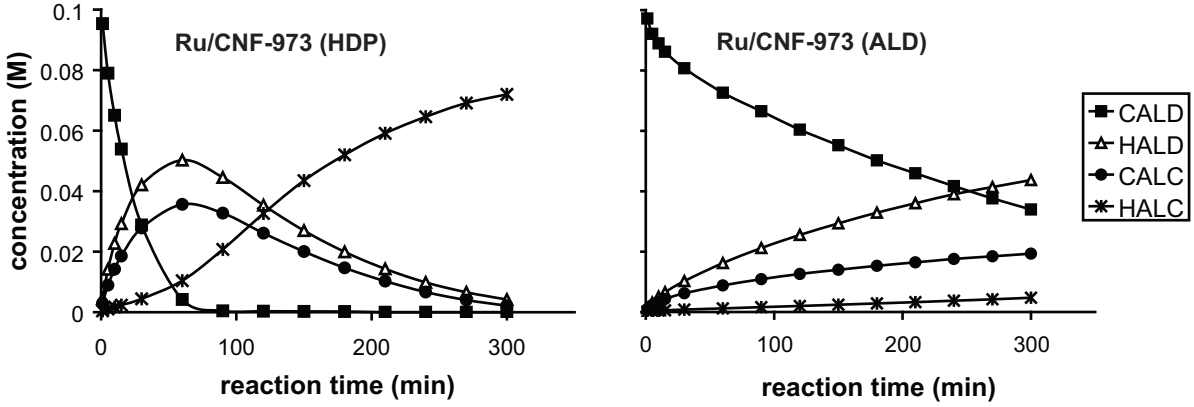

Fig. 9 Cinnamaldehyde hydrogenation results of the ruthenium catalysts.

also associated with catalytic deactivation for liquid-phase hydrogenations and may therefore explain the observed deactivation for the non heat-treated catalysts in this study [25].

The activity of Ru/CNF-973 (HDP) and Ru/CNF-973 (ALD) is depicted in Fig. 9. Ru/CNF-973 (HDP) converted all CALD within 90 min, while Ru/CNF-973 (ALD) converted 65% of CALD in 300 min. For both catalysts HALD was the major initial product. In Fig. 10 the conversion of CALD for the ruthenium catalysts is plotted versus the selectivity to CALC. The selectivity to CALC was higher for Ru/CNF-973 (HDP) compared to Ru/CNF-973 (ALD).

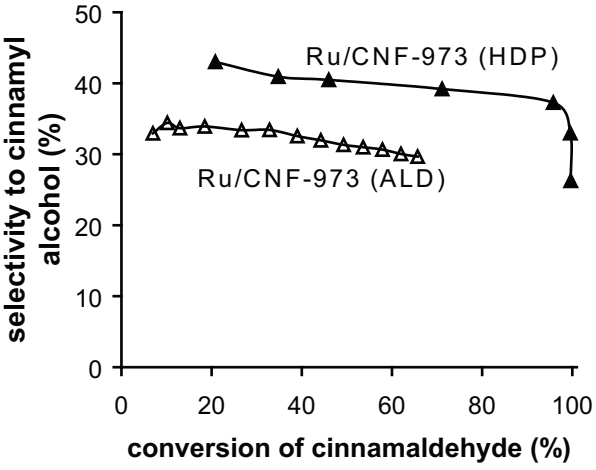

Fig. 10 Conversion vs. selectivity plot of the two ruthenium catalysts.

The aim of this study was to investigate platinum and ruthenium particle size effects on carbon nanofibers for the cinnamaldehyde hydrogenation, while the amount of oxygen surface groups was similar for all samples. The results summarized in Table 1 show that we were successful in preparing two platinum samples, one with small (on average 1.8 nm) particles (Pt/CNF (HDP)) and one with larger (on average 3.3 nm) particles (Pt/CNF (ALD)) while the amount of oxygen surface groups was the same (0.15 - 0.17 groups/nm^2). In addition two samples were prepared with similar particle sizes but without oxygen groups on the surface: Pt/CNF-973 (HDP) and Pt/CNF-973 (ALD). For ruthenium based catalysts only two samples were prepared with different particle sizes, i.e. 2.2 nm

(Ru/CNF-973 (HDP)) versus 3.5 nm (Ru/CNF-973 (ALD)) without oxygen groups on the surface.

The catalytic tests (Fig. 8) showed that when oxygen surface groups were present large platinum particles (Pt/CNF (ALD)) resulted in a higher selectivity to CALC compared to small platinum particles (Pt/CNF (HDP)). This is fully in line with results described in literature [1]. Unexpectedly, the catalysts which were heat-treated, i.e. without oxygen surface groups, showed a reversed particle size effect: small metal particles for both platinum and ruthenium catalysts resulted in a higher selectivity to cinnamyl alcohol compared to the larger metal particles (see Fig. 8 & 10). It was also observed that after heat-treatment, the activity and selectivity were strongly enhanced for the platinum catalysts (see Fig. 6).

Since the particle sizes were hardly influenced by the heat-treatment, the reversed particle size effect after heat-treatment must result from the decrease in amount of oxygen groups on the support surface. In earlier work from Toebes et al. [14] it was shown that the electronic state of platinum is not significantly changed by the presence or absence of oxygen surface groups. Therefore we propose that the change in adsorption properties is the main reason for the change in catalytic behavior of the samples.

An adsorption/repulsion model is proposed to explain the reversed particle size effect and is schematically depicted in Fig. 11. The catalysts with a high amount of oxygen surface groups (i.e. non heat-treated) may repel the phenyl ring from the support surface, as described before [15]. Small metal particles on Pt/CNF (HDP) interact with the C=O and C=C bonds of the α,β-unsaturated aldehyde group, whereas for large metal particles on Pt/CNF (ALD) the reactant phenyl ring is repelled from the polar support surface as well as from the metal

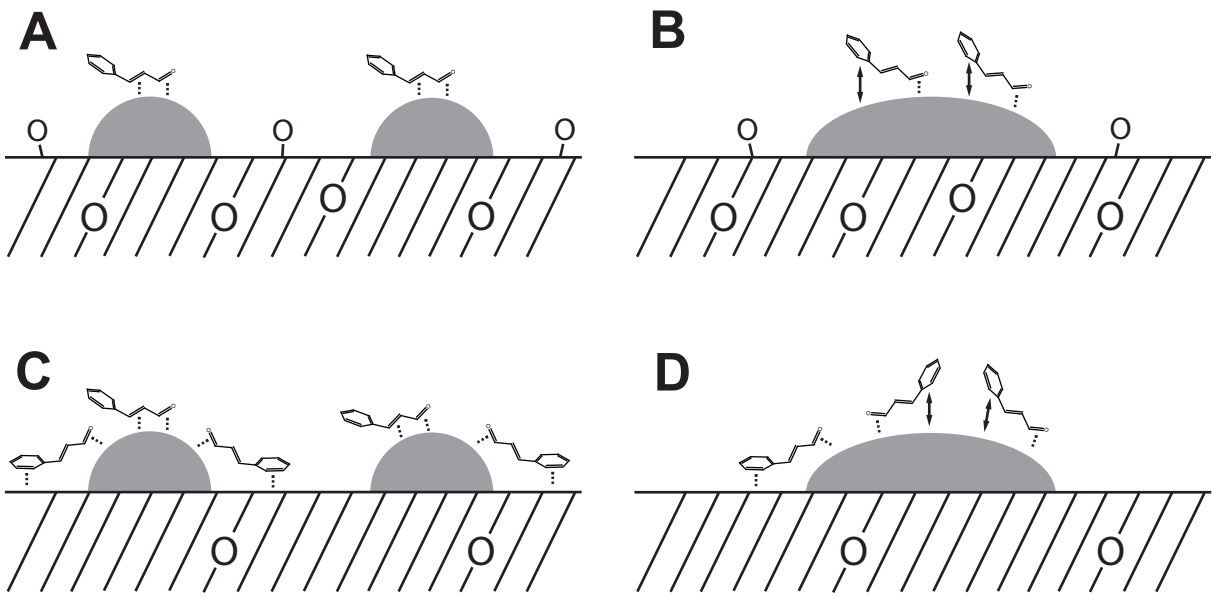

Fig. 11 Proposed model for the observed particle size effects: (A) small particles on polar surface (B) large particles on polar surface (C) small particles on non-polar surface (D) large particles on non-polar surface.

surface. In the latter situation, the C=O bond is directed towards the platinum surface [5], resulting in a higher selectivity towards cinnamyl alcohol compared to Pt/CNF (HDP) (see also Fig. 1). After removal of the oxygen surface groups, cinnamaldehyde adsorption via the phenyl ring is enhanced due to the less polar catalyst surface, resulting in a higher activity [15]. In the latter case, the reactant is adsorbed in the vicinity of platinum and the metal periphery is involved in the hydrogenation as well. The reactant may direct the C=O bond towards the metal periphery leading to an increase in selectivity and activity. This will occur for both small and larger metal particles, but the metal periphery area is much lower for the catalyst with larger particles. Therefore, the overall increase in activity and selectivity for Pt/CNF-973 (ALD) is lower compared to Pt/CNF-973 (HDP). The reversed particle size effect observed for the non-oxygen containing ruthenium catalysts are in line with the results for the non-oxygen containing platinum catalysts. Therefore, the results with ruthenium support the proposed model.

The cinnamaldehyde hydrogenation results observed for Pt/CNF (HDP) and Pt/CNF-973 (HDP) catalysts described in this study show an enhanced selectivity upon heat-treatment. This is the opposite trend as observed by Toebes et al. [14], who observed a decrease in selectivity upon heat-treatment. It is described in a review of Gallezot et al. [1] that for osmium-catalyzed crotonaldehyde hydrogenation the selectivity trend upon increased hydrogenation pressure may either increase or decrease depending on the support and pre-treatment. This is confirmed by Mäki-Arvela et al. [26], who described in a review that for the selective hydrogenation of cinnamaldehyde the selectivity may decrease or remain constant upon increased hydrogenation pressure depending on the support used. Therefore, the observed difference in selectivity trends is ascribed to the use of different temperatures and pressures during reaction in this study and the study of Toebes et al.

Conclusions

Different sized platinum and ruthenium particles were deposited on CNF via ALD and HDP, resulting in metal particles of 2-6 nm via ALD and metal particles of 1-3 nm via HDP. The platinum catalysts with oxygen groups on the CNF surface showed the highest selectivity towards cinnamyl alcohol for the largest metal particles, which is in line with results described in literature. After removal of the oxygen surface groups via a heat-treatment, the smallest metal particles resulted in the highest selectivity towards cinnamyl alcohol, resulting in a reversed particle size effect compared to the catalytic results obtained with polar supports. The observed particle size effects are explained by a change in the adsorption mode of the reactant as a function of the polarity of the support. After removal of oxygen surface groups,

the non-polar support favors the adsorption of the phenyl ring, which enables the metal periphery to participate in the hydrogenation. This may result in the direction of the C=O bond to the metal periphery. For smaller metal particles, a higher metal periphery area is present and this will result in a higher increase in activity and selectivity compared to larger metal particles.

Literature

1. P. Gallezot, D. Richard, Cat. Rev. - Sci. Eng., 40(1-2), 1998, 81-126.
2. R.G. Eilerman, in: R.E. Kirk, D.F. Othmer (Eds.), Concise encyclopedia of chemical technology, 4th ed., Wiley, New York, 1999.
3. L. Mercadante, G. Neri, C. Milone, A. Donato, S. Galvagno, J. Mol. Catal. A: Chem., 105(3), 1996, 93-101.
4. D. Richard, P. Fouilloux, P. Gallezot, Proc. Int. Congr. Catal., 9th, 3, 1988, 1074-1081.
5. A. Giroir-Fendler, D. Richard, P. Gallezot, Catal. Lett., 5(2), 1990, 175-182.
6. S. Galvagno, C. Milone, G. Neri, A. Donato, R. Pietropaolo, Stud. Surf. Sci. Catal., 78(Heterogeneous Catalysis and Fine Chemicals III), 1993, 163-170.
7. B. Coq, P.S. Kumbhar, C. Moreau, P. Moreau, M.G. Warawdekar, J. Mol. Catal., 85(2), 1993, 215-228.
8. S. Galvagno, G. Capannelli, G. Neri, A. Donato, R. Pietropaolo, J. Mol. Catal., 64(2), 1991, 237-246.
9. M. Lashdaf, J. Lahtinen, M. Lindblad, T. Venalainen, A.O.I. Krause, Appl. Catal. A, 276(1-2), 2004, 129-137.
10. M. Englisch, A. Jentys, J.A. Lercher, J. Catal., 166(1), 1997, 25-35.
11. Y. Nitta, K. Ueno, T. Imanaka, Appl. Catal., 56(1), 1989, 9-22.
12. S. Galvagno, C. Milone, A. Donato, G. Neri, R. Pietropaolo, Catal. Lett., 18(4), 1993, 349-355.
13. B. Coq, F. Figueras, P. Geneste, C. Moreau, P. Moreau, M. Warawdekar, J. Mol. Catal., 78(2), 1993, 211-226.
14. M.L. Toebes, Y. Zhang, J. Hájek, T.A. Nijhuis, J.H. Bitter, A.J. van Dillen, D.Y. Murzin, D.C. Koningsberger, K.P. de Jong, J. Catal., 226(1), 2004, 215-225.
15. M.L. Toebes, T.A. Nijhuis, J. Hájek, J.H. Bitter, A.J. van Dillen, D.Y. Murzin, K.P. de Jong, Chem. Eng. Sci., 60(21), 2005, 5682-5695.
16. K.P. de Jong, J.W. Geus, Cat. Rev. - Sci. Eng., 42(4), 2000, 481-510.

17. G.L. Bezemer, P.B. Radstake, V. Koot, A.J. van Dillen, J.W. Geus, K.P. de Jong, J. Catal., 237(2), 2006, 291-302.
18. M.L. Toebes, J.H. Bitter, A.J. van Dillen, K.P. de Jong, Catal. Today, 76(1), 2002, 33-42.
19. M.L. Toebes, F.F. Prinsloo, J.H. Bitter, A.J. van Dillen, K.P. de Jong, J. Catal., 214(1), 2003, 78-87.
20. T. Vergunst, PhD-thesis, Delft University of Technology, Delft, 1999.
21. M.L. Toebes, J.M.P. van Heeswijk, J.H. Bitter, A.J. van Dillen, K.P. de Jong, Carbon, 42(2), 2004, 307-315.
22. J.J.F. Scholten, A.P. Pijpers, M.L. Hustings, Cat. Rev. - Sci. Eng., 27(1), 1985, 151-206.
23. M. Utriainen, M. Kroger-Laukkanen, L.S. Johansson, L. Niinisto, Appl. Surf. Sci., 157(3), 2000, 151-158.
24. H.P. Boehm, Carbon, 32(5), 1994, 759-769.
25. P. Maki-Arvela, N. Kumar, K. Eranen, T. Salmi, D.Y. Murzin, Chem. Eng. J., 122(3), 2006, 127-134.
26. P. Maki-Arvela, J. Hajek, T. Salmi, D.Y. Murzin, Appl. Catal. A, 292, 2005, 1-49.

6

Catalysts based on Platinum-Tin and Platinum-Gallium in Close Contact for the Selective Hydrogenation of Cinnamaldehyde

Abstract

Bimetallic platinum-tin and platinum-gallium catalysts supported on carbon nanofibers (CNF) were prepared via reductive deposition precipitation and impregnation. Detailed EXAFS, TEM-EDX and XPS studies showed that reductive deposition precipitation resulted in a close contact of tin with platinum. These bimetallic catalysts displayed an improved selectivity for cinnamaldehyde hydrogenation towards the desired cinnamyl alcohol as compared to the monometallic platinum catalyst and a bimetallic catalyst prepared by impregnation in which such a close interaction was absent. The general applicability of reductive deposition precipitation as synthesis technique was demonstrated using tin and gallium as promoters.

Introduction

Platinum supported on carbon nanofibers (CNF) turned out as one of the most active catalysts for the hydrogenation of cinnamaldehyde [1, 2]. To achieve this high activity, it was crucial to remove the majority of the oxygen surface groups from the CNF catalysts. These oxygen surface groups were initially indispensible for obtaining a high platinum dispersion [1, 3]. In general the activity for hydrogenation was high, while the selectivity towards the desired cinnamyl alcohol was low [1, 2, 4]. Therefore the challenge is to increase the selectivity of these Pt/CNF catalysts while maintaining a high activity. Addition of a promoter metal(oxide) to CNF supported platinum catalysts is a promising route, since successful promotion of platinum based catalysts by tin, germanium, gallium or iron has been reported [5-10]. In early studies, the promoter salts were added in the reactor during the hydrogenation [7-9]. Though successful in enhancing the selectivity, it is not a very practical method for application in a continuous process. It is more convenient to make the promoter part of the catalyst. Various ways to prepare bimetallic catalysts for different applications have been reported [10]. The majority of these bimetallic catalysts are prepared using impregnation techniques. Unfortunately, this technique does not necessarily result in a close contact of the two metals, which is assumed to be of importance. Moreover, identification of the nature of the bimetallic phase remains challenging [10]. Controlled surface reactions of organometallic compounds have also been reported [10]. In that method one of the organic ligand moieties of the promoter-complex reacts with adsorbed hydrogen on the metal surface to bind the organometallic compound to the metal surface. Major drawback of this route is the risk of deposition of the organometallic complex on the support surface which results in multiple (inactive) phases on the catalyst [10].

Another promising technique to prepare bimetallic catalysts is the deposition of the second metal(oxide) via redox chemistry catalyzed by the first metal [11]. This technique is here referred to as reductive deposition precipitation (RDP). Barbier and co-workers [12, 13] were among the first to use this technique to prepare bimetallic catalysts. In this case hydrogen was adsorbed on a metal based catalyst and the promoter was deposited via reduction of promoter-salt by the adsorbed hydrogen. Platinum-tin and platinum-iron catalysts have been prepared successfully in that way [13-16]. In a review of Mallat et al. [17] deposition of lead, bismuth or copper on palladium catalysts using RDP has also been described. Preparation of bimetallic catalysts via RDP can also be performed below the equilibrium potential of the redox reaction. The latter situation results in underpotential deposition: adatoms can be deposited on particular sites of the metal surface whereby the equilibrium potential is shifted and enables creation of submonolayers of adatoms [12, 17].

Though the advantage of RDP for catalytic performance has been demonstrated [13, 14], detailed characterization of the interaction of promoters with the active metal is lacking thus far. Therefore, in this study we investigated the platinum-promoter interaction for RDP-prepared, CNF-supported bimetallic catalysts using TEM-EDX, XPS and EXAFS. These results will be related to catalytic results using the selective hydrogenation of cinnamaldehyde as a showcase [5, 18]. Bimetallic Pt/CNF catalysts were prepared by deposition of tin(IV), tin(II) and gallium(III) compounds on the monometallic Pt/CNF catalyst via RDP. Tin(II) and gallium(III) combinations with platinum were prepared and characterized to investigate the role of underpotential deposition on the selective hydrogenation of cinnamaldehyde. To the best of our knowledge, deposition of gallium in this way has not been reported before. For comparison, a catalyst without a close platinum-promoter interaction prepared via impregnation of tin(IV)chloride on Pt/CNF has been included in the study.

Experimental

A Ni/SiO_2 (20 wt-% nickel) growth catalyst was prepared via homogeneous deposition precipitation (HDP) using 17.0 g silica (Degussa, Aerosil 200), 21.1 g nickel nitrate hexahydrate (Acros; 99%) and 13.9 g urea (Acros; p.a.) in 1 L demineralized water according to an earlier described procedure [19].

CNF were grown from $CO/H_2/N_2$ at 823 K using Ni/SiO_2 (2 g) as reported earlier [4]. The raw CNF material (30 g) was collected and refluxed three times for 1 h per reflux in an aqueous KOH solution (1 M; 0.6 L; Merck; p.a.) to remove the SiO_2. After washing, the material was refluxed two times for 1 h per reflux in concentrated nitric acid (0.6 L; Merck; 65%) to remove exposed nickel and introduce oxygen surface groups on the CNF surface. After subsequent washing for three times with demineralized water and drying overnight at 393 K, the sample was denoted as CNF-ox.

Platinum was deposited via HDP on CNF-ox using $Pt(NH_3)_4(NO_3)_2$ and urea as base as described earlier [1]. The catalyst was reduced at 473 K for 1 h (heating rate 5 K/min) in a H_2/N_2 flow (100 mL/min; 10% v/v). The obtained material was denoted as Pt/CNF. Part of this monometallic catalyst was treated at 973 K for 2 h, to remove the oxygen surface groups, in N_2-flow (heating rate 5 K/min) and the resulting catalyst was denoted as Pt/CNF-973.

Tin and gallium were deposited on Pt/CNF via RDP (see Table 1 for precursors). Pt/CNF (4.00 g; 3.2 wt-%) was stirred for 1 h under hydrogen (1.2 bar) in the required solvent (100 mL; see Table 1 for details). Meanwhile, tin and gallium solutions were prepared in their corresponding solvents (see Table 1). Note that $Sn(HCOO)_2$ solutions were prepared by

Table 1. Synthesis details of RDP-prepared catalysts.

Precursor	Solvent	Intended Pt/promoter molar ratio
$SnCl_4$ (Sigma-Aldrich)	Aqueous HCl-solution, pH=1	5,3,1
$Sn(HCOO)_2$ (prepared from SnC_2O_4 (Fluka))	60 wt-% formic acid at pH=3.9 (via addition of ammonium hydroxide)	5
$Ga(NO_3)_3.xH_2O$ (Acros)	Demineralized water	5

dissolving SnC_2O_4 in 60 wt-% formic acid, which was prepared from concentrated formic acid (Merck). This formic acid solution (60 wt-%) was previously adjusted to a pH value of 3.9 using ammonium hydroxide (Merck, conc.), as was described by Meima et al. [20]. Next, 5 mL of the promoter solutions were added via a septum to the Pt/CNF slurry and the mixture was stirred for another 30 min under hydrogen atmosphere. The slurry was filtered and the catalysts were successively dried overnight at 393 K, reduced and heat-treated as described for Pt/CNF-973. The intended Pt/Sn molar ratios on the catalysts were 5, 3, and 1 when $SnCl_4$ was used and thus prepared catalysts were denoted respectively as: Pt-SnCl4/RDP-5, Pt-SnCl4/RDP-3 and Pt-SnCl4/RDP-1. When $Sn(HCOO)_2$ and $Ga(NO_3)_3$ were used, the intended Pt/promoter molar ratio was 5. These catalysts were denoted as Pt-SnForm/RDP-5 and Pt-Ga/RDP.

For reasons of comparison, tin was also added via incipient wetness impregnation (IWI). Pt/CNF-973 (2.2 g; 3.0 wt-%) was evacuated for 30 minutes. Subsequently, $SnCl_4.5H_2O$ (Sigma-Aldrich) was dissolved in demineralized water and 0.85 gram of the tin-solution was impregnated on the catalyst, resulting in a platinum/tin molar ratio of 5. The impregnated catalyst was kept under static vacuum for 40 hours, dried overnight at 393 K at ambient conditions and reduced as described for Pt/CNF. The resulting catalyst was denoted as Pt-SnCl4/IWI-5.

The catalysts were tested for the cinnamaldehyde hydrogenation at low (1.2 bar) and at high (30 bar) hydrogenation pressure. The hydrogenation of cinnamaldehyde (CALD) can result in cinnamyl alcohol (CALC), hydrocinnamaldehyde (HALD) and the fully hydrogenated product hydrocinnamyl alcohol (HALC) (Fig. 1). The formation of CALC is desired [5, 18]. Low pressure tests were performed at 313 K and 1.2 bar H_2 as described earlier [4]. The solvent used was 2-propanol/water and 1 g of catalyst (sieve fraction 25-90 μm) per run was used. High pressure tests were performed at 313 K and 30 bar H_2 in a batch wise mode. The stainless steel autoclave reactor (Autoclave Engineers, USA) was equipped with gas inlet, stirrer and temperature and pressure control. The catalyst (0.2 g; sieve fraction 25-90 μm) was suspended in a mixture of isopropanol (189.2 mL; Merck, p.a.), demineralized water (30.8 mL) and t-cinnamaldehyde (0.33 g; Sigma-Aldrich; p.a.). The slurry was heated to 313 K and saturated with hydrogen without stirring. Next, the reaction

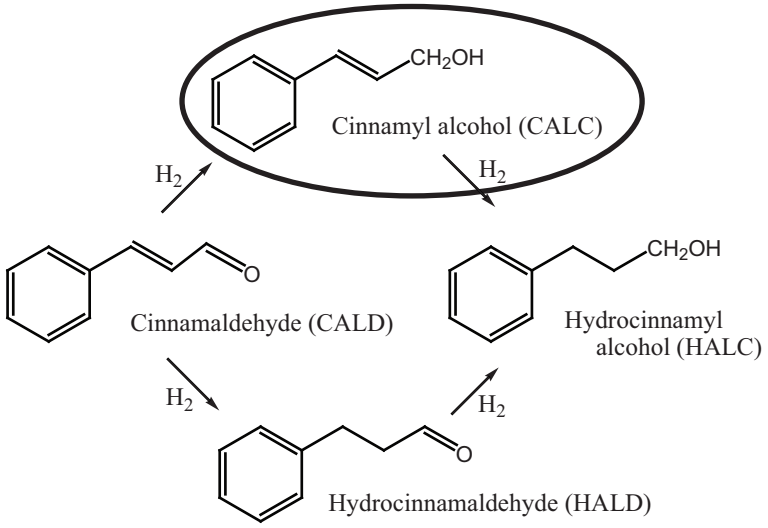

Fig. 1 The hydrogenation pathway of cinnamaldehyde; the desired product is encircled.

was started by starting to stir (1500 rpm) and samples were taken at different time intervals for 90 min. Samples were analyzed using GC Agilent 6890N equipped with autoinjector, FID detector and Agilent DB-1 column. Initial cinnamaldehyde hydrogenation activities were calculated for all tests. The conversion of CALD and selectivity to CALC were calculated as described before [4].

Platinum weight-loadings were determined either using calibrated X-ray fluorescence or ICP-OES. X-ray fluorescence analysis was performed on a calibrated Spectro X-lab 2000 apparatus using 2 – 4 g of the dry catalyst powder. ICP-OES, which was also used to analyze the gallium loading, was performed on a SPECTRO CIROS^{CCD} ICP-Spectrometer. Each sample was destructed by heating in aqua regia (1:3 mixture of HNO_3: HCl) before analysis. For Pt-SnCl4/RDP-1, the tin loading was determined by analyzing the amount of tin left in the filtrate solution using ICP-OES on the same apparatus as described above.

TEM was performed on a Tecnai 20 FEG operating at 200 kV (point resolution of 2.7 Å). The instrument was equipped with an EDAX EDS system, a STEM option and a Gatan Imaging Filter 2000. Samples were suspended in ethanol using an ultrasonic treatment and brought onto a holey carbon film on a copper grid.

Hydrogen chemisorption measurements were performed using a Micromeritics ASAP 2020. Samples were dried at 373 K in vacuum followed by cooling to room temperature. Next, the samples were re-reduced in flowing hydrogen at 473 K for 60 min (heating rate 5 K/min). Afterwards, the samples were degassed for at least 30 min at a pressure of <13.3 Pa at 473 K to remove chemisorbed hydrogen and water. The isotherms were measured at 313 K and the mass was determined afterwards. The presented H/Pt ratios are based on the amounts of hydrogen adsorbed at zero pressure, which are calculated by extrapolation of the linear part

of the isotherm and the amount of platinum in the sample. Nitrogen physisorption measurements were performed as described earlier [4].

The XPS data were obtained with a Vacuum Generators XPS system, using a CLAM-2 hemispherical analyzer for electron detection. Non-monochromatic Al (Kα) X-ray radiation was used for exciting the photoelectron spectra using an anode current of 20 mA at 10 keV. The pass energy of the analyzer was set at 50 eV.

Sn K and Pt L_3 XAFS spectra for several catalysts were either measured at HasyLab (beamline C) in Hamburg equipped with a Si(311) double-crystalmonochromator (detuned to 70% of maximum intensity to avoid higher harmonics present in the X-ray beam) or at the ESRF (beamline BM26A DUBBLE) in Grenoble equipped with a Si(111) double-crystalmonochromator (higher harmonics were reduced by the presence of a secondary Si mirror after the crystalmonochromator). Pt L_3 spectra were measured in transmission mode and Sn K spectra were measured in the fluorescence mode. For the latter measurements, self-absorption of the fluorescence signal was negligible due to the low tin-loading on the samples. The powdered catalysts were pressed into self-supporting wafers and mounted in a stainless-steel in situ cell equipped with Kapton windows, resulting in a total absorption of 0.5 - 0.7 for the Pt L_3 transmission measurements. The samples were re-reduced in situ at 473 K for 60 min (5 K/min) in flowing hydrogen, cooled down in hydrogen atmosphere and XAFS data were collected (T = 77 K). Three scans were averaged and the EXAFS data from the measured absorption spectra were extracted with the XDAP code (version 2.2.7, 2006) [21]. Preedge subtraction, background subtraction and normalization of the data were performed as described by Toebes et al. [1]. The phase shift and backscattering amplitude functions for the Pt-Sn absorber-backscatterer pair at the Pt L_3 edge, was extracted from experimental XAFS data using a Pt-Sn complex, i.e. $(Pt(SnCl_3)_5).(Ph_3PCH_3)_3$ (N=5, R=2.57 Å, k-range=2.3-14.3 $Å^{-1}$, k^1-weighting, filtered FT range=1.7-2.9 Å [22]). This complex was prepared as described by Nelson et al. (according to method A) [23]. The reference data for Pt-Sn was measured at the same temperature as the samples (T = 77 K) and the first shell scattering atoms (Pt-Sn) were well separated from the higher shells. Therefore, back transformation of the first shell in the Fourier-Transformed data was used to obtain the backscattering amplitude and phase shift function of the Pt-Sn absorber-backscatterer pair. Phase shift and backscattering amplitude functions for Pt-Pt and Pt-O were obtained from FEFF7 as described by Van Dorssen et al. [24]. For Sn-Pt, Sn-Cl, Sn-O and Sn-Sn absorber-backscatterer pairs (see also [22]) these functions were obtained from FEFF8. In Table 2 the used parameters for the FEFF8 calculations are summarized. Backscattering amplitude and phase shift functions were optimized with respect to S_0^2 and V_r. These functions were accepted when they could successfully describe the first shells of experimentally measured

tin(II)oxide for Sn-O and Sn-Sn (i.e. Sn^{2+}-Sn^{2+}) absorber-backscatterer pairs, and for experimentally measured $(Pt(SnCl_3)_5).(Ph_3PCH_3)_3$ for Sn-Pt and Sn-Cl absorber-backscatterer pairs with respect to the expected values for distance and coordination number [22, 25]. Data analysis of the catalysts was performed by multiple shell fitting using the difference file technique in R-space (1.0<R<3.5 Å) with the XDAP code using both k^1 and k^3 weighting [26]. Variances of the fits were calculated as described earlier [1].

Table 2. Used input parameter for FEFF8 calculations.

Absorber-Backscatterer	**N**	**R (Å)**	**S_0^2**	**σ^2 ($Å^{-1}$)**	**V_r (eV)**	**V_i (eV)**	**Reference compound**
Sn-Pt	1	2.57	1	0	0	1	Pt-Sn complex
Sn-Cl	1	2.28	1	0	0	1	Pt-Sn complex
Sn-O	1	2.22	1	0	12	1	tin(II)oxide
Sn-Sn	1	3.54	0.9	0	5	1	tin(II)oxide

Hedin-Lundqvist potentials were used for calculations

Results and Discussion

All samples had a BET surface area of about 180 m^2/g and a mesopore volume of about 0.26 mL/g. No micropores were found. The platinum loading was similar for all samples (3.0 to 3.3 wt-%). In Table 3 the intended and for some catalysts also the actual promoter loadings are summarized. The gallium loading in Pt-Ga/RDP was 0.1 wt-%. The actual tin weight loading for Pt-SnCl4/RDP-1 (0.7 wt %) was lower than the intended loading (1.8 wt%) thus it must be concluded that high loadings were not achieved by RDP. This can be expected since the theoretical maximum weight-loading is about 0.8 wt-% when assuming a $Sn/Pt_{surface}$ of 1 and a H/Pt of 0.45 (Table 3). Nevertheless we intended for a higher loading to obtain the highest possible actual tin loading.

Table 3. Physical and chemical properties of the catalysts.

Sample	**Intended promoter loading (wt-%)**	**Actual promoter loading (wt-%)**	**H/Pt ratio based on H_2-chemisorption**	**Average particle size based on TEM (nm)**	**XPS Sn $3d_{5/2}$ peak maximum (eV)**
Pt/CNF-973			0.45	2.0	-
Pt-SnCl4/RDP-5	0.4	n.a.	0.32	2.3	486.0
Pt-SnCl4/RDP-3	0.6	n.a.	0.17	2.8	486.0
Pt-SnCl4/RDP-1	1.8	0.7	0.22	3.2	486.0
Pt-SnForm/RDP-5	0.4	n.a.	0.32	n.a.	486.0
Pt-SnCl4/IWI-5	0.4	0.4	0.41	2.0	486.8
Pt-Ga/RDP	0.2	0.1	0.33	2.1	-

n.a. = not analyzed

The number of accessible available platinum sites was determined using hydrogen chemisorption. The hydrogen chemisorption results are also summarized in Table 3 and expressed as H/Pt ratio. The highest H/Pt ratio was observed for monometallic Pt/CNF-973. In general an increasing intended tin-loading resulted in a lower H/Pt ratio for the RDP prepared samples. This suggests that upon deposition of higher concentrations of promoter, a lower amount of hydrogenation sites is available on the catalysts, which can be ascribed to an increased coverage of platinum by tin. This indicates that tin is well dispersed over the platinum surface which suggests a good contact between platinum and tin for RDP prepared samples. For the sample prepared by IWI the decrease in hydrogen chemisorption capacity was less significant. Thus indicating that tin was not, to a significant extent, present on the platinum surface, i.e. not in close contact.

TEM-EDX was used to determine platinum particle sizes (Table 3), size distributions and chemical composition of the samples. In Fig. 2 representative TEM images are displayed for Pt-SnCl4/IWI-5, Pt-SnCl4/RDP-5, Pt-SnCl4/RDP-3 and Pt-SnCl4/RDP-1. In Fig. 3 the platinum particle size distributions for the latter samples and for Pt-Ga/RDP and Pt/CNF-973 are shown. For Pt/CNF-973, Pt-Ga/RDP and Pt-SnCl4/IWI-5 a platinum particle size range of 1-3 nm is observed. After deposition of tin via RDP, the platinum particle size range increased i.e., 1-4 nm for Pt-SnCl4/RDP-5, 1-6 nm for Pt-SnCl4/RDP-3 and 1-7 nm for Pt-SnCl4/RDP-1. Increasing metal particle sizes upon addition of larger amounts of tin has been observed as well by Neri et al. [27]. Apparently, combining monometallic platinum catalysts with tin via RDP resulted in larger platinum particles, i.e. sintering, after reduction.

Dark field TEM images and elemental maps obtained via EDX analysis are shown in Fig. 4 for Pt-SnCl4/RDP-3 and for Pt-Ga/RDP. Analysis of the elemental maps was limited to areas of 25 nm. For both samples it was observed that the presence of platinum and tin or platinum and gallium, which are depicted as the brighter areas in Fig. 4, coincide at this scale. Based on this characterization technique, it is therefore tentatively concluded that platinum and promoters are in close vicinity.

To get a more detailed picture of the interaction between platinum and tin, XAFS studies both on the Pt L_3 and Sn K edge for Pt-SnCl4/RDP-5, Pt-SnCl4/RDP-1 and Pt-SnCl4/IWI-5 were performed. The absorption edge energy position measured for the Pt L_3 spectra was at 11564 eV, corresponding to platinum in the metallic state. Results of the data fitting are reported in Table 4A. An example of the raw, Fourier-Transformed and fitted data is depicted in Fig. 5. The number of free parameters (N_I) which are allowed to use for the fitting procedure, is calculated using $N_I=(2\Delta k\Delta R/\pi)+2$ (Δk: Fourier Transform range of the raw data, ΔR: fit range) [28]. For the Pt L_3-fits it is calculated that $N_I=14.9$. Since the Pt-Pt distance is known (i.e. 2.76-2.77 Å [24, 29]), this parameter was fixed for all fits thereby

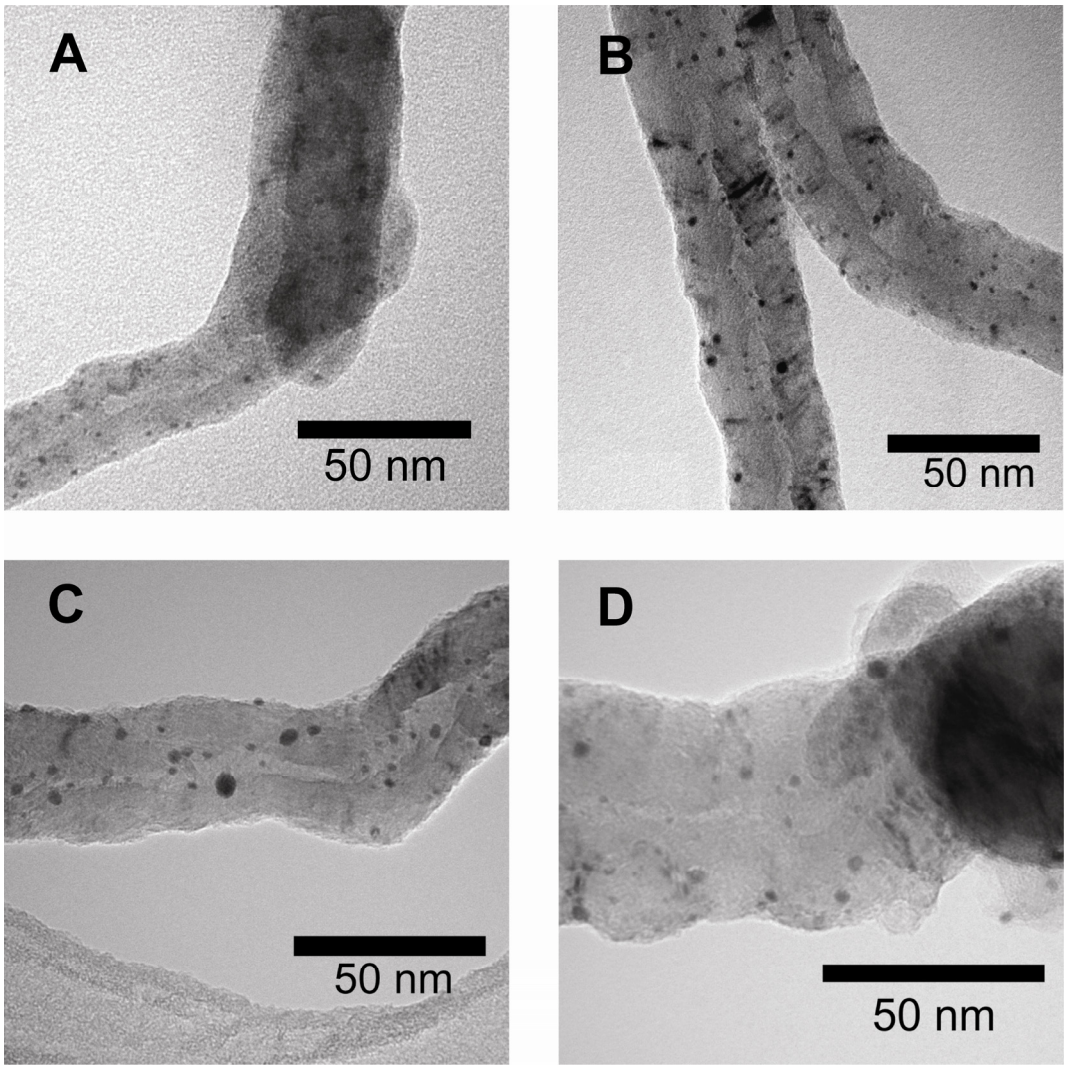

Fig. 2 TEM images of A) Pt-SnCl4/IWI-5 (1-3 nm) B) Pt-SnCl4/RDP-5 (1-4 nm) C) Pt-SnCl4/RDP-3 (1-6 nm) D) Pt-SnCl4/RDP-1 (1-7 nm).

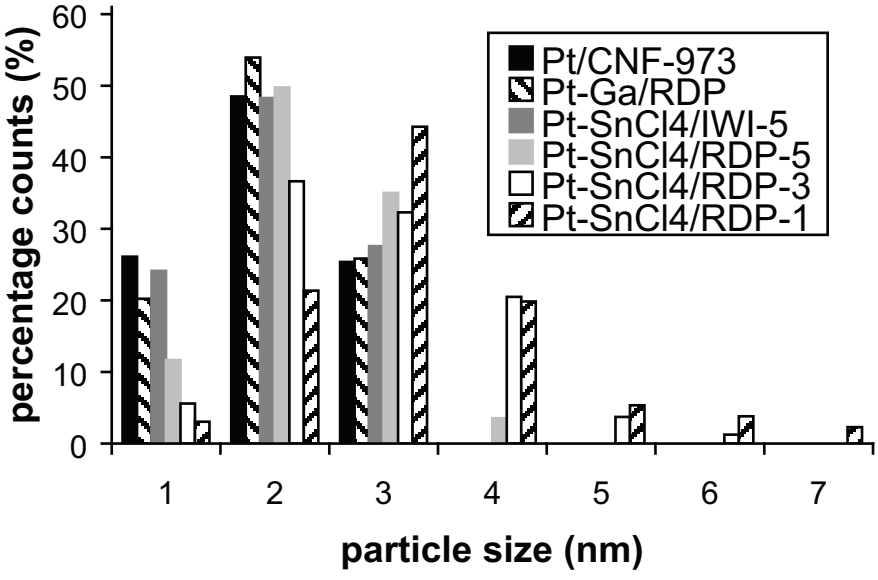

Fig. 3 TEM histograms of the analyzed samples showing the particle size distribution for several catalysts.

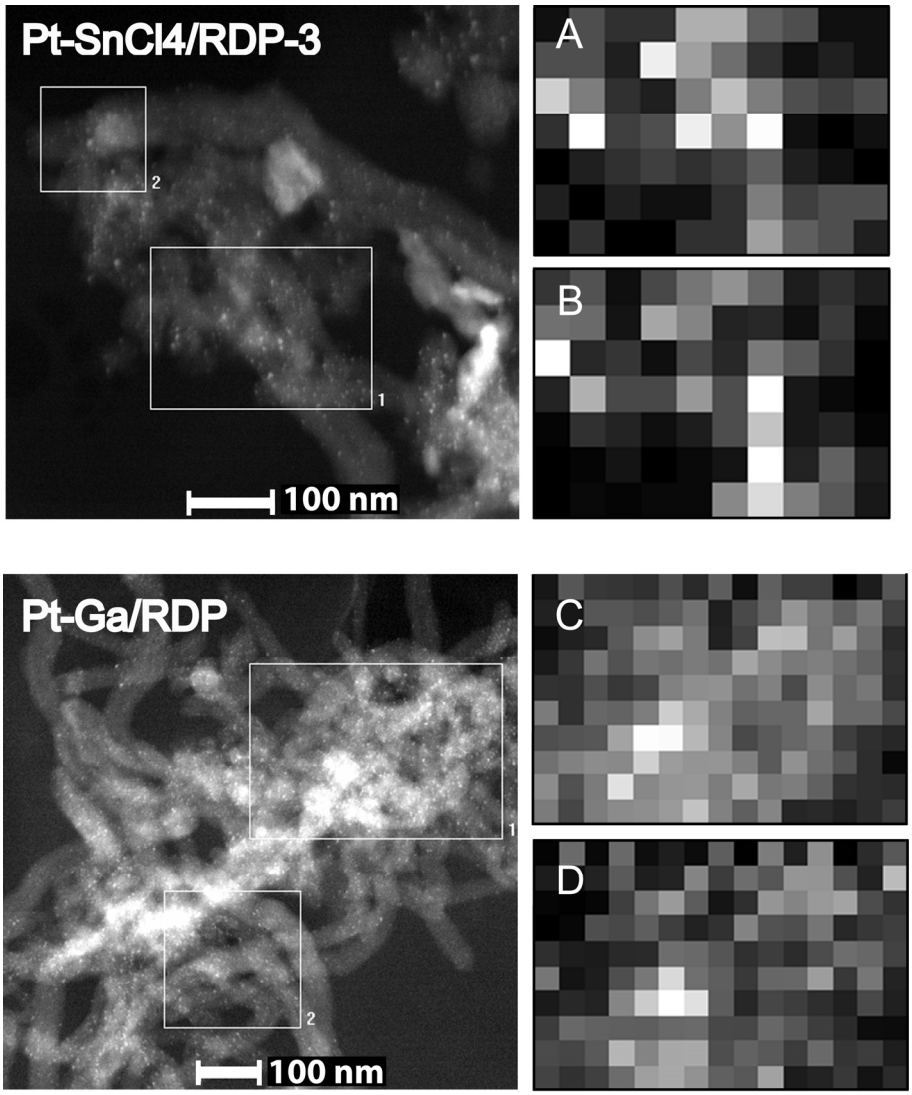

Fig. 4 TEM dark field images of Pt-SnCl4/RDP-3 and Pt-Ga/RDP. Elemental EDX maps were taken from area 1. Area 2 was used to correct for any drift of the samples. Map A reflects the measured Sn L intensity and map B the measured Pt M intensity of Pt-SnCl4/RDP-3. Map C reflects the measured Ga L intensity and map D the measured Pt M intensity of Pt-Ga/RDP. Going from dark to light correspond to increasing metal intensities.

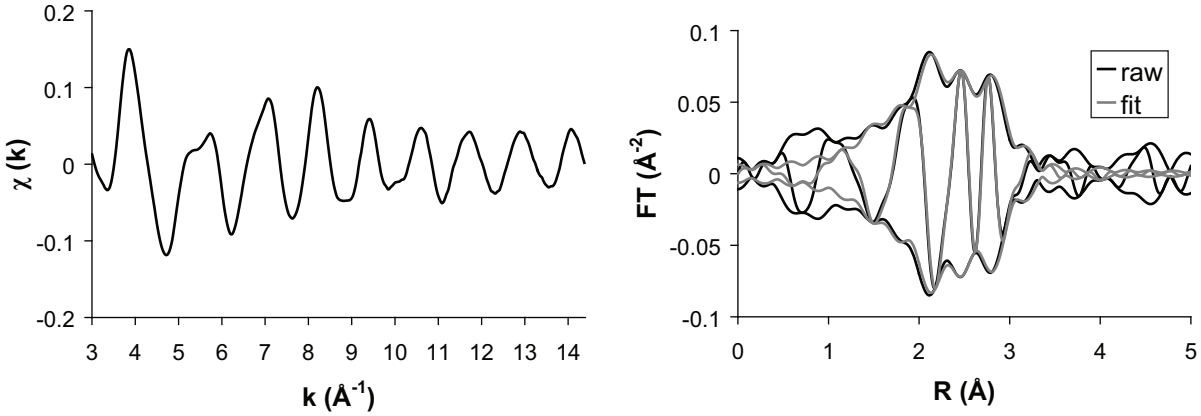

Fig. 5 Left: experimental Pt L_3 EXAFS data (k^1 weighted) of Pt-SnCl4/IWI-5 (Δk = 3-14.3 $Å^{-1}$) Right: Pt L_3 Fourier-Transform of the data and the fit for Pt-SnCl4/IWI-5 (k^1 weighted; Δk = 3-14.3 $Å^{-1}$; ΔR = 1.5-3.3 Å).

Tables 4. EXAFS fit results for the analyzed catalysts at the Pt L_3-edge or Sn K-edge using four or three different absorber-backscatterer pairs (scatter). The resulting coordination numbers (N), scatter distances (R), Debye-Waller factor ($\Delta\sigma^2$) and energy shifts are summarized. The k-range, R-space and variances of the magnitude and imaginary part of the Fourier-Transforms are also summarized.
A) Fit results at Pt L_3-edge.

Catalyst	Scatter	N	R (Å)	$\Delta\sigma^2$ (Å^2) x 10^{-3}	ΔE_0 (eV)	Δk (Å^{-1})	ΔR (Å)	k^1 variance (%)	
								Abs	Im
Pt-SnCl4/IWI-5	Pt-Pt	5.7	2.76	2.7	0.9	3.0-14.3	1.5-3.3	0.34	0.95
	Pt-Os	1.0	1.99	9.7	2.9				
	Pt-Ol	0.7	2.61	2.3	3.5				
	Pt-Sn	0.5	2.74	4.2	3.0				
Pt-SnCl4/RDP-5	Pt-Pt	6.4	2.76	1.7	2.5	3.0-14.3	1.5-3.3	0.18	0.36
	Pt-Os	0.4	2.00	9.0	4.2				
	Pt-Ol	0.8	2.62	3.8	0.9				
	Pt-Sn	0.8	2.75	6.2	0.1				
Pt-SnCl4/RDP-1	Pt-Pt	6.7	2.76	3.0	4.0	3.0-14.3	1.5-3.3	0.15	0.81
	Pt-Os	0.6	2.00	9.9	1.2				
	Pt-Ol	0.4	2.63	4.1	2.4				
	Pt-Sn	1.2	2.73	6.4	4.5				

B) Fit results at Sn K-edge.

Catalyst	Scatter	N	R (Å)	$\Delta\sigma^2$ (Å^2) x 10^{-3}	ΔE_0 (eV)	Δk (Å^{-1})	ΔR (Å)	k^1 variance (%)	
								Abs	Im
Pt-SnCl4/IWI-5	Sn-Sn	0.5	3.18	2.1	2.2	3.5-12.4	1.0-3.3	0.28	0.77
	Sn-Pt	1.6	2.71	7.8	-6.9				
	Sn-O	5.1	2.04	9.4	5.4				
Pt-SnCl4/RDP-5	Sn-Sn	-	-	-	-	2.9-12.0	1.2-3.5	0.35	0.60
	Sn-Pt	4.8	2.74	9.9	-6.1				
	Sn-O	1.1	2.08	9.9	5.9				
Pt-SnCl4/RDP-1	Sn-Sn	0.6	3.34	7.2	-6.9	2.85-12.0	1.2-3.5	0.45	0.82
	Sn-Pt	5.2	2.75	8.0	-5.7				
	Sn-O	0.8	2.06	9.9	6.9				

allowing 4 shells for fitting. The low variances of the fit indicate that the data could be fitted well with the given parameters. For all samples Pt-Pt, Pt-Sn and two Pt-O (long: Pt-Ol and short: Pt-Os) contributions were found. The latter is in agreement with observations of Zhang et al. [29] for reduced platinum on CNF catalysts. Platinum EXAFS is mainly dominated by the Pt-Pt contributions and its coordination number increased from 5.7 to 6.7 when going from Pt-SnCl4/IWI-5, Pt-SnCl4/RDP-5 to Pt-SnCl4/RDP-1. This indicates that the platinum particles sizes increased with increasing tin content which is in agreement with the above discussed TEM results.

When assuming spherical particles, the resulting Pt-Pt coordination numbers (5.7 to 6.7) correspond to particle sizes of 1.1 – 1.4 nm in diameter [30]. Table 3 indicated that the particle sizes determined by TEM are around 2 nm. This discrepancy in particle size has been observed earlier for small particles and has been ascribed to the fact that TEM may not detect

the metal particles smaller than about 1 nm thereby resulting in overestimation of the average particle size [29]. EXAFS on the other hand averages over all platinum coordination numbers thus including also the very small particles which results in a lower average particle size.

The coordination numbers for the Pt-O contributions at long and at short distance do not show a trend as function of the synthesis method. Moreover, the coordination numbers are small, i.e. 0.4 – 1.0, and therefore, definite conclusions with respect to these contributions were not drawn.

The Pt-Sn contribution was the lowest (0.5) for Pt-SnCl4/IWI-5 and increased to 0.8 and 1.2 for Pt-SnCl4/RDP-5 and Pt-SnCl4/RDP-1. These coordination numbers are also rather small, though it indicates that RDP resulted in more tin atoms being in close contact with platinum as compared to IWI, which is in agreement with the hydrogen chemisorption results described above. Moreover, a higher tin-loading for RDP prepared samples also resulted in a higher concentration of tin in close contact with platinum. This is also in agreement with the hydrogen chemisorption results.

Platinum-tin interactions were also investigated using Sn K-edge XAFS. The absorption edge energy position for the RDP prepared samples (29201.2 eV) was close to the absorption edge energy of tin(II)oxide reference material (29201.7 ev) indicating the presence of tin(II). Thus tin became reduced during RDP synthesis and the subsequent reductive treatment, since originally tin(IV) was used at the start of the synthesis. For the IWI synthesized sample, a stronger white line, as compared to the RPD samples, is observed and its edge position shifted by about 2 eV to higher energy which is close to the edge position of tin(IV)oxide reference material (i.e. 29203.5 eV). Hence, tin does not become reduced when deposited via IWI. The reduction of tin for RDP-prepared samples is speculated to result from the interaction of tin obtained with the hydrogen saturated platinum surface. In Fig. 6 the background subtracted and normalized Sn K-edge EXAFS data of Pt-SnCl4/IWI-5 and Pt-SnCl4/RDP-5 are depicted as representative examples and indicate a good signal/noise ratio up to k=12. The resulting EXAFS data were fitted and fit results are compiled in Table 4B. The number of free parameters for the Sn K-edge fits ranges from 15.0-15.4, which allows the use of 3 shells for fitting. Fig. 7 and 8 show the Fourier-Transformed plots of the experimental and fitted data for Pt-SnCl4/IWI-5 and Pt-SnCl4/RDP-5.

The fit results for Pt-SnCl4/IWI-5 show that a substantial Sn-O contribution is observed with a coordination number of 5.1, while the Sn-Pt and Sn-Sn contributions are 1.6 and 0.5 respectively. The Sn-O (2.04 Å) and Sn-Sn (3.18 Å) distances found here correspond to that of tin(IV)oxide [31]. Moreover, a strong white line is observed, indicating tin is in a high oxidation state and in addition, the edge position is close to tin(IV)oxide. This shows that small tin(IV)oxide clusters were present which were not in close contact with platinum.

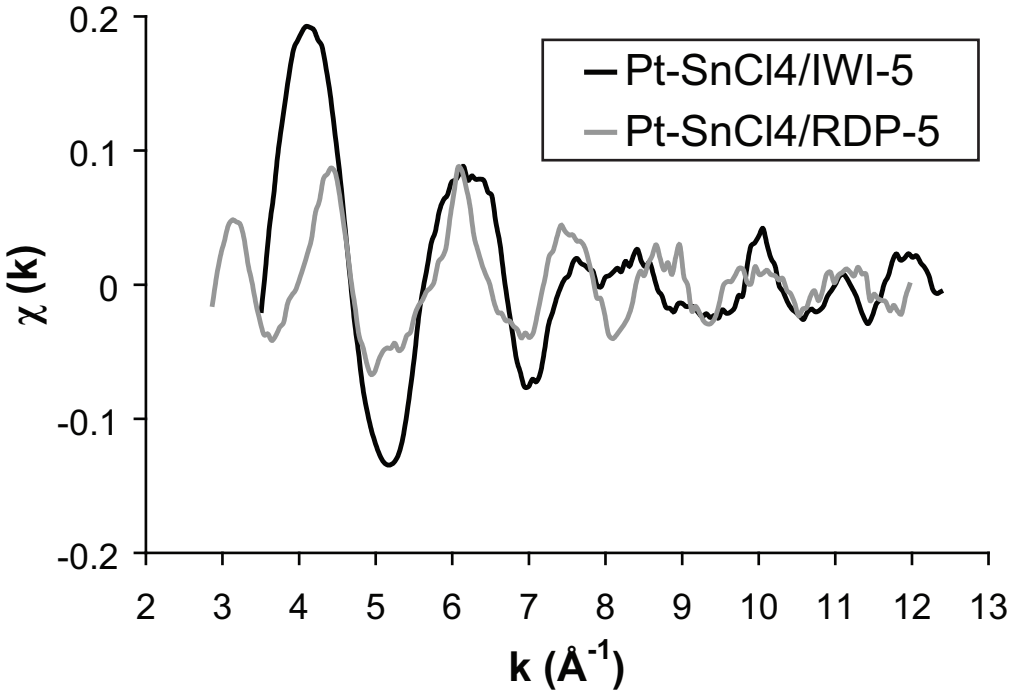

Fig. 6 The experimental Sn K EXAFS data (k^1 weighted) of Pt-SnCl4/IWI-5 (Δk = 3.5-12.4 $Å^{-1}$) and Pt-SnCl4/RDP-5 (Δk = 2.9-12.0 $Å^{-1}$).

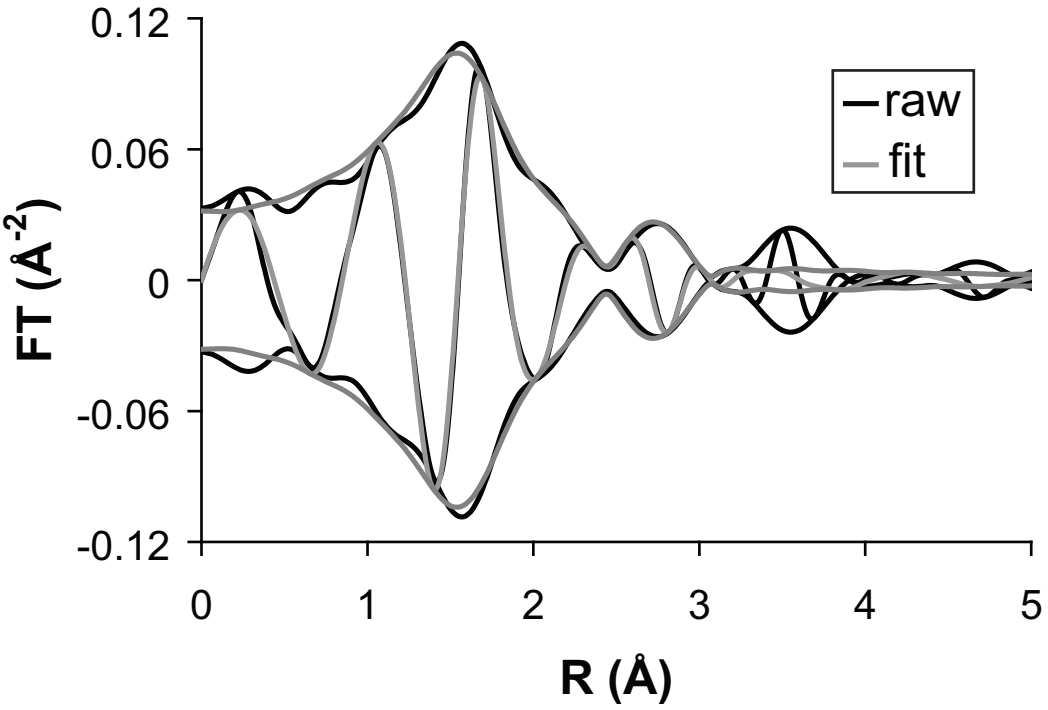

Fig. 7 The Sn K Fourier-Transform of the data and the fit for Pt-SnCl4/IWI-5 (k^1 weighted; Δk = 3.5-12.4 $Å^{-1}$; ΔR = 1.0-3.3 Å).

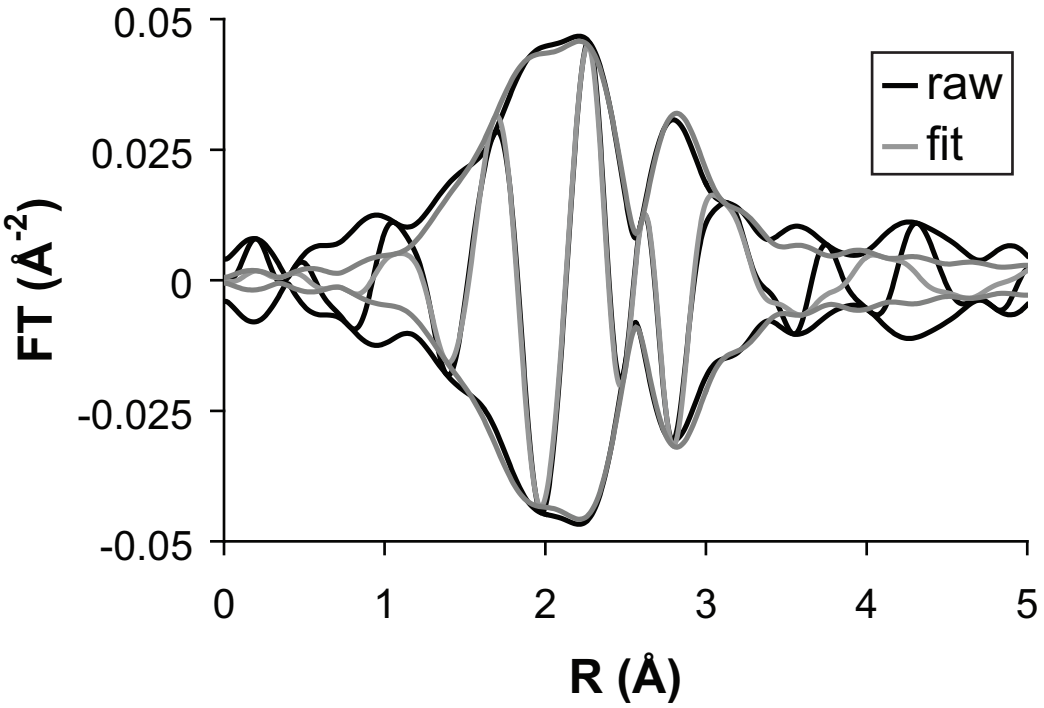

Fig. 8 The Sn K Fourier-Transform of the data and the fit for Pt-SnCl4/RDP-5 (k^1 weighted; Δk = 2.9-12.0 $Å^{-1}$; ΔR = 1.2-3.5 Å).

This is in contrast to the RDP prepared catalysts which resulted in significant Sn-Pt contributions with coordination numbers of 4.8 and 5.2 for Pt-SnCl4/RDP-5 and Pt-SnCl4/RDP-1 respectively. These results show that RDP leads to a close contact of tin on platinum, thereby forming a bimetallic system, while for the IWI sample this interaction is low. The coordination numbers for Sn-O for Pt-SnCl4/RDP-5 and Pt-SnCl4/RDP-1 are low (1.1 and 0.8 respectively) and therefore, firm conclusions with respect to this contribution cannot be drawn. The Sn-Sn contribution is low (coordination number of 0.6) for Pt-SnCl4/RDP-1 and could not be determined at all for Pt-SnCl4/RDP-5, which is again an indication that large tin oxide clusters were not formed by RDP. The distance for the Sn-O contribution (i.e. 2.06-2.08 Å) is lower than expected for tin(II)oxide (i.e. 2.2 Å [25]), which indicates that this oxygen has a different nature as compared to that in tin(II)oxide.

All platinum-tin catalysts were analyzed using XPS for platinum, tin, carbon, and oxygen. Chlorine, if present, was below the detection limit for all analyzed samples. The measured Sn 3d peak position is depicted in Fig. 9 and the Sn $3d_{5/2}$ peak maximum positions are summarized in Table 3. For reasons of comparison, a reference material was prepared by impregnation and treatment of $SnCl_4$ on CNF at 473 K in H_2/N_2 flow, referred to as SnCl4/CNF. Synthesis of platinum-tin on CNF via IWI did not result in a shift of the peak maxima when compared to the reference sample, while synthesis via RDP resulted in a shift

of the peak maxima to lower binding energies close to tin(II) reference species [32]. Such a peak shift has not been observed for any of the other measured elements, i.e. platinum, carbon and oxygen. Both XAFS analysis as well as XPS analysis techniques indicated the presence of tin(II) for RDP-synthesized catalysts and tin(IV) for the IWI-synthesized catalyst. Please, note that XAFS measurements were measured in situ directly after reduction, while the XPS samples were shortly exposed to air before the measurements. Since the results agree with each other, it is concluded that tin is not reoxidized due to air exposure. The observed tin reduction is only possible when close interaction of tin with the hydrogen saturated platinum surface is present.

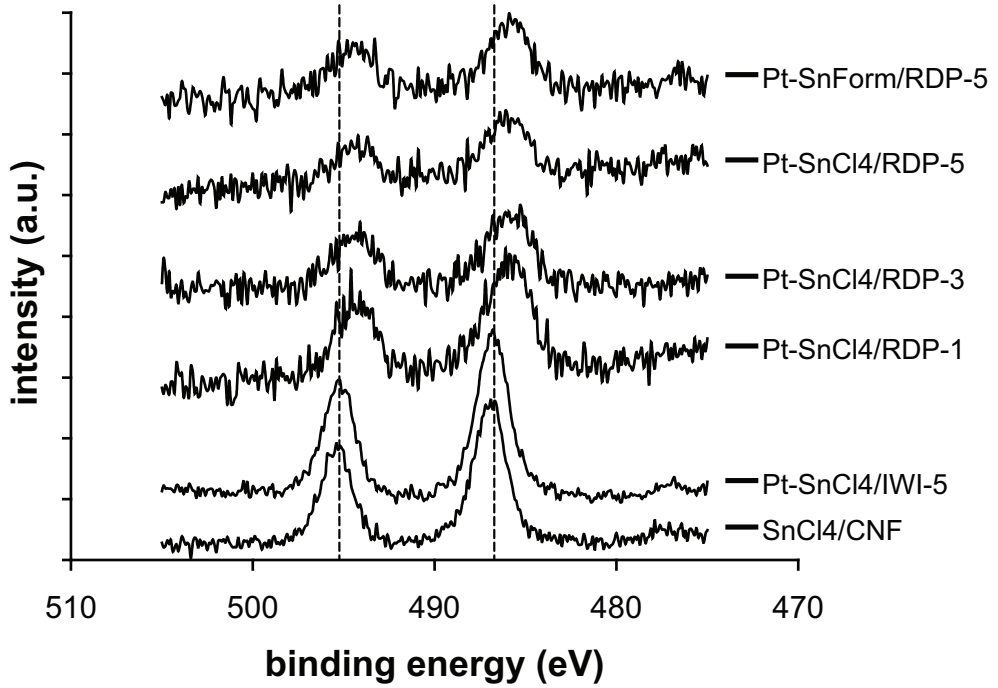

Fig. 9 The measured XPS Sn $3d_{3/2}$ (left peak) and Sn $3d_{5/2}$ (right peak) of the bimetallic samples. The vertical dotted lines indicate the peak maxima for the reference material, which was prepared via impregnation and treatment at 473 K in H_2/N_2 of $SnCl_4$ on CNF.

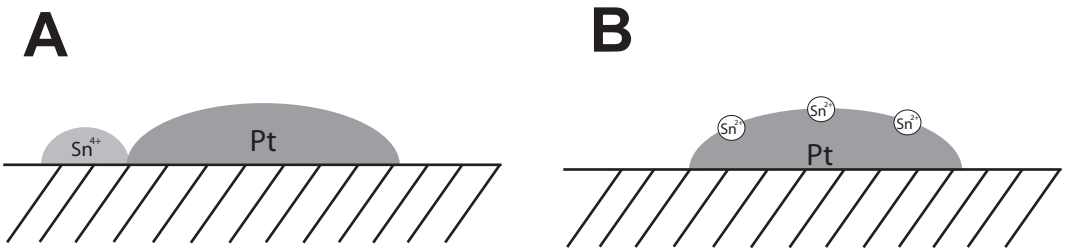

Fig. 10 Schematic representation of the location of the tin cations in A) platinum-tin catalyst prepared via IWI and B) platinum-tin catalyst prepared via RDP.

Thus to summarize, using TEM-EDX, EXAFS and XPS it is demonstrated that RDP resulted in a close contact of the two metals and partial reduction of tin on the platinum sites, which is not observed for the IWI prepared catalyst. A schematic representation of these catalysts is depicted in Fig. 10.

The catalysts were tested for CALD hydrogenation at low pressure and for some catalysts also at high pressure. Representative examples of the low-pressure test reactions are displayed in Fig. 11. In Table 5 the initial hydrogenation activities, the reaction time required to obtain 50% CALD conversion and the selectivity towards CALC are shown. From Fig. 11 and Table 5 it can be seen that at low pressure, catalysts prepared via RDP are more selective and active compared to the monometallic catalyst. The platinum-gallium catalyst resulted in the highest selectivity at this pressure. In contrast to the RDP prepared catalysts, the IWI prepared catalyst resulted in a decreased activity and selectivity as compared to the monometallic Pt/CNF. It has been observed that for all test reactions (also when performed at high pressure) < 3.8% by-products were formed. These by-products were mainly propylbenzene and β-methylstyrene, while ethylbenzene has not been observed for any test reaction. Only for Pt-SnCl4/IWI-5 the formation of acetals, 0.5%, was observed during

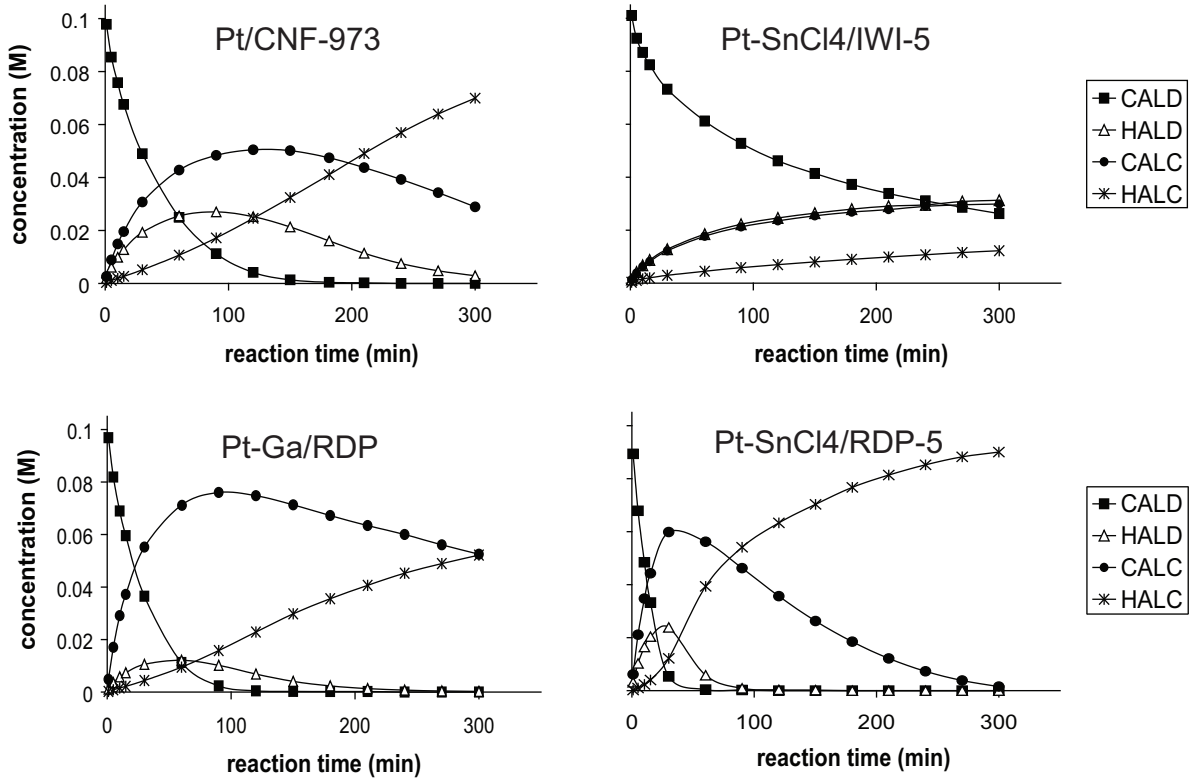

Fig. 11 Cinnamaldehyde hydrogenation results of several of the tested catalysts. Test reactions were performed at 313 K under 1.2 bar H_2 in 2-propanol/water mixture.

Table 5. Results of the catalytic tests.

Sample	LOW PRESSURE TESTS			HIGH PRESSURE TESTS		
	Initial activity ($mmol.s^{-1}.g_{Pt}^{-1}$)[a]	**Reaction time (min)[b]**	**Selectivity (%)[c]**	**Initial activity ($mmol.s^{-1}.g_{Pt}^{-1}$)[a]**	**Reaction time (min)[d]**	**Selectivity (%)[e]**
Pt-SnCl4/RDP-5	0.37	10	72	0.59	4.5	42
Pt-SnCl4/RDP-3	0.32	12	79	n.t.	n.t.	n.t.
Pt-SnCl4/RDP-1	0.27	15	81	n.t.	n.t.	n.t.
Pt-SnForm/RDP-5	0.29	13	74	0.49	5.0	31
Pt-SnCl4/IWI-5	0.18	85	43	0.55	5.5	17
Pt-Ga/RDP	0.25	20	88	0.40	8.0	39
Pt/CNF-973	0.21	30	59	0.75	3.5	19

[a] = Initial activity based on the first two reaction data points
[b] = Reaction time (min) required to reach 50% CALD conversion at low pressure
[c] = Selectivity to CALC (%) at 50% CALD conversion at low pressure
[d] = Reaction time (min) required to reach 50% CALD conversion at high pressure
[e] = Selectivity to CALC (%) at 50% CALD conversion at high pressure
n.t. = not tested

testing. For this catalyst tin(IV) species are present as promoter and we believe that this is mainly in the form of tin(IV)oxide, since chlorine has not been detected using XPS. It has been described earlier that the presence of tin(IV)oxide may result in the formation of acid sites on the catalyst surface, which is associated with acetal formation [33, 34]. The formation of this type of by-products often result in a decreasing catalytic activity and selectivity [33, 34].

Industrial application of CALD hydrogenations are in general performed at high hydrogenation pressures [35]. Therefore some catalysts were tested at high hydrogenation pressures (30 bar) to investigate catalytic behavior under these conditions. In Table 5 an overview of the obtained test results is given for the following catalysts: Pt-SnCl4/RDP-5, Pt-SnForm/RDP-5, Pt-SnCl4/IWI-5, Pt-Ga/RDP and Pt/CNF-973. Please note that some screening experiments, in which either the catalyst particle sizes or stirring speeds were varied, indicated that the selectivity was not affected by the presence or absence of mass transfer limitation. As for the low pressure experiments also at high hydrogenation pressure, RDP synthesized bimetallic catalysts resulted in enhanced selectivities irrespective the used precursor, while the IWI prepared catalyst resulted in a slightly lower selectivity compared to the monometallic catalyst. This means that the observed trend with respect to selectivity both at low and at high hydrogenation pressure is the same. It must be noted here that Pt-SnCl4/RDP-5 resulted in a higher selectivity compared to Pt-Ga/RDP, which is not expected based on the low hydrogenation pressure results. An explanation for the latter behavior is lacking.

To investigate the stability of the catalyst we filtered the reaction mixture after a catalytic run. The solvent in the filtrate was evaporated and the resulting solid was treated in aqua regia and analyzed for leached platinum using ICP-OES. Since no platinum was detected it was concluded that leaching did not occur.

The absolute selectivities decreased when comparing high pressure test reactions with low pressure test results. In literature, it has been reported that higher CALD concentrations resulted in a higher selectivity [36, 37]. It has also been reported that higher hydrogenation pressures can result in a lower selectivity compared to lower hydrogen pressures [34, 37]. Since in this study the hydrogenation pressure was increased and the CALD concentration was decreased at the same time when going from the low to the high pressure experiments, a combination of these two factors might have resulted in the observed decrease in absolute selectivities at high pressure.

At higher pressure the activity of Pt/CNF was higher compared to that of the bimetallic catalysts, while the opposite trend is observed for the low pressure tests. It has been reported before that the addition of a second metal can result an increasing as well as a decreasing activity [5, 34, 38]. Increased activities have been ascribed to the presence of ionic promoters directing the C=O bond towards the platinum, thereby enhancing both selectivity and activity. Decreased activities have been ascribed to the presence of high promoter concentrations resulting in a dramatically decreasing hydrogenation capacity [5]. Our results suggest that the optimum activity does not depend on a particular amount of promoter only, but may shift due to application of different test conditions as well. Since multiple variables are present when comparing high pressure tests to low pressure tests, e.g. different reactant concentrations and different hydrogenation pressures, this behavior cannot be ascribed to one particular reaction parameter yet.

For RDP synthesis we reported that platinum does sinter after reduction and heat-treatment (Table 3). In our previous study, it is concluded that for heat-treated platinum on CNF larger metal particles result in a decreasing selectivity [4]. Therefore, the selectivity increase observed here can only be attributed to the presence of promoters and not to the presence of larger platinum particles.

The RDP synthesis results in close contact of tin with platinum, thereby forming a close interaction of the two metals. This results in a higher selectivity to cinnamyl alcohol for the cinnamaldehyde hydrogenation, irrespective the applied hydrogenation pressure. The increase in selectivity observed with RDP synthesized catalysts is not observed for the bimetallic catalyst prepared via IWI synthesis where close platinum-tin interaction is absent.

Conclusions

In this study, tin and gallium promoted Pt/CNF catalysts were prepared by reductive deposition precipitation (RDP, i.e. deposition under hydrogen atmosphere) and incipient wetness impregnation (IWI). TEM-EDX, XPS and EXAFS showed that RDP synthesis resulted in a close contact between promoter and platinum. Catalysts which displayed a close and significant contact between platinum and promoter were more selective in the hydrogenation of cinnamaldehyde to cinnamyl alcohol as compared to the samples in which such an interaction is not present. For activity such a clear conclusion could not be drawn since activity is mainly influenced by the reaction conditions, such as pressure and reactant concentration.

Literature

1. M.L. Toebes, Y. Zhang, J. Hájek, T.A. Nijhuis, J.H. Bitter, A.J. van Dillen, D.Y. Murzin, D.C. Koningsberger, K.P. de Jong, J. Catal., 226(1), 2004, 215-225.
2. M.L. Toebes, T.A. Nijhuis, J. Hájek, J.H. Bitter, A.J. van Dillen, D.Y. Murzin, K.P. de Jong, Chem. Eng. Sci., 60(21), 2005, 5682-5695.
3. M.L. Toebes, M.K. van der Lee, L.M. Tang, M.H. Huis in 't Veld, J.H. Bitter, A.J. van Dillen, K.P. de Jong, J. Phys. Chem. B, 108(31), 2004, 11611-11619.
4. A.J. Plomp, H. Vuori, A.O.I. Krause, K.P. de Jong, J.H. Bitter, Appl. Catal. A, 351(1), 2008, 9-15.
5. P. Gallezot, D. Richard, Cat. Rev. - Sci. Eng., 40(1-2), 1998, 81-126.
6. V. Ponec, Appl. Catal. A, 149(1), 1997, 27-48.
7. W.F. Tuley, R. Adams, J. Am. Chem. Soc., 47, 1925, 3061-3068.
8. D. Richard, J. Ockelford, A. Giroir-Fendler, P. Gallezot, Catal. Lett., 3(1), 1989, 53-58.
9. S. Galvagno, A. Donato, G. Neri, R. Pietropaolo, D. Pietropaolo, J. Mol. Catal., 49(2), 1989, 223-232.
10. O.S. Alexeev, B.C. Gates, Ind. Eng. Chem. Res., 42(8), 2003, 1571-1587.
11. K.P. de Jong, Curr. Opin. Solid State Mater. Sci., 4(1), 1999, 55-62.
12. J. Barbier, in: G. Ertl, H. Knözinger, J. Weitkamp (Eds.), Preparation of Solid Catalysts, WILEY-VCH, Weinheim, 1999, pp. 526-540.
13. E. Lamy-Pitara, L. El Ouazzani-Benhima, J. Barbier, J. Electroanal. Chem., 335(1-2), 1992, 363-370.

14. G. Corro, P. Marecot, J. Barbier, Stud. Surf. Sci. Catal., 111(Catalyst Deactivation), 1997, 359-366.
15. F. Epron, C. Carnevillier, P. Marecot, Appl. Catal. A, 295(2), 2005, 157-169.
16. C. Carnevillier, F. Epron, P. Marecot, Appl. Catal. A, 275(1-2), 2004, 25-33.
17. T. Mallat, A. Baiker, Appl. Catal. A, 200(1-2), 2000, 3-22.
18. S. Schimpf, J. Gaube, P. Claus, Springer Series in Chemical Physics, 75(Basic Principles in Applied Catalysis), 2004, 87-123.
19. M.L. Toebes, J.H. Bitter, A.J. van Dillen, K.P. de Jong, Catal. Today, 76(1), 2002, 33-42.
20. G.R. Meima, B.G. Dekker, A.J. van Dillen, J.W. Geus, J.E. Bongaarts, F.R. van Buren, K. Delcour, J.M. Wigman, Stud. Surf. Sci. Catal., 31(Preparation of Catalysts IV), 1987, 83-101.
21. M. Vaarkamp, J.C. Linders, D.C. Koningsberger, Physica B, 209(1-4), 1995, 159-160.
22. H.H.C.M. Pinxt, PhD-thesis, Eindhoven University of Technology, Eindhoven, 1997.
23. J.H. Nelson, N.W. Alcock, Inorg. Chem., 21 (3), 1982, 1196-2000.
24. G.E. van Dorssen, D.C. Koningsberger, D.E. Ramaker, J. Phys.: Condens. Matter, 14(49), 2002, 13529-13541.
25. W.J. Moore, L. Pauling, J. Am. Chem. Soc., 63, 1941, 1392-1394.
26. D.C. Koningsberger, B.L. Mojet, G.E. van Dorssen, D.E. Ramaker, Top. Catal., 10(3-4), 2000, 143-155.
27. G. Neri, C. Milone, S. Galvagno, A.P.J. Pijpers, J. Schwank, Appl. Catal. A, 227(1-2), 2002, 105-115.
28. E.A. Stern, Phys. Rev. B, 48(13), 1993, 9825-9827.
29. Y. Zhang, M.L. Toebes, A. van der Eerden, W.E. O'Grady, K.P. de Jong, D.C. Koningsberger, J. Phys. Chem. B, 108(48), 2004, 18509-18519.
30. A. Jentys, Phys. Chem. Chem. Phys., 1(17), 1999, 4059-4063.
31. W.H. Baur, A.A. Khan, Acta Cryst., B27, 1971, 2133-2139.
32. C.D. Wagner, W.M. Riggs, L.E. Davis, J.F. Moulder, Handbook of X-ray Photoelectron Spectroscopy, Perkin-Elmer Corporation, Eden Prairie, 1979.
33. M.d.C. Aguirre, P. Reyes, M. Oportus, I. Melian-Cabrera, J.L.G. Fierro, Appl. Catal. A, 233(1-2), 2002, 183-196.
34. P. Maki-Arvela, J. Hajek, T. Salmi, D.Y. Murzin, Appl. Catal. A, 292, 2005, 1-49.
35. T. Vergunst, PhD-thesis, Delft University of Technology, Delft, 1999.
36. T. Vergunst, F. Kapteijn, J.A. Moulijn, Catal. Today, 66(2-4), 2001, 381-387.
37. M. Shirai, T. Tanaka, M. Arai, J. Mol. Catal. A: Chem., 168(1-2), 2001, 99-103.
38. G. Neri, S. Galvagno, Recent Research Developments in Catalysis, 2, 2003, 121-141.

7A

Summary and Concluding Remarks

The aim of the work described in this thesis was to investigate the role and nature of nanostructured carbon materials, oxygen surface groups and promoters on platinum-based catalysts for the selective hydrogenation of cinnamaldehyde. The selective hydrogenation of cinnamaldehyde to cinnamyl alcohol was chosen as a showcase, since the selectivity and activity of this reaction can be tuned by multiple catalyst variables such as the support and presence of promoters. To establish structure-activity relations, it is crucial to prepare well-defined carbon nanofibers (CNF) supports and well-defined catalytic metal phases on these supports.

In **Chapter 2** an exploratory study on the selective hydrogenation of cinnamaldehyde is described. The influence of the reactant concentration, reaction solvent and nature of the metal and support was evaluated. Based on the results, it was decided to use 2-propanol/water as solvent due to the high activity and selectivity of the catalyst in this solvent and the limited formation of acetals. Cinnamaldehyde concentration effects turned out to be in line with literature, i.e. higher cinnamaldehyde concentrations resulted in enhanced selectivities towards cinnamyl alcohol. A cinnamaldehyde concentration of 0.1 M was chosen for further studies, since catalyst deactivation was not observed at this reactant concentration while the higher concentration (1 M) did result in deactivation. This exploratory study was extended by investigating the influence of heat-treatments on various CNF-supported metals for cinnamaldehyde hydrogenation. To that purpose, iridium, ruthenium, platinum, palladium and rhodium were deposited on CNF and before heat-treatment the sequence in selectivity was Ir > Ru > Rh > Pt > Pd. After heat-treatment, the sequence in selectivity changed and followed Pt > Ru > Ir > Pd ≈ Rh. Heat-treated platinum on CNF resulted in the highest selectivity combined with reasonable activity, while the catalyst did not deactivate. Therefore, it was decided to perform further studies on this catalyst.

The role of the nature and stability of oxygen surface groups in anchoring and stabilizing platinum particles was investigated. To that purpose CNF and platinum-containing CNF with different amounts and types of oxygen surface groups were analyzed using XPS and titrations. The results are described in **Chapter 3**. With respect to stability of oxygen surface groups, it was found that after heat-treatment at 973 K all initially present acidic oxygen surface groups were removed. This decomposition temperature for acidic oxygen surface groups decreased to 773 K when platinum particles were present. Platinum anchoring occurs on both carboxyl and phenol type groups during catalyst synthesis. It is proposed that during synthesis and with increasing pH, both types of oxygen surface groups become deprotonated, first the carboxylic acid groups and then the phenol groups, which bring about platinum-ion adsorption on both groups.

In **Chapter 4** the influence of graphene orientations on platinum deposition and reduction behavior was analyzed. To that purpose, platinum was deposited on oxidized nanostructured carbon materials, i.e. CNF, carbon nanoplatelets (CNP) and carbon nanotubes (CNT). It was demonstrated that platinum deposited on CNT resulted in 20 K higher reduction temperature as compared to platinum on CNF and CNP. We related this to the high amount of acidic oxygen surface groups detected on this support, resulting in a strong stabilization of the platinum cation during reduction. Application of the required higher reduction temperature resulted in complete reduction for that sample, accompanied by sintering of platinum to large agglomerates. The prepared catalysts were tested and Pt/CNP

and Pt/CNF turned out to be active catalysts for the cinnamaldehyde hydrogenation, while fully reduced and sintered platinum on CNT was not very active for this reaction. Pt/CNP resulted in a higher selectivity towards cinnamyl alcohol when compared to Pt/CNF. Since for the latter two catalysts the amount of oxygen surface groups, platinum particle sizes as well as initial hydrogenation activities are similar, it is concluded that the orientation of the graphene sheets must have a significant influence on the selectivity for cinnamaldehyde hydrogenation.

In **Chapter 5** particle size effects for cinnamaldehyde hydrogenation using platinum and ruthenium on CNF with similar amounts of acidic oxygen surface groups, i.e. before and after heat-treatment, were investigated. Different sized platinum and ruthenium particles were deposited on CNF via atomic layer deposition (ALD) and homogeneous deposition precipitation (HDP), resulting in metal particles of 2-6 nm via ALD and metal particles of 1-3 nm via HDP. These catalysts were tested for the selective hydrogenation of cinnamaldehyde. Before heat-treatment, the platinum catalysts with larger metal particles turned out to be more selective, which is in line with particle size effects described in literature. After heat-treatment, which resulted in removal of oxygen surface groups, smaller metal particles resulted in a higher selectivity for the platinum and ruthenium catalysts. Thus, a reversed particle size effect was observed after heat-treatment as compared to the catalytic results obtained with polar, i.e. non heat-treated supports. This is ascribed to a changing adsorption mode of the reactant, whereby the non-polar, i.e. heat-treated support favors the adsorption of the phenyl ring. This enables the metal periphery to participate in the hydrogenation and may result in the direction of the C=O bond to the metal periphery. Since the metal periphery area is larger for smaller metal particles, an increase in activity and selectivity is observed as compared to larger metal particles.

Promoters were added to platinum on CNF to obtain enhanced selectivities towards cinnamyl alcohol. We aimed to characterize platinum-promoter interactions and relate this to the catalytic performance. In **Chapter 6**, CNF-supported platinum was combined with tin and gallium as promoters via incipient wetness impregnation (IWI) and via reductive deposition precipitation (RDP). For the latter technique, promoters were added to platinum catalysts under hydrogen atmosphere. Via detailed characterization using EXAFS, TEM-EDX and XPS, it was demonstrated that tin became partially reduced when deposited via RDP, thereby resulting in a close contact of the two metals. Via IWI synthesis such a close interaction was not obtained. The prepared catalysts were tested for the selective hydrogenation of cinnamaldehyde both at low as well as at high hydrogenation pressures and enhanced selectivities towards cinnamyl alcohol were observed when close platinum-promoter interactions were present. For activity such a clear conclusion could not be drawn since it was mainly influenced by the reaction conditions, such as pressure and reactant concentration.

Gallium deposition on platinum catalysts via RDP demonstrated the wider applicability of this synthesis technique.

The results described in this thesis showed that we successfully investigated the role and nature of oxygen surface groups for platinum deposition, the influence of graphene sheet orientation on platinum, particle size effects for cinnamaldehyde hydrogenation before as well as after heat-treatments for platinum on CNF and the influence of platinum-promoter interactions for cinnamaldehyde hydrogenation. Future research can be devoted to reveal the mechanism of reactant adsorption on CNF and reactant adsorption via promoters towards platinum.

7B

Samenvatting en Conclusies

Het doel van het werk beschreven in dit proefschrift is om de rol en de aard van nano-gestructureerd koolstof, oppervlakte-zuurstofgroepen en promoter-elementen op platina-gebaseerde katalysatoren voor de selectieve hydrogenering van kaneelaldehyde te onderzoeken. De selectieve hydrogenering van kaneelaldehyde naar kaneelalcohol is gebruikt als demonstratie-reactie, omdat de selectiviteit en activiteit van deze reactie geregeld kan worden door meerdere katalysator-variabelen, zoals het dragermateriaal en de aanwezigheid van promotoren. Om structuur-activiteits relaties op te stellen, is het cruciaal om goed gedefinieerde koolstofnanovezels (KNV) als dragermateriaal en goed gedefinieerde metaalfasen op deze dragermaterialen te bereiden.

In **Hoofdstuk 2** is een verkennend onderzoek naar de selectieve hydrogenering van kaneelaldehyde beschreven. De invloed van de reactantconcentratie, reactie-oplosmiddel en het type metaal en dragermateriaal is onderzocht. Gebaseerd op deze resultaten, is ervoor gekozen om 2-propanol/water als oplosmiddel te gebruiken, vanwege de hoge activiteit en selectiviteit van de katalysator in dit oplosmiddel. Kaneelaldehyde concentratie-effecten bleken in lijn te zijn met de literatuur, dat wil zeggen dat hogere concentraties van kaneelaldehyde resulteerden in hogere selectiviteiten naar het kaneelalcohol. Voor verdere studies is een kaneelaldehyde concentratie van 0.1 M gekozen, omdat bij deze concentratie geen deactivering van de katalysator werd waargenomen terwijl bij hogere concentratie (1 M) wel deactivering werd waargenomen. Dit verkennend onderzoek werd uitgebreid door de invloed van warmtebehandelingen op verschillende metalen op KNV te bestuderen voor de hydrogenering van kaneelaldehyde. Met dat doel werden iridium, ruthenium, platina, palladium en rhodium afgezet op KNV. Voor de warmtebehandeling was de volgorde in selectiviteit: Ir > Ru > Rh > Pt > Pd. Na warmtebehandeling veranderde deze volgorde in selectiviteit naar Pt > Ru > Ir > Pd ≈ Rh. Warmtebehandeld platina op KNV resulteerde in de hoogste selectiviteit gecombineerd met een behoorlijke activiteit, terwijl de katalysator niet deactiveerde. Daarom werd deze katalysator verkozen voor verdere studies.

De rol van oppervlakte-zuurstofgroepen voor het verankeren en stabiliseren van platinadeeltjes werd onderzocht, waarbij in het bijzonder de aard en stabiliteit van deze oppervlakte-zuurstofgroepen werd geanalyseerd. Met dat doel werden KNV en Pt/KNV met verschillende hoeveelheden en typen oppervlakte-zuurstofgroepen geanalyseerd met behulp van XPS en titraties. De resultaten zijn beschreven in **Hoofdstuk 3**. Met betrekking tot de stabiliteit van de oppervlakte-zuurstofgroepen is gevonden dat na warmtebehandeling bij 973 K alle initieel aanwezige zure zuurstofgroepen werden ontleed. Deze ontledings-temperatuur voor zure zuurstofgroepen zakte naar 773 K wanneer platinadeeltjes aanwezig waren. Platina verankering vindt plaats op zowel carboxyl- als fenol-type zuurstofgroepen gedurende de synthese van de katalysator. Het voorgestelde model is, dat tijdens synthese beide typen zuurstofgroepen deprotoneren: bij lagere pH de carboxyl-groepen en bij hogere pH de fenol-groepen. Dit resulteert uiteindelijk in platina-ionen adsorptie op beide groepen.

In **Hoofdstuk 4** is de invloed van de oriëntatie van grafeenlagen op platina afzetting en reductie onderzocht. Daartoe werd platina afgezet op geoxideerde nano-gestructureerde koolstof materialen, te weten KNV, koolstofnanoplaten (KNP) en koolstofnanobuizen (KNB). Platina op KNB resulteerde in een 20 K hogere reductietemperatuur in vergelijking tot KNV en KNP. Deze verschuiving in reductietemperatuur is gerelateerd aan de grote hoeveelheid zure oppervlakte-zuurstofgroepen gedetecteerd op dit dragermateriaal, resulterend in een sterke stabilisatie van platina kationen tijdens reductie. Bij toepassing van de benodigde,

hogere reductie-temperatuur werd volledige reductie bereikt, maar het platina vormde daarbij grote deeltjes. De katalysatoren werden getest en Pt/KNP en Pt/KNV bleken actieve katalysatoren te zijn voor de kaneelaldehyde hydrogenering, terwijl het gereduceerde Pt/KNB nauwelijks actief was voor deze reactie. Pt/KNP resulteerde in een hogere selectiviteit naar kaneelalcohol in vergelijking met Pt/KNV. Omdat voor deze laatste katalysatoren de hoeveelheid oppervlakte-zuurstofgroepen, platina deeltjesgrootte en initiële hydrogenerings-activiteiten gelijk zijn, kan worden geconcludeerd dat de oriëntatie van de grafeenlagen een significante invloed heeft op de selectiviteit tijdens de hydrogenering van kaneelaldehyde.

In **Hoofdstuk 5** zijn effecten van de metaal deeltjesgrootte onderzocht voor de hydrogenering van kaneelaldehyde met behulp van platina en ruthenium op KNV met dezelfde hoeveelheid oppervlakte-zuurstofgroepen, zowel voor als na warmtebehandeling. Verschillende platina en ruthenium deeltjesgroottes werden afgezet op KNV via atomaire laag depositie (ALD) en homogene depositie precipitatie (HDP) en dat resulteerde in metaaldeeltjes van 2-6 nm via ALD en 1-3 nm via HDP. Deze katalysatoren werden getest voor de selectieve hydrogenering van kaneelaldehyde. Voor warmtebehandeling vertoonden de platinakatalysatoren met grotere metaaldeeltjes een hogere selectiviteit, wat in lijn is met deeltjesgrootte-effecten beschreven in de literatuur. Na warmtebehandeling, die ontleding van de oppervlakte-zuurstofgroepen tot gevolg had, gaven kleinere metaaldeeltjes een hogere selectiviteit voor zowel de platina- als ruthenium-katalysatoren. Dus een omgekeerd deeltjesgrootte-effect werd waargenomen na warmtebehandeling in vergelijking met de katalytische resultaten voorafgaand aan de warmtebehandeling, dat is op polaire dragermaterialen. Dit is toegeschreven aan een veranderende wijze van adsorptie van de reactant, waarbij de apolaire, dat zijn warmtebehandelde, dragermaterialen de adsorptie van de fenyl ring bevorderen. Dit maakt het mogelijk dat de metaalperiferie deelneemt aan de hydrogenering en kan resulteren in een sturing van de C=O binding naar de metaalperiferie. Omdat de lengte van de metaalperiferie groter is voor kleinere metaaldeeltjes, is er een toename aan activiteit en selectiviteit waargenomen in vergelijking met grotere metaaldeeltjes.

Aan platina op KNV werden promotoren toegevoegd om een hogere selectiviteit naar kaneelalcohol te bewerkstelligen. Het was daarbij de uitdaging om de interactie van platina en het promoter-element te karakteriseren en dat te relateren aan de katalytische prestatie. In **Hoofdstuk 6** werd platina op KNV gecombineerd met tin en gallium via porie volume impregnatie (PVI) en via reductieve depositie precipitatie (RDP). Voor de laatstgenoemde methode werden promoter-elementen toegevoegd aan de platinakatalysatoren onder een atmosfeer van waterstof. Via gedetailleerde karakterisering met behulp van EXAFS, TEM-EDX en XPS werd aangetoond dat tin gedeeltelijk werd gereduceerd tijdens afzetting via

RDP, dat resulteerde in een zeer goede interactie tussen platina en tin. Via PVI werd een dergelijke goede interactie niet verkregen. De bereide katalysatoren werden getest voor de selectieve hydrogenering van kaneelaldehyde zowel bij lage als bij hoge waterstofdruk. Een toegenomen selectiviteit naar kaneelalcohol werd waargenomen indien een goede interactie van platina en promoter-element aanwezig was. Wat betreft activiteit kon een dergelijke heldere conclusie niet worden getrokken omdat deze voornamelijk werd beïnvloed door de reactiecondities, zoals druk en concentratie van reactant. Afzetting van gallium op platinakatalysatoren via RDP liet de brede toepasbaarheid van deze synthesemethode zien.

De resultaten in dit proefschrift laten zien dat de rol en aard van oppervlakte-zuurstofgroepen tijdens afzetten van platina, de invloed van oriëntatie van grafeenlagen op platina, deeltjesgrootte-effecten voor de hydrogenering van kaneeladehyde zowel voor als na warmtebehandeling van platina op KNV en de invloed van interactie van platina met promotoren voor de kaneeldehyde hydrogenering, succesvol zijn onderzocht. Toekomstig onderzoek kan worden gewijd aan het ontrafelen van het mechanisme van reactantadsorptie op KNV en reactantadsorptie via promotoren richting het platina.

7C

Samenvatting voor Leken

Korte Introductie

Een katalysator is een stof die een chemische reactie versnelt. Een katalysator wordt daarbij niet zelf verbruikt en kan dus gerecycled worden. Katalyse wordt veelvuldig toegepast, meer of minder bewust, en is onmisbaar voor de samenleving. Zeer bekende katalysatoren zijn o.a. de enzymen in gist voor het laten rijzen van deegproducten of voor de productie van alcohol (een natuurlijke katalysator), zeolieten voor het kraken van aardolie tot brandstof en uitlaatgaskatalysatoren voor het terugdringen van schadelijke emissies. Dergelijke processen zouden anders niet of zeer veel trager verlopen.

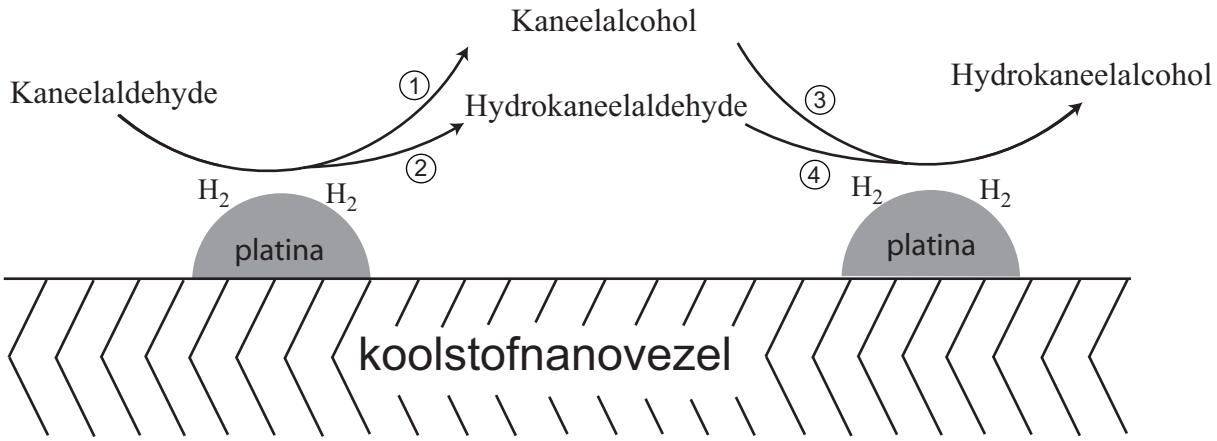

Fig. 1 Reactie van kaneelaldehyde met waterstof (dat is H_2) op de platina op KNV katalysator. De gevormde producten (hydrokaneelaldehyde en het gewenste kaneelalcohol) kunnen verder reageren tot hydrokaneelalcohol (voor structuurformules zie hoofdstuk 2, fig. 2).

Een ander gekatalyseerd proces is de reactie van kaneelaldehyde met waterstof (zie Fig. 1). Dit proces is zowel vanuit wetenschappelijk als industrieel oogpunt interessant. Het gewenste product is kaneelalcohol (als geur- en smaakstof en als bouwsteen voor medicijnen) en daarom is reactie 1 gewenst. Van nature verloopt echter reactie 2 (vorming van hydrokaneelaldehyde) sneller en er zal dus relatief veel hydrokaneelaldehyde worden gevormd. Daarnaast kunnen beide producten (dat zijn kaneelalcohol en hydrokaneelaldehyde) verder reageren tot hydrokaneelalcohol (reactie 3 en 4). Het is dus de uitdaging een katalysator te ontwerpen die selectief reactie 1 laat verlopen en alle andere mogelijke reacties voorkomt.

Voor dit proefschrift werden platinakatalysatoren onderzocht. Voor dit type katalysatoren vindt de gekatalyseerde reactie plaats op het oppervlak van het platina (zoals schematisch is weergegeven in Fig. 1). Om zo efficiënt mogelijk het katalysatormetaal te gebruiken, is het dus van belang om een zo groot mogelijk oppervlak met zo min mogelijk metaal te creëren. Dat kan door kleine platinadeeltjes te maken en deze stabiel te verankeren op een ander materiaal, het zogenaamde dragermateriaal. Een relatief nieuw dragermateriaal zijn koolstofnanovezels (verder afgekort tot KNV). Dit materiaal is opgebouwd uit lagen van koolstof. Eerder onderzoek toonde al aan dat platina succesvol als kleine deeltjes (ongeveer

2 nm, dat is 0.000002 millimeter) verankerd kan worden op KNV en in deze vorm een zeer actieve katalysator is voor de eerder besproken reactie van kaneelaldehyde met waterstof. Het was daarbij opvallend dat de katalysator eerst een warmtebehandeling (bij 700°C) moest ondergaan, voordat deze hoge activiteit werd gehaald.

Deze katalysator was wel zeer actief voor de reactie van kaneelaldehyde met waterstof, maar hierbij ontstond relatief veel hydrokaneelaldehyde. Om de productie naar kaneelalcohol om te buigen (dus de gewenste reactie 1), kan aan de platina katalysator een tweede element worden toegevoegd, een zogenaamde promoter. Een goed voorbeeld van een dergelijke promoter is tin.

Samenvatting

In **Hoofdstuk 2** is allereerst onderzocht onder welke condities de reactie van kaneelaldehyde met waterstof het beste uitgevoerd kan worden. Daartoe werd kaneelaldehyde opgelost in verschillende oplosmiddelen waar de katalysator aan werd toegevoegd. Door dit mengsel te roeren en er waterstofgas aan toe te voegen, kan de reactie verlopen. Het bleek dat een mengsel van 2-propanol met water het meest praktisch is als oplosmiddel voor de studies hier beschreven. Dit werk werd uitgevoerd met platina op KNV katalysatoren. Nu werden ook andere katalytische metalen op KNV gebracht, namelijk ruthenium, rhodium, iridium en palladium. Deze katalysatoren werden ook getest, zowel voor als na een warmtebehandeling van de katalysatoren. Daaruit bleek dat platina op KNV (na warmtebehandeling) resulteerde in de hoogste hoeveelheid kaneelalcohol gecombineerd met een behoorlijke activiteit. Daarom werd platina op KNV verkozen voor verdere studies.

Het is bekend dat voor de bereiding van kleine platina deeltjes op KNV, het laatste materiaal eerst zodanig behandeld moet worden dat er op het oppervlak van KNV zuurstofgroepen ontstaan. Dit zijn oppervlaktegroepen met als kenmerkend bestanddeel zuurstof. Deze zuurstofgroepen dienen als ankerpunten en binden dus het platina. In **Hoofdstuk 3** is onderzocht welke typen zuurstofgroepen het platina nu specifiek binden tijdens de katalysatorbereiding en daarvoor zijn KNV met en zonder platina en zowel voor als na warmtebehandeling geanalyseerd. Het bleek dat twee typen zuurstofgroepen daarbij de voornaamste rol spelen: zogenaamde fenol-groepen en carboxyl-groepen. Overigens ontleden deze zuurstofgroepen tijdens de eerder genoemde warmtebehandeling. Het is niet helemaal duidelijk hoe de platina deeltjes daarna precies gebonden zijn op het oppervlak van KNV.

Zoals eerder beschreven, bestaan KNV uit lagen van koolstof. Deze koolstoflagen kunnen op verschillende manieren geordend zijn en vrijwel al het werk in dit proefschrift is uitgevoerd op KNV met een zogenaamde vissegraatstructuur (zoals schematisch is

weergegeven in Fig. 1). Deze koolstoflagen kunnen echter ook parallel of haaks op het oppervlak staan. De invloed van deze verschillende structuren op platina is beschreven in **Hoofdstuk 4**. Het voornaamste resultaat was dat op parallel-georiënteerd koolstof het moeilijk was om geschikte platina deeltjes te maken. In dit geval waren er teveel zuurstofgroepen: het platina bindt wel goed, maar deeltjes van geschikte grootte kunnen dan niet eenvoudig verkregen worden. Deze katalysator was daarom nauwelijks actief voor de gebruikte reactie.

In **Hoofdstuk 5** is beschreven hoe, via twee verschillende methoden, platina deeltjes met verschillende grootte op KNV zijn gemaakt: deeltjes van ongeveer 2 nm (benaming: klein platina op KNV) en deeltjes van ongeveer 3½ nm (benaming: groot platina op KNV). Deze beide katalysatoren werden getest zowel voor als na de warmtebehandeling. De activiteit voor beide katalysatoren nam toe na de warmtebehandeling, zoals al eens eerder was waargenomen. Wat betreft de hoeveelheid gevormd kaneelalcohol: voor de warmte-behandeling resulteerde groot platina op KNV in meer kaneelalcohol in vergelijking met klein platina op KNV; dit is overigens in lijn met eerder beschreven resultaten in de literatuur. Verrassend was echter dat na de warmtebehandeling precies het omgekeerde werd waargenomen: klein platina op KNV resulteerde in meer kaneelalcohol tijdens de reactie. Het effect van de grootte van platinadeeltjes hangt dus af van de warmtebehandeling. Aangezien deze behandeling leidt tot ontleding van de eerder besproken zuurstofgroepen, was de vorming van kaneelalcohol direct te relateren aan de aan- of afwezigheid van zuurstofgroepen. Een mogelijke verklaring is dat bij afwezigheid van zuurstofgroepen, kaneelaldehyde een interactie heeft met het KNV-oppervlak en samen met kleine platinadeeltjes resulteert in relatief veel kaneelalcohol ten opzichte van grote platina deeltjes.

Tenslotte werd in **Hoofdstuk 6** op twee verschillende methoden tin als promoter toegevoegd aan de platina op KNV-katalysator, waarbij het de bedoeling was tin specifiek aan het platina te binden. De gemaakte platina-tin katalysatoren werd uitgebreid geanalyseerd en daaruit bleek dat via één van de methoden het tin inderdaad nauwkeurig en goed verdeeld op de platina deeltjes werd geplaatst en niet elders op het KNV-oppervlak terecht kwam: een goede platina-tin interactie werd dus verkregen. Via de andere methode kwam het merendeel van het tin wel op het KNV-oppervlak terecht en vormde daar grote deeltjes: een slechte platina-tin interactie werd bereikt. Deze katalysatoren werden getest en in het geval van een goede platina-tin interactie nam de hoeveelheid gevormd kaneelalcohol verder toe, terwijl bij een slechte platina-tin interactie juist het tegenovergestelde werd bereikt: de hoeveelheid gevormd kaneelalcohol nam af en hydrokaneelaldehyde nam toe. Daarmee is onomstotelijk vastgesteld dat een promoter op het platina oppervlak moet worden geplaatst om de hoeveelheid kaneelalcohol tijdens de reactie te verhogen.

Concluderend kan worden gezegd dat platina op KNV een veelbelovende katalysator is en de hier beschreven resultaten laten zien welke factoren belangrijk zijn voor de bereiding en het testen van de katalysator. Bovendien is aangetoond dat met een goede platina-tin interactie de reactie kan worden omgebogen zoals gewenst en ook hoe deze katalysator gemaakt kan worden.

List of Publications and Presentations

Publications:

H. Markus, A.J. Plomp, P. Mäki-Arvela, J.H. Bitter and D.Y. Murzin 'The influence of acidity of carbon nanofibre-supported palladium catalysts in the hydrogenolysis of hydroxymatairesinol' Catalysis Letters 113 (2007) 141-146.

H. Markus, A.J. Plomp, T. Sandberg, V. Nieminen, J.H. Bitter and D.Y. Murzin 'Dehydrogenation of hydroxymatairesinol to oxomatairesinol over carbon nanofibre-supported palladium catalysts' Journal of Molecular Catalysis A: Chemical 274 (2007) 42-49.

A.J. Plomp, H. Vuori, A.O.I. Krause, K.P. de Jong and J.H. Bitter 'Particle size effects for carbon nanofiber supported platinum and ruthenium catalysts for the selective hydrogenation of cinnamaldehyde' Applied Catalysis A: General 351 (2008) 9-15.

H. Bernas, A.J. Plomp, J.H. Bitter and D.Y. Murzin 'Influence of reaction parameters on the hydrogenolysis of hydroxymatairesinol over carbon nanofibre supported palladium catalysts' Catalysis Letters 125 (2008) 8-13.

A.J. Plomp, T. Schubert, U. Storr, K.P. de Jong and J.H. Bitter 'Reducibility of platinum supported on nanostructured carbons' Topics in Catalysis, accepted.

A.J. Plomp, D.M.P. van Asten, A.M.J. van der Eerden, P. Mäki-Arvela, D.Y. Murzin, K.P. de Jong and J.H. Bitter 'Catalysts based on platinum-tin and platinum-gallium in close contact for the selective hydrogenation of cinnamaldehyde' Journal of Catalysis, accepted.

A.J. Plomp, D.S. Su, K.P. de Jong and J.H. Bitter 'On the nature of oxygen-containing surface groups on carbon nanofibers and their role for platinum deposition' Journal of Physical Chemistry C, submitted.

H. Vuori, A.J. Plomp, K.P. de Jong, A.O.I. Krause and J.H. Bitter 'Gas phase deposition of palladium on carbon nanofibers', in preparation.

Oral Presentations:

A.J. Plomp, K.P. de Jong and J.H. Bitter 'Preparation of platinum nano-particles on carbon nano-materials' 7th Netherlands' Catalysis and Chemistry Conference, Noordwijkerhout, The Netherlands, March 2006.

A.J. Plomp, K.P. de Jong and J.H. Bitter 'Surface oxidation of carbon nanofibers – characterization and utilization' Invited lecture, Fritz-Haber Institute, Berlin, Germany, October 2006.

A.J. Plomp, K.P. de Jong and J.H. Bitter 'Platinum combined with tin on carbon nanofibers' 8th Netherlands' Catalysis and Chemistry Conference, Noordwijkerhout, The Netherlands, March 2007.

E.V. Murzina, A.V. Tokarev, A.J. Plomp, J.H. Bitter, I.L. Simakova and D.Y. Murzin 'Lactose oxidation over carbon supported palladium catalysts' 20th North American Meeting, Houston, USA, June 2007.

D.Y. Murzin, A.J. Plomp, P. Mäki-Arvela and J.H. Bitter 'Selective hydrogenation of cinnamaldehyde over Pt/CNF' 9th Netherlands' Catalysis and Chemistry Conference, Noordwijkerhout, The Netherlands, March 2008.

H. Vuori, A.O.I. Krause, A.J. Plomp, K.P. de Jong and J.H. Bitter 'Pt, Ru and Pd catalysts on carbon nanofibers for selective hydrogenation' IDECAT WP5 workshop, Ghent, Belgium, March 2008.

A.J. Plomp, H. Vuori, A.O.I. Krause, K.P. de Jong and J.H. Bitter 'Reversed particle size effect for Pt on carbon nanofibers in the cinnamaldehyde hydrogenation' E-MRS Fall Meeting, Warsaw, Poland, September 2008.

Poster Presentations:

A.J. Plomp, K.P. de Jong and J.H. Bitter 'Structure of platinum-tin on carbon nanofibers related to its performance for cinnamaldehyde hydrogenation' 20th North American Meeting, Houston, USA, June 2007.

A.J. Plomp, K.P. de Jong and J.H. Bitter 'On the effects of the preparation of carbon nanofibers supported PtSn catalysts used for cinnamaldehyde hydrogenation' Europacat 8, Turku/Åbo, Finland, August 2007.

A.J. Plomp, H. Vuori, A.O.I. Krause, K.P. de Jong and J.H. Bitter 'Reversed particle size effect for carbon nanofiber supported Pt catalysts in the hydrogenation of cinnamaldehyde' 9th Netherlands' Catalysis and Chemistry Conference, Noordwijkerhout, The Netherlands, March 2008.

A.J. Plomp, H. Vuori, A.O.I. Krause, K.P. de Jong and J.H. Bitter 'Reversed particle size effect for carbon nanofiber supported Pt catalysts in the hydrogenation of cinnamaldehyde' 14th International Congress on Catalysis, Seoul, Korea, July 2008.

Dankwoord

Ik wil bij deze iedereen bedanken, die op wat voor wijze dan ook heeft bijgedragen aan mijn promotieonderzoek. Zonder de kennis, inzet en vaardigheden van anderen zou ik dit werk nooit uit hebben kunnen voeren. De volgende personen wil ik in het bijzonder noemen.

Mijn promotor Krijn de Jong en co-promotor Harry Bitter ben ik veel dank verschuldigd voor hun begeleiding en bijdrage aan het hier beschreven werk. Krijn, je hebt mij erg gemotiveerd de afgelopen vier jaren door al je enthousiasme en interesse in het onderzoek. Je nuchtere kijk op zaken en geduldige aanpak hebben de afronding van dit proefschrift sterk bevorderd, zeker in de laatste fase als ik het soms zelf even niet meer overzag. Harry, de afgelopen vier jaren was je mijn eerste begeleider. Gedurende deze periode heeft de deur van je kamer wagenwijd opengestaan: ik kon altijd terecht voor een korte vraag, die steevast langer was dan ik tevoren aangaf, en je had steeds tijd voor het onderzoek en al het correctiewerk. Ook je gezelschap tijdens de verscheidene reizen die we kriskras door Europa hebben gemaakt voor projectbijeenkomsten, congressen en metingen heb ik erg gewaardeerd. En bij de diverse diners kon ik me verheugen op een dubbele portie groente.

As a PhD student I cooperated with many people from various universities. I therefore wish to acknowledge in particular prof. Dmitry Murzin, Päivi Mäki-Arvela and Heidi Bernas (Heidi Markus before marriage) from the Åbo Akademi in Turku, Finland for all research performed on our catalysts and for giving me the opportunity to perform test experiments myself in your group. Also Ulrich Storr and Tim Schubert from FutureCarbon in Bayreuth, Germany are acknowledged for their kind provision of carbon materials for research. My gratitude goes to Dangsheng Su and Ute Wild from the Fritz-Haber Institute in Berlin, Germany for giving me the opportunity to measure on their machine. I wish to thank Heli Vuori and prof. Outi Krause from the Helsinki University of Technology in Espoo, Finland for all research we performed in which two different synthesis techniques were combined. Heli, I hope you enjoyed this time as well and that you still use the poffertjespan. Technical staff from beamline C at HasyLab in Hamburg, Germany and beamline BM26A at ESRF in Grenoble, France allocated measurement time for me, for which I owe gratitude. In addition, I wish to thank all partners from our Nanocat project team for all interest and valuable comments on my research.

Verschillende studenten hebben bijgedragen aan het hier beschreven werk. In het bijzonder noem ik Niek Smeenk, Aitziber Errecacho en David van Asten die qua praktisch onderzoek hebben bijgedragen en Paul Radstake en Andre Sonke die twee informatieve scripties hebben geschreven.

Veel metingen zijn mede mogelijk gemaakt of verzorgd door de technische staf, die ik dan ook erkentelijk ben vanaf het enkele vrijdagmiddag-experiment tot en met de forse hoeveelheden die soms werden ingeleverd voor analyses. Ook bij mijn zoveelste 'spoedje' kwamen de resultaten op een of andere manier toch weer op tijd. In het bijzonder noem ik Ad van der Eerden (XRF, EXAFS en hulp met data-analyse als ik er zelf weer niet uitkwam), Cor van der Spek (TEM), Marjan Versluijs (XRD en XRF), Vincent Koot (chemisorptie en TPR) en Ad Mens (opstellingen in elkaar zetten, fysisorptie en XPS, dat laatste zelfs tot het apparaat ermee ophield). Een bijzonder woord van dank richting emeritus prof. John Geus, die al vanaf mijn studententijd met veel enthousiasme verschillende materialen voor mij heeft geanalyseerd met behulp van TEM en me zeker ook met raad en daad terzijde heeft gestaan voor wat betreft het onderzoek. Zonder de geweldige administratieve ondersteuning van Dymph Serree en Monique Lamers had ik beslist minder tijd in onderzoek kunnen steken.

De hele vakgroep Anorganische Chemie & Katalyse heeft in al zijn verscheidenheid een plezierige werksfeer gecreëerd, die ik zeker zal missen. Dit werd mede bepaald door ontspanning in de vorm van borrels, BBQ's, vakgroepsuitjes en kerstdiners. Mijn kamergenoten Daphne Keller, Ingmar Swart en Mariska Wolters hebben de dagelijkse beslommeringen meer dan eens doorbroken met levendige gesprekken, discussies en muziek. Het leven in Went N209 werd daardoor bijzonder veraangenaamd. Ingmar, vanaf de allereerste uurtjes in de collegebanken, tegelijk afstuderen en daarna promoveren kennen we elkaar. Jij en Charlotte alle goeds gewenst. Johan den Breejen wil ik ook vermelden als mijn trouwe EXAFS-compagnon. Samen met Ingmar maakten we regelmatig een lunch-wandeling om even te bespreken hoe zwaar het allemaal wel niet was. Nu lopen jullie het laatste stukje mee als paranimf.

Pa en Ma, jullie hadden altijd vertrouwen in me. Ik houd van jullie. Willemein en Piet, Edwin, Sander en Jacqueline, schoonfamilie en vrienden: ik vrees dat ik er niet altijd in ben geslaagd in 'normaal Nederlands' weer te geven waar ik al die tijd zo druk mee was. Ik bewonder jullie geduld in deze... Toch hebben jullie op geheel eigen wijze aan dit boekje bijgedragen. Bedankt voor alles.

De laatste woorden zijn voor jou, mijn lieve Annemieke. Zonder jouw onvoorwaardelijk vertrouwen, aanmoediging en steun in alle opzichten zou dit proefschrift er volgens mij niet liggen. Ik hoop nog lang samen met jou gelukkig te zijn.

ARJAN

Curriculum Vitae

Arie Jan Plomp werd op 18 juli 1980 geboren in Zeist. In juni 1999 behaalde hij het VWO diploma aan het Van Lodensteincollege in Amersfoort en in hetzelfde jaar begon hij aan zijn studie Scheikunde aan de Universiteit Utrecht. In september 2000 behaalde hij zijn propedeuse met genoegen. Zijn afstudeeronderzoek verrichtte hij in de fysisch organische chemie onder begeleiding van dr. P. Loffeld en prof. dr. L.W. Jenneskens. Van november 2003 tot juli 2004 liep hij stage bij Engelhard De Meern B.V. onder begeleiding van dr. A.E.W. Beers en dr. P.H. Berben, waarna hij in augustus 2004 het doctoraal examen aflegde met genoegen. Vanaf oktober in datzelfde jaar was hij werkzaam als Assistent in Opleiding (AIO) bij de vakgroep Anorganische Chemie & Katalyse onder begeleiding van dr. J.H. Bitter en prof. dr. ir. K.P. de Jong. Een deel van de verkregen onderzoeksresultaten staat beschreven in dit proefschrift.